CLONING, EXPRESSION AND STUDY OF TWO PROTEINS IMPLICATED IN HUMAN CANCER: ASPARAGINE SYNTHETASE AND EPIDERMAL GROWTH FACTOR RECEPTOR

By

MIHAI CIUSTEA

A DISSERTATION PRESENTED TO THE GRADUATE SCHOOL
OF THE UNIVERSITY OF FLORIDA IN PARTIAL FULFILLMENT
OF THE REQUIREMENTS FOR THE DEGREE OF
DOCTOR OF PHILOSOPHY

UNIVERSITY OF FLORIDA

2003

To Mom and Dad

ACKNOWLEDGMENTS

I thank my advisor Dr Nigel G J Richards for giving me a wonderful opportunity to learn and grow as a biochemist while working on very [illegible] projects I thank Dr W Clay Smith for his daily help assistance and [illegible] for teaching me almost all the molecular biology techniques that I have used I am grateful for allowing me to work in the laboratories of the Ophthalmology Department I thank Dr Gregory S Schultz for his support and advice for being always enthusiastic whenever I made unscheduled appearances in his office door to ask for help I thank the members of my committee Dr Steven A Benner Dr Jon D Stewart Dr James A. Deyrup and all the professors in whose classes I was introduced to the wonderful world of science I would like to give special thanks to my mathematics professor from high school Prof Dumitru Buturuga the person who had the biggest influence on my formation I would like to thank all the students and personnel who made our labs a very pleasant place to be and work I thank my friends for their friendship and for all the good time that we had together Finally I thank my parents for everything

TABLE OF CONTENTS

page

ACKNOWLEDGMENTS iii

LIST OF TABLES vii

LIST OF FIGURES viii

ABSTRACT xi

CHAPTER

1 ASPARAGINE SYNTHETASE 1

- L-Asparaginase in Cancer Treatment 1
- Role of Asparagine Synthetase in L-Asparaginase Resistant Tumors 3
- Asparagine Synthetase Inhibitors 4
- Structure of Glutamine Dependent AS 5
- Catalytic Mechanisms of the Two Active Sites in Glutamine Dependent AS 10

2 EPIDERMAL GROWTH FACTOR RECEPTOR 18

- Growth Factors and Cancer 18
- Activation of Receptor Tyrosine Kinases 19
- Structure and Function of Epidermal Growth Factor Receptor 20
  - Extracellular Domain 20
  - Transmembrane Domain 22
  - Intracellular Domain 23
- Structure of Epidermal Growth Factor and Transforming Growth Factor α 23
- Epidermal Growth Factor Receptor Antagonists and Agonists 25

3 PROTEIN EXPRESSION IN BACULOVIRUS 27

- Baculovirus Expression Systems 27
- Experimental Methods and Materials 30
  - Materials 30
    - Enzymes 30
    - Oligonucleotides 30
  - Methods 31
    - Ligation and transformation reactions 31
    - Bacterial strains and vectors 31

Plasmid DNA preparation 31
Viral DNA preparations 31
DNA Sequencing 32
Sequence analysis of the expressed human asparagine synthetase 33
Growth and maintenance of insect cells 33
Subcloning of human asparagine synthetase cDNA 34
Cloning of human asparagine synthetase in pBAC-1 35
Oligonucleotide-directed in vitro mutagenesis 36
Transfection of insect cells and preparation of human asparagine synthetase recombinant baculovirus 36
Isolation, amplification and analysis of recombinant virus 37
Preparation of high titer viral stock 38
Time course of human asparagine synthetase expression 39
Western blotting 40
Expression and purification of human asparagine synthetase 40
Purification of messenger RNA from A431 human epidermoid carcinoma cells 41
First-strand cDNA synthesis and amplification 42
Subcloning and restoration of the EGFR-ED wild-type sequence 43
Cloning of EGFR-ED in the pMelBac transfer plasmid 43
Transfection of insect cells and preparation of EGFR-ED recombinant virus 44
Expression and purification of EGFR-ED 45
Results and Discussions 46
Subcloning of Human Asparagine Synthetase cDNA 46
Cloning of Human Asparagine Synthetase in pBAC-1 47
Transfection of Insect Cells and Preparation of Human Asparagine Synthetase Recombinant Virus 48
Virus Analysis, Purification and Amplification 49
Time Course of Human Asparagine Synthetase Expression 50
Expression and Purification of Human Asparagine Synthetase 51
N-Terminal Sequence Analysis of the Expressed Human Asparagine Synthetase 52
Cloning, Expression and Purification of Human Asparagine Synthetase Mutants 52
Synthesis and Cloning of EGFR-ED cDNA 53
Human EGFR-ED Recombinant Baculovirus 56
Expression and Purification of EGFR-ED 57

4 KINETIC CHARACTERIZATION OF HUMAN ASPARAGINE SYNTHETASE AND ITS MUTANTS 71

Expression and Characterization of Human Asparagine Synthetase Mutants 71
Pyrophosphate Determination Assay 72
Glutaminase Activity Assay 73
Kinetic Characterization of Human Asparagine Synthetase and its Mutants 74
Discussion 77

5 IDENTIFICATION OF EPIDERMAL GROWTH FACTOR RECEPTOR BINDING PEPTIDES BY PHAGE DISPLAY 103

Phage Display 105
Panning of the Phage Display Library against EGFR-ED 108
  Materials and Methods 108
    Iodination of human TGFα 108
    Binding of ^{125}I TGFα to EGFR-ED 108
    Solution panning of phage library against EGFR-ED 109
    Competition binding assay 111
    Cell proliferation assay 111
  Results 112
  Discussions 114

LIST OF REFERENCES 129

BIOGRAPHICAL SKETCH 151

LIST OF TABLES

Table page

3-1 Human AS DNA oligonucleotide primers 59

3-2 Human EGFR-ED cloning primers 59

3-3 Time course of human AS expression measured by the rate of pyrophosphate formation 62

3-4 Cell densities and viabilities during human AS expression. 63

4-1 Kinetic constants for the ammonia-dependent activity of wild type hAS, C1A and C1S 100

4-2 Kinetic constants of wild type hAS for L-glutamine in the glutaminase and glutamine dependent synthetase activities at saturating amounts of chloride 101

4-3 Kinetic constants of human AS for L-glutamine in the glutaminase reaction at various chloride concentrations 101

4-4 Effect of anions and other chemical species on the glutaminase and glutamine dependent synthetase activities. 102

5-1 Amount of phage (plaque forming units) selected in three consecutive panning rounds against EGFR-ED 120

LIST OF FIGURES

Figure page

1-1 Overall transformation catalyzed by glutamine-dependent asparagine synthetase 13

1-2 Schematic view of the ammonia channel 14

1-3 Comparison of the chemical mechanisms of BLS and AS 15

1-4 Cartoon representations of X-ray crystal structures A) BLS B) *Escherichia coli* AS-B 16

1-5 Hypothetical mechanism for the AS catalyzed formation of βAspAMP 17

2-1 Side view of the back to back EGFR/TGFα dimer 26

3-1 The pBAC/hAS cloning sites 60

3-2 Viral plaques on the Sf9 cell monolayer 61

3-3 Relative rate of pyrophosphate formation of human AS samples collected during the time course 62

3-4 Human AS purification on Ni-agarose 64

3-5 Analysis of the human AS preparation by SDS-PAGE and anti-histidine tag Western blot 65

3-6 N-terminus sequence analysis of human AS expressed in insect cells 66

3-7 Gel picture of the cDNA amplification product 67

3-8 Insert size analysis of potential EGFR ED cDNA fragments cloned in pCR2.1 67

3-9 Sequence of EGFR ED cloned in pMelBac B 68

3-10 Recombinant EGFR ED viral plaques that stained blue on Sf9 cell monolayer overlaid with medium-agarose containing X gal 69

3-11 Purification of untagged EGFR ED. SDS/PAGE of fractions eluted from Q-Sepharose column with NaCl gradient 69

3-12 Purification of histidine tagged EGFR-ED. SDS/PAGE of fractions eluted from Ni-agarose column with imidazole gradient 70

4-1 Determination of human AS K_m for ATP 86

4-2 Determination of human AS K_m for NH_4 87

4-3 Determination of human AS K_m for L-Aspartate 88

4-4 Determination of human AS K_m for L-Glutamine 89

4-5 Determination of C1A/hAS K_m for ATP 90

4-6 Determination of C1A/hAS K_m for NH_4 91

4-7 Determination of C1A/hAS K_m for L-Aspartate 92

4-8 Determination of C1S/hAS K_m for ATP 93

4-9 Determination of C1S/hAS K_m for NH_4^+ 94

4-10 Determination of C1S/hAS K_m for L-Aspartate 95

4-11 Human AS inhibition by ATP at concentrations above 2 mM 96

4-12 Effect of chloride on glutaminase activity 97

4-13 Amino acid sequence of the expressed human AS and the expected fragments produced by trypsin digestion 98

4-14 A) Structure of the N-acylsulfonamide inhibitor 4. B) Progress curves showing the effect of N-acylsulfonamide 4 on pyrophosphate production. 99

5-1 Competition binding of ^{125}I-TGFα and unlabeled TGFα to biotinylated EGFR-ED expressed in insect cells 121

5-2 Sequences of seventeen peptides selected by panning a random 12-mer phage-displayed library against EGFR-ED 122

5-3 Sequences of the peptides that were synthesized and characterized 123

5-4 Displacement of ^{125}I-EGF from MDA-231 cells by synthetic peptide 1 124

5-5 Displacement of ^{125}I-EGF from MDA-231 cells by synthetic peptide 2 125

5-6 Effect of TGFα on proliferation of human skin fibroblasts. 126

5-7 Effect of synthetic peptides on TGFα induced cell proliferation at 10^{-11} M TGFα 127

Abstract of Dissertation Presented to the Graduate School
of the University of Florida in Partial Fulfillment of the
Requirements for the Degree of Doctor of Philosophy

CLONING, EXPRESSION AND STUDY OF TWO PROTEINS IMPLICATED IN HUMAN CANCER: ASPARAGINE SYNTHETASE AND EPIDERMAL GROWTH FACTOR RECEPTOR

By

Mihai Ciustea

December 2003

Chair: Nigel G.J. Richards
Major Department: Chemistry

Epidermal growth factor receptor, the primary member of the tyrosine kinase family of signaling cell surface receptors, and asparagine synthetase, the eukaryotic enzyme responsible for the synthesis of asparagine from ATP, glutamine and aspartate, have been the focus of intense structural, mechanistic and inhibitory studies, as they represent two molecular targets for anti-cancer drug discovery. Human asparagine synthetase and five of its mutants were cloned and expressed in a baculovirus expression system under the control of the very late *polyhedrin* promoter. The recombinant proteins fused to a C-terminal histidine tag were purified to homogeneity in a single-step, nickel-chelation chromatography and the apparent affinity constants were determined. The wild-type asparagine synthetase was properly processed, as N-terminus sequence analysis showed that the starting methionine residue was cleaved off. The recombinant enzyme had both glutaminase and glutamine-dependent asparagine synthetase activities. As expected, Cys-1 mutants showed no glutamine-dependent activity, but were able to use ammonia as a nitrogen source for asparagine synthesis. Mutation of the conserved position Arg-339 to alanine or lysine completely eliminated the synthetase activity, while preserving the ability to hydrolyze glutamine. A possible thermolabile mutant, Lys413-Phe, showed an activity even at lower temperatures. The glutaminase and glutamine-dependent asparagine synthetase activities required chloride ions, which could be replaced by bromide or iodide, but with less activity. Compounds analogous to the reaction transition state or the β-aspartyl-AMP intermediate were effective inhibitors of the synthetase activity, but did not interfere with the glutaminase activity of the recombinant enzyme.

The extracellular domain of epidermal growth factor receptor was expressed in insect cells with a baculovirus secretion system and purified from the serum-free medium based on a C terminal histidine tag. The domain was biotinylated and used as a target to select 12-residue peptides displayed on bacteriophage from a 1.9 x 10^9-member library. After three rounds of affinity selection, binding phage were purified and clones were analyzed to identify the sequences of selected peptides. Analysis of the amino-acid sequences of selected peptides showed a high content of histidine residues, indicating that selection was directed against Ni^{2+} ions that are possibly contaminating the target by binding to the C-terminal tag. Two peptides were synthesized and evaluated. While both peptides were able to displace TGFα bound to the epidermal growth factor receptor, only the peptide with no histidines had an antagonistic activity against growth factor-induced cell proliferation.

CHAPTER 1
ASPARAGINE SYNTHETASE

L-Asparaginase in Cancer Treatment

The association of L-aspargine and cancer began with the observation made in 1953 that guinea pig serum has therapeutic effects against certain lymphomas of mouse and rat (1 2) The antitumor properties of the guinea pig serum were shown to be due to its L asparaginase activity (3 5) L-Asparaginases from *Escherichia coli* and other bacteria were also effective against lymphomas by causing a profound lowering of the level of free asparagine in the blood and tissues of treated mice (6-10) L Asparaginase catalyses the hydrolysis of L-asparagine to L aspartate depleting the circulating asparagine and antagonizing the cellular systems that undergo rapid protein synthesis (8)

A wide variety of human cancers have been treated with L asparaginase but acute lymphocytic leukemia (ALL) appears to be almost uniquely sensitive (11 12) Tumors of lymphoid origin are incapable of intracellular asparagine synthesis making them sensitive to the L asparaginase treatment. When *Escherichia coli* L asparaginase is used as a single agent there is nearly complete remission in 40 to 60% of ALL cases (13 14) More importantly when the enzyme is administered in combination with drugs such as vincristine and prednisone, complete remission is observed in 95% of cases of untreated ALL (15)

In an interesting and apparently poorly investigated observation T-cell based immunosuppresion is often seen in patients who are undergoing initial treatment with L-asparaginase (16)

Although administration of L-asparaginase is accepted as an essential component of modern therapy, it is fraught with serious side effects and overwhelmed by the appearance of resistant leukemias (17,18). The clinical utility of L-asparaginase in cancer therapy is limited by three factors. First, most neoplasms can synthesize asparagine and do not depend on an exogenous supply (15). Second, even in those neoplasms that are initially sensitive to L-asparaginase, selection of cell lines that are asparagine independent occurs during therapy and a large number of patients who achieve remission suffer a relapse with resistant cancerous cells (19-21). Finally, L-asparaginase enhances the growth of resistant tumors and increases their metastatic activity (13,22). Because L-asparaginase sensitivity in tumors cannot be reliably predicted, the major use of this enzyme remains confined to the treatment of ALL, despite estimates that 5 to 10% of all solid tumors may be sensitive to asparagine depletion (20).

There is a remarkable correlation between the requirement for external asparagine and the susceptibility of leukemia cells to L-asparaginase therapy (18). The lymphoma cell lines that respond to treatment require approximately 10^{-5}M asparagine for optimal growth in tissue cultures (23-25), while resistant tumors were shown to synthesize and excrete L-asparagine into the medium (17). Resistant cells, whether naturally resistant or selected for resistance by treatment with L-asparaginase, respond to deprivation of exogenous asparagine by increasing their rate of asparagine synthesis, producing sufficient amino acid for normal protein synthesis (8,17). When a human lymphoma cell line highly sensitive to L-asparaginase was made resistant to either L-asparaginase or asparagine deprivation, the activity of asparagine synthetase increased to 80 or 7 fold of the wild type, respectively (26).

Role of Asparagine Synthetase in L-Asparaginase Resistent Tumors

The molecular basis of L-asparaginase resistance is poorly understood and remains the major clinical problem in treating relapsed patients (27,28). The phenomenon appears to be related to alterations in Asparagine Synthetase (AS) gene expression (21-29), which is controlled at both the transcriptional and translational levels in mammalian cells (30-34), and also appears to be induced by activation of the unfolded protein response and amino acid response pathways (35,36).

A number of investigations into the correlation between L-asparaginase resistance and AS gene amplification/methylation have been reported, but have yielded only indirect support for this hypothesis (37-39). Direct evidence showing that overexpression of AS is sufficient for the induction of L-asparaginase resistance has, however, been acquired in a recent series of elegant *in vitro* studies with MOLT-4 human leukemia cells (29). Thus, it was shown that short term treatment (12 h) of drug sensitive leukemia cells with L-asparaginase caused elevated AS expression, at least as judged by mRNA levels. Having demonstrated this correlation, it was shown that the elevated AS activity could be mimicked by transformation of drug-sensitive MOLT-4 cells using a retrovirus containing the AS gene under a constitutively active promoter. The consequent overexpression of the AS gene in the transformed cells was sufficient to induce the cellular L-asparaginase resistant phenotypes obtained by exposure of untransformed MOLT-4 cells to L-asparaginase. The molecular role of AS in inducing drug resistance remains to be elucidated, however. Thus, it is not yet completely clear whether the resistant phenotype arises as a result of increased levels of asparagine biosynthesis or is caused by participation of AS in signaling pathways that modulate cell growth and/or transformation. Leukemia cells transformed to become L-asparaginase resistant use a set of adaptive mechanisms to reduce the amino acid efflux and to increase the uptake and synthesis of L-glutamine, the nitrogen-providing substrate for the AS catalyzed reaction (40).

The AS gene can be specifically induced by a hormonal factor before cells advance from G_1 to S-phase in the cell cycle (41-43), indicating that expression of this enzyme may be closely related to cell differentiation and, in some cases, to oncogenesis (42,44,45).

Asparagine Synthetase Inhibitors

On the basis of the studies outlined above, potent, specific inhibitors of human AS have significant potential both as agents for treating cancers and as tools for investigating the cellular basis of resistance to L-asparaginase treatment. Despite the effort that has been devoted to obtaining compounds that can inhibit AS, extensive screening studies using hundreds of analogs of aspartic acid, glutamine, and ATP have failed to yield any specific AS inhibitors (46-49).

The several glutamine analogs capable of covalent attachment to the enzyme that have been described possess little selectivity, modifying all cellular glutamine dependent amidotransferases (50). 5-Diazo-4-oxo-L-norvaline (DON), a diazoketo analogue of L-asparagine and alkylator of L-asparaginase, and 5-chloro-4-oxo-L-norvaline (CONV) at a concentration of 1 mM almost completely inhibited the utilization *in vitro* of L-glutamine by AS, but did not affect the utilization of ammonium. Dithiothreitol prevented the inhibition, suggesting that endogenous sulfhydryl compounds are possibly responsible for the ineffectiveness of these substances *in vivo* (51). Ethacrynic acid has been shown to inhibit the AS activity from L-asparaginase resistant leukemia cells through the formation of an adduct with the sulfhydryl functions on the enzyme (52). The asparagine analog that most effectively inhibits AS, β-aspartyl methylamide, was competitive with both glutamine ($K_i = 2\times10^{-4}$ M) and ammonia, but only managed to increase the life span from 31 to 79% when administered to mice bearing various L-asparaginase resistant tumors (53).

Given recent success in the discovery of drugs based upon transition state analogs (54), elucidation of the mechanistic details underlying the AS reaction mechanism may prove an alternate approach to obtaining potent AS inhibitors.

Structure of Glutamine-Dependent AS

Two families of AS have been described that do not exhibit sequence or structural homology (55,56). The first enzyme family, which seems to be present only in prokaryotes, can only use ammonia as a nitrogen source and appears evolutionary related to aminoacyl tRNA synthetases on the basis of sequence comparison (57) and three-dimensional structure (58). The AS encoded by the *asnA* gene of *Escherichia coli* (AS-A) is a representative member of this family (59-61).

Human AS (62) and *Escherichia coli* AS-B (63), however, are members of the second class, the glutamine-dependent asparagine synthetases, which are present in both eukaryotes and prokaryotes. These enzymes catalyze the biosynthesis of L-asparagine from L-aspartate in an ATP-dependent reaction for which L-glutamine is the nitrogen source under physiological conditions (Figure 1.1) (55).

Glutamine-dependent AS has been cloned or isolated from a number of organisms including yeast (64,65), various plants (66-72), bacteria (63,73-76), archaebacteria (77-79), parasites (80,81), and mammals (44,82-89). The detailed kinetic and structural characterization of asparagine synthetases from mammalian sources (44,83-86) has proven difficult, however, because of the low abundance and instability of these enzymes. In this respect, the native AS from bovine pancreas represents the only mammalian enzyme to be purified and characterized in some detail (90-93). Only small amounts of recombinant, wild-type human AS could be obtained using a variety of expression systems, the enzyme being purified to homogeneity using an affinity chromatography protocol (94-97). Access to recombinant human enzyme, albeit in small quantities, in these early experiments did, however, allow some limited studies of its properties including substrate specificity with respect to glutamine (94-97).

A key breakthrough in studying the structure (98) and mechanism (55) of glutamine-dependent AS was therefore the development of procedures for obtaining large amounts of AS-B, which is encoded by the *asnB* gene in *Escherichia coli* (99). The recombinant AS-B is active, the expressed enzyme being processed correctly to give cysteine as the N-terminal residue after post-translational removal of methionine.

Eukaryotic asparagine synthetases and *Escherichia coli* AS-B catalyze the following reactions (87,99):

Reaction (1) $\text{Gln} + \text{H}_2\text{O} \longrightarrow \text{Glu} + \text{NH}_3$
Reaction (2) $\text{NH}_3 + \text{Asp} + \text{ATP} \longrightarrow \text{Asn} + \text{AMP} + \text{PP}_i$
Reaction (3) $\text{Gln} + \text{Asp} + \text{ATP} \longrightarrow \text{Asn} + \text{Glu} + \text{AMP} + \text{PP}_i$

The importance of Cys-1 in mediating the glutamine-dependent activities of AS has been shown using AS mutants in which this residue is replaced by either alanine (C1A) or serine (C1S) (94,95,99). This observation when coupled with the primary structure of the N-terminal GAT domain places AS in the Class II, or Ntn, family of glutamine-dependent amidotransferases (100,101), which also include glutamine 5-phosphoribosyl-α-pyrophosphate (PRPP) amidotransferase (GPATase) (102,103), glutamine fructose-6-phosphate amidotransferase (GFAT) (104,105), and glutamine synthase (106-108).

Access to the bacterial form of the enzyme and to a system that allowed the expression of large amounts of highly pure recombinant protein (99) was essential for obtaining a high-resolution crystal structure of the ternary complex between glutamine, AMP, and the C1A/AS-B mutant (98). The lack of glutamine-dependent activity in the C1A/AS-B mutant, and the observation that glutamine binds to this variant with a K_D of approximately 6 μM, were also essential elements in allowing crystallization of the enzyme in an "active" conformation.

As expected from sequence alignment studies (109) and experimental characterization of bovine AS using monoclonal antibodies (91), the enzyme is composed of two distinct domains. Comparison of the crystal structures of GPATase (110-114), GFAT (115-119), and glutamate synthase (108,120) shows that all Ntn amidotransferases possess a homologous N-terminal catalytic domain, constructed from two layers of six-stranded anti-parallel β-sheet, that mediates the hydrolysis of glutamine to yield glutamate and ammonia (98). This domain is observed in members of an enzyme superfamily (121-123) termed Ntn hydrolases (124-126), which perform a number of biologically important transformations (127-133). In the N-terminal domain of AS, residues that position glutamine within the binding pocket include Arg-49, Asn-74, Glu-76 and Asp-98, consistent with recent studies on site directed AS-B mutants.

Another interesting aspect of the C1A/Gln/AMP structure was the observation that the C-terminal domain, responsible for catalyzing the formation and breakdown of β-aspartyl-AMP (Figure 1-1) to yield asparagine (98), was found to be structurally homologous to guanosine 5′ monophosphate synthetase (GMPS) (134) rather than to rather the ammonia-dependent asparagine synthetases (AS-A) that are found in bacteria (58-61) or to the C-terminal domain of GPATase (110-114). This is consistent with the functional properties of both AS-B and GMPS in that catalysis leads to the formation of PP_i from ATP, placing them in the family of ATP pyrophosphatases (135,136). Thus bioinformatic analysis has suggested that the motif SGGXDS is present in all enzymes that convert ATP to AMP and PP_i in carrying out their particular chemical transformation (135). This conserved "pyrophosphatase loop" motif is not only observed in AS and GMPS (136-139), but also in argininosuccinate synthetase (140-142) and ATP sulfurylase (143-145). The AMP moiety in the C1A/Gln/AMP complex is anchored to the protein via hydrogen bonds with O of Ser-346 and the backbone carbonyl and amide groups of Val-272, Leu-232 and Gly-347. Superimposition of the C-terminal domain structures of AS-B and GMPS did, however, reveal altered nucleotide binding. Thus, although the pyrophosphate binding loop regions (PP-loops) of the two enzymes (Ser-234 to Ser-240 in AS-B and Ser-235 to Ser-241 in GMPS) are virtually identical in sequence, these loops have significantly different structures (98,134). Presumably this reflects the fact that different substituents are bound in this region of the proteins (*i.e.*, uranyl ions in AS-B and PP_i in GMPS), and aspartate is absent from the synthetase active site in AS-B.

The glutaminase and synthetase active sites in the C1A/Gln/AMP structure are separated by about 19 Å and are connected by a molecular channel that can be visualized using the GRASP software package (Figure 1.2) (146). The side chain of Arg-30 appears hydrogen bonded to the carboxamide groups of Asn-74 (N-terminal domain) and

Asn 389 (C-terminal domain), a series of interactions that might represent a vestigial pathway for mediating communication between the two active sites of the enzyme.

Unfortunately for the efforts to use rational approaches in the discovery of potent, selective AS inhibitors, disorder in the C-terminal domain of the C1A/Gln/AMP complex did not permit the observation of two loop regions (Ala-250 to Leu-267 and Cys-422 to Ala-426) and the final forty residues of the enzyme.

Insight into the structure of the AS synthetase site during turnover, and the potential role of residues involved in aspartate activation and ammonia addition has been provided, however, by showing that β-lactam synthetase (BLS) (147,148), a key enzyme in the biosynthesis of the secondary metabolite clavulanic acid, and AS have likely evolved from a common ancestor (147,149). There is a striking similarity in the chemical reactions that lead to asparagine and β-lactam formation in the two enzymes, in that both substrates are activated as their AMP derivatives, and the carbonyl group is attacked by a nitrogen nucleophile (Figure 1-3). The common ancestry of the two enzymes is further highlighted by the degree of similarity observed for the three-dimensional structures of AS (98) and BLS (150) (Figure 1-4). It is therefore reasonable to assume that the catalytic machinery for substrate activation by adenylation is conserved in both enzymes, and this hypothesis is supported by the fact that the contiguous segment comprising residues Ser-234 to Ser-239 in AS-B, which likely mediates the pyrophosphatase activity, is also present in the BLS active site. Alanine scanning mutagenesis of residues Ser-234 to Ser-239 in AS-B support this hypothesis, even though AMP is bound to this loop in the C1A/Gln/AMP crystal structure (98). Furthermore, recent elegant studies have provided a series of crystallographic "snapshots" of BLS at various steps in its catalytic cycle (151)

Catalytic Mechanisms of the Two Active Sites in Glutamine-Dependent AS

Glutamine-dependent asparagine synthesis is accomplished by using ammonia as a common intermediate to couple two "half reactions" that are carried out in independent active sites within the enzyme. Thus, in the C-terminal domain, ATP is used to activate the side chain carboxylate of aspartate by forming β-aspartyl-AMP (βAspAMP) **1** and inorganic pyrophosphate (PP_i) (Figure 1-1), while glutamine is hydrolyzed to glutamate and ammonia in the N-terminal domain. After being channeled from the glutaminase site along an intramolecular tunnel, the reaction of ammonia with βAspAMP takes place in the C-terminal synthetase site to give asparagine and AMP.

The essential role of the N-terminal cysteine residue (Cys-1) in mediating the glutamine dependent activities is consistent with the hypothesis that this domain catalyzes amide bond cleavage using a similar mechanism to thiol proteinases (152), such as cathepsins (153), papain (154) and caspases (155,156). In such a mechanism, the amide of glutamine initially reacts with the nucleophilic thiolate anion of Cys-1, forming a tetrahedral intermediate in which C-N bond cleavage can occur after nitrogen-protonation to give an amine and an acyl thioenzyme intermediate (154). The formation of the tetrahedral oxyanion intermediate implies the existence of an oxyanion hole in the glutaminase active site. In this regard, it is noticeable that all Ntn amidotransferases possess a conserved asparagine residue (Asn-74 in AS-B) that defines an oxyanion hole (157-159), presumably stabilizing the intermediate in a similar manner to the Gln-19 side chain of the cysteine protease papain (160-163). Support for this hypothesis has been provided by mutagenesis experiments showing that catalytic activity can be similarly reengineered in the two enzymes by replacement of Asn-74 or Glu-19

(159-161). There is also evidence for the existence of an acyl-thioenzyme intermediate in the mechanism of AS-catalyzed hydrolysis (164-165). Subsequent hydrolysis of this thioester regenerates the thiolate and yields glutamate. In thiol proteases, protonation of the leaving group nitrogen by histidine is a key step in facilitating subsequent C-N bond cleavage in the catalytic mechanism and these enzymes therefore possess an active site Cys-His dyad (154). In papain, for example, the His 159 side chain is specifically oriented so as to promote breakdown of the initial tetrahedral intermediate, and to stabilize the thiolate of Cys-25 (166). Site specific GPATase mutants initially supported the idea that His 101 in the GAT-domain played a role in catalyzing Gln hydrolysis (167), a conclusion that was supported by chemical modification studies on GFAT using diethylpyrocarbonate (168). The crystal structures of homologous glutaminase domains in Ntn amidotransferases (98,113,119,120), however, provide no evidence for the existence of a Cys-His dyad equivalent to that observed in thiol proteinases (154). Also, identification of an important histidine residue using an extensive series of site-directed AS-B mutants has failed (99). It has been proposed that protonation of the leaving group before C-N bond cleavage and thioester formation is carried out by the N-terminal amino group functioning as a general acid/base catalyst. This hypothesis is also supported by the demonstration that the amino group of the N-terminal proline in 4-oxalocrotonate tautomerase is catalytically active as a general acid/base, having a pKa of 6.4±0.2 as determined by ^{15}N NMR measurements (169). On the other hand, experimental efforts to investigate the catalytic role of the N-terminal amino group in the Ntn amidotransferases using mutants of GPATase (114) and GFAT (116) in which an N-terminal glycine residue has been placed in the sequence in front of the catalytic cysteine, have yielded contradictory results Direct evidence for the participation of the AS N-terminal amino group in catalysis remains to be obtained

In contrast to the N-terminal glutaminase site there is a lack of similarly detailed knowledge concerning the catalytically important residues that mediate the synthesis of βAspAMP 1 (Figure 1-1) and the subsequent reaction of this reactive intermediate with ammonia. The current working model is that the carboxylate of bound aspartate reacts with the α phosphate of ATP to yield a pentacoordinate intermediate 3 that collapses to give **1** and PP_i (Figure 1-5) Experiments with non-natural, conformationally constrained aspartate analogs have suggested that aspartate binds in a conformation such that all of the polar functional groups are located on one face of the molecule (170 171) While the AS-B crystal structure does not provide any definitive information on the residues defining the aspartate binding site alanine-scanning mutagenesis experiments have shown that modifications of the conserved residues Thr-321 Thr-322 and Arg-324 have significant effects on the steady state kinetic parameters of both aspartate and ATP (172) For example R324A and R324K AS-B mutants have no detectable synthetase activity but retain their ability to hydrolyze glutamine with catalytic efficiency (k_{cat}/K_M) similar to that of the wild-type enzyme

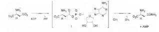

Figure 1-1 Overall transformation catalyzed by glutamine-dependent asparagine synthetase, showing the β-aspartyl-AMP intermediate **1**. Ammonia may replace glutamine as a nitrogen source *in vitro*

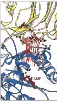

Figure 1-2 Schematic view of the ammonia channel (lines are positioned on interior surface) linking the glutaminase and synthetase active sites in the crystal structure of the Cys-1→Ala mutant of *Escherichia coli* AS-B complexed with glutamine (top) and AMP (bottom).

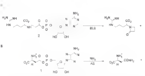

Figure 1-3 Comparison of the chemical mechanisms of BLS and AS A) CEA, the substrate for BLS is activated as its acyl-AMP derivative which then undergoes intramolecular nitrogen attack to give the β-lactam product. B) Aspartate is activated as an analogous AMP derivative that then undergoes intermolecular nitrogen attack to yield asparagine

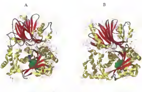

Figure 1-4 Cartoon representations of X-ray crystal structures. A) BLS complexed to its substrate (CPK-colored space-filling model) and AMPCPP (green space-filling model) in the C-terminal domain (150). B) *Escherichia coli* AS-B complexed with glutamine (not shown) and AMP (green space-filling model) (98). The striking structural conservation in both enzymes suggest that they shared a common ancestor, or perhaps that AS was recruited to provide BLS during the evolution of secondary metabolism (clavulanic acid biosynthesis). In both structures, helices and β-strands are shown in yellow and red, respectively, while water molecules are represented as red spheres.

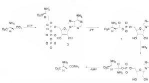

Figure 1.5 Hypothetical mechanism for the AS-catalyzed formation of βAspAMP 1 via the pentacoordinate intermediate 3 and the subsequent reaction of ammonia with 1 to yield asparagine and AMP

CHAPTER 2
EPIDERMAL GROWTH FACTOR RECEPTOR

Growth Factors and Cancer

Multicellular organisms have highly coordinated mechanisms for controlling cellular interactions. These complex signaling and communication systems that normally mediate vital cell functions like growth, differentiation, migration, and wound healing, can be subverted and lead to cancers. Malignant cells arise from a stepwise progression of genetic events that include the unregulated expression of growth factors or components of their signaling pathways. Growth factors act as cell modulators by interacting with their specific membrane receptors and triggering cascades of biochemical signals that result in the activation or repression of various genes. One group of growth factors, that includes neuregulins and epidermal growth factor (EGF)-like proteins, stimulates cells to divide by activating members of the EGF receptor (EGFR) family. While growth-factor-induced EGFR signalling is essential for many normal morphogenic processes and is involved in numerous cellular responses, the aberrant activity of members of this receptor family has been shown to play a key role in the development and growth of tumour cells (173).

The earliest evidence for the involvement of growth factors in cancer came with the observation that neoplastic cells need decreased amounts of serum and growth factors for proliferation in cultures (174-176). Loss of requirement for growth factors is a common occurence in many types of cancer cells (177,178) and could be mediated by the autocrine secretion of growth factors, expression of an altered growth factor receptor that is constitutively active or activation of a postreceptor pathway that bypasses the growth factor receptor requirement

More convincing evidence linking growth factors and cancer emerged when oncogene products were found to be similar to growth factor receptors both having transmembrane and tyrosine kinase domains (179) Growth factors increase transcription of proto-oncogenes like *myc* and *fos* (180 183) which suggests that oncogene products may be involved in the growth factor receptor response pathway and indicates points where alterations may occur leading to the development of neoplastic transformations

Transfection of normal hematopoietic cells with the *erbB* proto-oncogene whose product is the EGFR has produced cells that have a mitogenic response to growth factor treatment (184) This indicates that for this type of cells other than the EGFR and its activating ligands all the necessary signaling components for mitogenic response are present

Activation of Receptor Tyrosine Kinases

As a result of over 20 years of intense research the mechanism by which the growth factor binding to the extracellular domain regulates the receptor's intracellular kinase activity is coming to light Extensive evidence has proved that growth-factor induced receptor oligomerization (185) is responsible for the activation of receptor tyrosine kinase (186) Although it was initially believed that the activated receptor complex involved a single ligand molecule subsequent studies have shown that the stoichiometry of dimerization is 2 2 (187 188) Studies using the receptor s extracellular domain (EGFR-ED) have shown that this fragment retains its ligand binding and dimerization properties (189 190) Growth factor induced receptor dimerization is followed by intermolecular transphosphorylation of key tyrosine residues in the activation loop of the [illegible] protein tyrosine kinase domain (191). Upon tyrosine phosphorylation, the activation loop is rearranging from a close configuration that prevents the access of ATP to an open configuration that enables the access of substrates, thus switching on the kinase activity (192). The activation of the cytoplasmic kinase domain starts a signaling cascade through docking and phosphorylation of a wide range of substrates that are recruited through their SH2 and PTB subunits (193).

Structure and Function of Epidermal Growth Factor Receptor

The epidermal growth factor receptor, or erb B1, was the first receptor tyrosine kinase to be discovered (194) and is prototypical for the erb B tyrosine kinase family of receptors, which is comprised of four homologous members (195-197). The basic organizational motif of these transmembrane protein receptors is identical and includes a single hydrophobic membrane anchor sequence that separates an extracellular ligand-binding domain from a cytoplasmic domain with a tyrosine kinase activity (194,198,199). The mature EGFR has a molecular mass of about 170 kDa and is composed of a single polypeptide chain of 1186 amino acid residues, with a substantial amount of N-linked oligosaccharide (approximately 40 kDa).

Extracellular Domain

The 623-residue EGFR ED is characterized by its capacity to bind EGF and EGF-like ligands with high affinity. This portion of the receptor contains about 10 N-linked oligosaccharide chains (200,201) and is composed of four subdomains L1, CR1, L2, and CR2 (202,203), also referred as domains I to IV (204). Domains II and IV have an unusually high content of cysteine residues that give rise to as many as 25 disulfide bonds (205). The N terminus has a significant homology with the C-terminal region of the extracellular domain, suggesting a symmetrical structure. Affinity labelling experiments have pointed to the region between the two cysteine rich clusters as involved in ligand binding (204) and it was proposed that domains I and III form the binding region, while other parts of the EGFR-ED mediate receptor dimerization (206). Studies with truncated EGFR-ED showed that a domain III fragment, isolated by limited proteolysis, preserves some of the binding capacity for TGFα (207), while a 501-residue EGFR-ED that is missing the cysteine-rich domain IV, binds the human EGF or TGFα with 13- to 14-fold higher affinity (208).

Two recently described crystal structures of TGFα/EGFR-ED and EGF/EGFR-ED complexes revealed the molecular basis for ligand binding and receptor dimerization. The full-length EGFR-ED and the extracellular domain missing subunit IV were expressed in Chinese hamster ovary Lec8 cells, purified, deglycosylated, and crystallized with human EGF (209) and TGFα, respectively (210). The protein phases were determined by the multiwavelength anomalous dispersion method, using selenomethionine-labeled EGFR-ED. Since most of domain IV, which connects the extracellular domain to the transmembrane region in the native EGFR, is disordered in the EGF/EGFR-ED complex, this structure contains the same region as seen in the deletion mutant lacking domain IV that was crystallized with TGFα.

Both structures provide a very similar view of a 2:2 receptor:ligand complex (Figure 2-1). Each ligand molecule is bound exclusively to a single EGFR molecule, and dimerization is mediated entirely by receptor-receptor interactions. EGF and TGFα make similar interactions with large β sheets of the receptor domains I and III. The B loop of EGF interacts with domain I while residues from the A loop and from the C-terminal region of EGF interact with domain III. More than a third of the ligand's accessible surface area is buried between the two domains, and over 60% of the ligand's residues make contact with the receptor. The structure of ligands in the receptor bound complexes is very similar to that of the free ligands (211). The assignment of the EGF and TGFα binding domains in the two structures is consistent with previous mutagenesis and chemical crosslinking results.

Receptor dimerization is mediated by a loop in the cysteine rich domain II, which makes homophilic interactions with a specific region in domain II of the adjoining receptor. This model is supported by sequence conservation at the dimer interface throughout the EGFR family and by mutagenesis experiments showing that point mutations in key residues or deletion of the dimerization loop prevent EGF induced signaling via EGFR (209,210). It is probable that the dimerization loop in the unoccupied receptor adopts a conformation that does not facilitate receptor/receptor interactions. The conformation of this dimerization loop from domain II is coupled to ligand binding in the cleft between domains I and III. The structure is consistent with a receptor mediated dimerization mechanism (189) and suggests that ligand binding to EGFR induces a conformational change that exposes a receptor receptor interaction site on the opposite face of the molecule, resulting in dimerization of two EGFR monomers only when occupied by the ligand. In this "back-to back" dimmer, the two ligands are located on opposite sides of the complex, more than 70 Å apart.

Transmembrane Domain

The transmembrane spanning domain is made of a stretch of 26 hydrophobic amino acids and forms a single α helix that apparently extends for other eight residues inside the cytoplasm (212).

Intracellular Domain

The 542 amino acid cytoplasmic domain consists of a 50-residue juxtamembrane segment involved in ATP binding and feedback activity attenuation, a tyrosine kinase domain, and a 229 amino acid carboxy-terminal tail that includes autophosphorylation motifs, internalization motifs, and sites for proteolytic activation or degradation. Five tyrosine residues near the carboxyl terminus of the EGFR were identified as substrates for EGF-dependent autophosphorylation (213,214). These COOH-terminal tyrosines define an autoinhibitory region that can be relieved by autophosphorylation or truncation (215,216). The tyrosine kinase domain shows remarkable sequence conservation among the growth factor receptors and is similar to a substantial number of oncogene products.

The tyrosine kinase activity has a central role in cellular regulation, as it triggers numerous downstream signaling pathways. The activated EGFR was shown to be able to phosphorylate many substrates, such as erb B2, phospholipid-directed enzymes PI3 kinase, PLD and PLC γ, proto-oncogene cytoplasmic tyrosine kinases src, raf, ras and various other MAP kinases, small GTPases such as rho and rac, multiple signal transducer and activator of transcription isoforms.

The formation of ligand receptor complexes on the cell surface is followed by rapid internalization and degradation of ligand and receptor (217,218). A short segment of the EGFR (residues 973 to 991) has been identified as responsible for mediating the internalization of EGFR complexes (219).

Structure of Epidermal Growth Factor and Transforming Growth Factor α

All known ligands for the receptor tyrosine kinase family contain an EGF like motif. Depending on their receptor specificity, these ligands can be divided into three classes. EGF and TGFα belong to the class of ligands that bind EGFR, together with amphiregulin, heparin-binding EGF-like growth factor and a number of virally encoded factors. These peptides are essential elements of the signaling and communication systems involved in growth, differentiation and wound healing.

First described in 1962 (220), the EGF was shown to have a stimulatory effect on epidermal proliferation (221) in mice, resulting in precocious eyelid opening and accelerated tooth eruption. The abundance of EGF in male mouse submaxillary glands facilitated its purification (220) and the amino acid sequence determination (222) including the location of disulfide bonds (222,223). The human EGF was isolated from urine (224) and its structure was determined (225).

TGFα was detected in 1976 together with TGFβ, as the two components secreted by retrovirally transformed murine fibroblast cells (226). It was isolated and sequenced a few years later (227,228).

Human EGF and TGFα are small proteins of 53 and 50 residues, respectively, that have been expressed and purified in a number of systems. Given the large quantities of recombinant wild type EGF (229-231) and TGFα (232-234) that are available, the high resolution, three-dimensional structures of these growth factors have been characterized in aqueous solution using NMR measurements (235,236). In common with other ligands that bind to the EGFR, the conformation of EGF and TGFα is defined by three disulfide bonds that are formed by six conserved cysteine residues. Based on these disulfide bonds, the protein structure can be divided into three loops, designated as A, B and C. The native fold is essential for activity since disruption of any disulfide bond using site directed mutagenesis results in biologically inactive proteins. The cysteine motif of this mitogen family is also found in a much larger number of cell-associated and extracellular proteins that, while not ligands of EGFR, have important properties in development, cell adhesion and protein-protein interactions. Although the attempts to synthesize biologically active peptides corresponding to various portions of the EGF or TGFα molecules were largely unsuccessful (237), it has been possible to chemically synthesize the entire EGF (238) and TGFα (239) molecules with full biological activity.

Epidermal Growth Factor Receptor Antagonists and Agonists

As an essential step in the signaling and communication mechanisms involved in cell growth and differentiation, the binding of EGF or TGFα to EGFR has been the target of intense research efforts. Activation of EGFR is implicated in wound healing (225,240-241) and cancer development (242), indicating that compounds with agonistic or antagonistic activity would be effective in promoting the rate at which wounds heal or in cancer treatment. A number of different tumor cells exhibit elevated levels of EGFR and a synthetic ligand of these receptors or even a native growth factor coupled to a cytotoxic agent might be useful to specifically target these cancers.

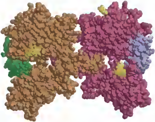

Figure 2-1 Side view of the back-to-back EGFR-TGFα dimer. The EGFR molecules are shown in orange and magenta. The two TGFα molecules are colored green and lilac. Reproduced from (210)

CHAPTER 3
PROTEIN EXPRESSION IN BACULOVIRUS

Baculovirus Expression Systems

The baculovirus, *Autographa californica* nuclear polyhedrosis virus (AcNPV) provides a eukaryotic expression system that is conducive to the proper folding, disulfide bond formation and post-translational modifications required for the biological activity of eukaryotic proteins. Post-translational modifications of the gene products of the insect virus closely parallel the signal peptide cleavage, glycosylation, fatty acid acylation, and phosphorylation in mammalian cells (243).

The baculovirus is capable of infecting a wide range of insect hosts, such as alfalfa leaf hopper, army worm, cabbage looper, salt marsh caterpillar, but it fails to infect mammalian cells, making it a safe vector for laboratory work.

The development of baculovirus expression systems was facilitated by the establishment of insect cell lines and refinement of the growing conditions and media. Most expression vectors are based on AcNPV infection of the fall army worm (*Spodoptera frugiperda*) or the cabbage looper (*Trichoplusia ni*) derived cell lines.

The baculovirus genome contains a number of non-essential genes that can be replaced by an exogenous coding DNA. Many of these genes, particularly the very late ones, are under the control of powerful promoters that allow abundant expression of the passenger recombinant gene.

Most baculovirus expression systems make use of the *polyhedrin* promoter. The *polyhedrin* gene codes for a protein that serves as a matrix, protecting the embedded virus particles from inactivation by environmental factors. When larvae feed on plants contaminated with polyhedral occlusion bodies released by the death of an infected insect, they ingest the polyhedra, which dissolve inside the gut, releasing the virus that invades its new host. Even though the viral occlusions are important in the natural virus life cycle as they provide the means for horizontal transmission, they are not necessary for cell to cell propagation. Deletion of the *polyhedrin* gene does not affect the replication of the virus in cell cultures (244 245) and the gene is deleted naturally when the virus is subjected to serial passages in cell culture at a high multiplicity of infection (246).

The 133 kilo base (kb) baculovirus genome is too large to permit easy manipulations for the insertion of foreign genes. The usual way to construct a recombinant baculovirus is to introduce the desired cDNA into a transfer vector that has a multiple cloning site downstream of the *polyhedrin* promoter. This vector contains a bacterial plasmid and a portion of the baculovirus genome flanking the locus to be replaced with the foreign gene. The use of a small transfer vector enables preliminary manipulations to be performed *in vitro* and subsequently amplified in bacterial cells. The foreign coding sequence is inserted into the baculovirus genome by co transfecting insect cells with viral DNA and the plasmid transfer vector. Recombination between the homologous sequences of the viral DNA and transfer vector effects exchange of genetic information.

The frequency of recombination is low, most of the viral DNA molecules not recombining with a plasmid DNA. Typically, only 0.1 to 0.2% of the progeny viruses are recombinant and therefore a large number of viral clones must be screened to find the recombinant virus. Because only circular viral DNA can function as a substrate for replication, the proportion of recombinants in the progeny viruses from co-transfection can be greatly increased by using linearized baculovirus DNA (247). Today's most widely used viral DNA is based on a recombinant baculovirus with β-galactosidase cloned at the *polyhedrin* locus and *Bsu*36 I restriction sites introduced in the flanking sequences, upstream the promoter and downstream the transcription terminator inside the essential gene 1629 (248). Digestion of this recombinant virus with *Bsu*36 I, an enzyme that does not cleave the wild type viral DNA, yields a linear, defective viral DNA that is missing the C terminus of the essential ORF1629 and cannot propagate. Inside the cells the linear viral DNA can be rescued by recombination with homologous regions in the transfer vector, thereby replacing the viral sequence flanking the cut with modified sequences from the transfer vector. Recombination on both sides of the break, within ORF603 (249) upstream and ORF1629 downstream the *polyhedrin* gene, generates a circular DNA that regains the complete gene 1629 and is competent for replication. In this process, any foreign DNA inserted between the two segments of viral sequence in the transfer vector is transferred to the viral genome. Recombinant plaques can be distinguished visually from plaques of the parental virus. Plaques of the parental virus will produce β-galactosidase and stain blue with X-gal, whereas recombinant viruses, in which the foreign gene from the transfer vector has replaced the *lacZ* gene, will not produce β-galactosidase and will make white plaques. The use of this linearized baculovirus DNA produces nearly 100% recombinant virus.

Viruses obtained by the co-transfection are plated out to give individual plaques, and a few putative recombinant plaques are picked for further analysis. The viruses in these plaques are purified, screened for the presence of the foreign gene, and then a larger stock is made from the confirmed recombinant virus This stock is used to determine the optimal times and conditions for protein expression

To express the target protein the insect cells are infected with the recombinant baculovirus bearing the gene of interest The infected cells undergo a burst of protein expression after which they die and lyse The very late *polyhedrin* promoter becomes active in infected insect cells during the final stages of the infection cycle

Experimental Methods and Materials

Materials

All materials and reagents not specifically listed were of the highest available commercial grade

Enzymes

All restriction endonucleases were purchased from Promega (Madison WI) or New England Biolabs Inc (Beverly MA) and used according to manufacturer s specifications Proteinase K was from Promega *T4* DNA ligase was obtained from Invitrogen Corp (Carlsbad CA) and New England Biolabs Inc Cloned *Pfu* polymerase was from Stratagene (La Jolla CA) *Taq* DNA polymerase was from BD Biosciences Clonetech (Palo Alto, CA)

The QuickPrep Micro mRNA Purification Kit and the First-Strand cDNA Synthesis Kit used to extract the mRNA and make the complementary cDNA were purchased from Amersham Biosciences (Piscataway NJ)

Oligonucleotides

All oligonucleotide primers were synthesized by GenoMechanix LLC (Gainesville FL)

Methods

Ligation and transformation reactions

Ligation and transformation reactions were done according to the published procedures (250) The only deviation from published procedure was done according to the recommended protocol provided by the manufacturer regarding the particular bacterial host strain and commercial source of *T4* DNA Ligase

Bacterial strains and vectors

Escherichia coli K-12 strain Nova Blue obtained from Novagen (Madison WI) was used for routine cloning experiments The GM2929 strain was received from the *Escherichia coli* Genetic Stock Center at Yale University (New Haven CT) The pCR2 1 pMelBac plasmids and the Bac-N-Blue baculovirus DNA were purchased from Invitrogen BacVector3000 baculovirus DNA and the pBAC1 plasmid were from Novagen

Plasmid DNA preparations

Commercially available kits were used for the purification of DNA fragments and plasmids. In all cases, the protocol followed was based on the manufacturers instructions DNA plasmid preparations were obtained with the Wizard Miniprep DNA Purification System from Promega PCR and digestion products were cleaned up with the PCR Purification Kit from QIAGEN (Valencia, CA) DNA fragments were extracted out of low-melting-point agarose gels with QIAquick Gel Extraction Kit from QIAGEN

Viral DNA preparations

Viral DNA used for PCR analysis was prepared by lysing 10 µL of high-titer virus stock with 1 µL Proteinase K (6 mg/mL) and lysis buffer (10 mM Tris 100 µg/mL gelatin 0 45% Triton X 100 0 45% Tween 20 50 mM KCl pH 8.3) in a 100 µL reaction. The mixture was incubated at 60°C for 1 hour and Proteinase K was inactivated by heating at 95°C for 10 min.

Viral DNA used for sequencing the exogenous insert of recombinant baculovirus was prepared from 100 mL of high-titer viral stock. The stock solution was clarified by centrifugation at 10 000×g for 10 min at 4°C and the supernatant was ultracentrifuged at 24 000 rpm in a Beckman SW28 rotor for 2 h at 4°C to pellet the viral particles. The virus was resuspended in 2 mL TE buffer (10 mM Tris, 1 mM EDTA, pH 8.0) and left overnight at 4°C. The virus suspension was layered on top of a sucrose gradient made of 10 mL 60% (w/v) sucrose and 10 mL 20% (w/v) sucrose. Following centrifugation at 24 000 rpm for 1 h at 4°C, the virus particles that banded at the 60%/20% sucrose interface were harvested, diluted 5-fold with TE buffer and repelleted as above. The purified virus was resuspended in 1 mL TE buffer and lysed by adding 10 µL Proteinase K (10 mg/mL), 50 µL 10% SDS and incubating for 30 min at 37°C. Following extraction with 1 volume of TE-buffered phenol, 1:1 mixture of phenol:CIAA, and CIAA, the DNA was precipitated from the aqueous phase with 0.1 volumes of 3 M sodium acetate, pH 5.2, and 2 volumes ethanol. The solution was incubated at room temperature for 5 min and centrifuged at 12 000×g for 5 min to pellet the DNA. The pellet was rinsed with 70% ethanol, air dried briefly and resuspended in 250 µL TE buffer. Wide bore pipette tips were used and vortexing was avoided throughout the procedure to reduce shredding of the viral DNA.

DNA Sequencing

Double stranded DNA sequencing was performed manually by the dideoxy chain termination method (251), with the Sequenase version 2.0 sequencing kit (Amersham

Biosciences), separating the products by electrophoresis on an 8% denaturing polyacrylamide gel (Sequagel-8, National Diagnostics). Preparation of templates for sequencing was performed using alkaline lysis followed by polyethylene glycol precipitation. Sequencing of long DNA segments was performed on Perkin Elmer/Applied Biosystems automated DNA sequencers at the DNA Sequencing Facility of the Interdisciplinary Center for Biotechnology Research (ICBR) at the University of Florida.

Sequence analysis of the expressed human asparagine synthetase

Purified protein was electrophoresed on SDS gel and electroblotted on a PVDF membrane, in 10 mM MES buffer, pH 6.0 containing 20% methanol. The membrane was stained with 0.02% Coomassie Brilliant Blue in 40% methanol/5% acetic acid for 30 sec and destained with 40% methanol/5% acetic acid for 1 min. After rinsing five times with water, the membrane was dried and a small piece with the protein banded at ~60 kDa was excised for N terminal sequencing. The protein sequencing was performed at the Protein Chemistry Core Facility of the Interdisciplinary Center for Biotechnology Research at University of Florida.

Growth and maintenance of insect cells

All materials used for insect cell cultures were supplied by Gibco/Invitrogen Corporation. Serum free adapted *Spodoptera frugiperda* Sf9 cells were maintained in Sf 900 II serum free medium containing 10 μg/mL gentamicin, 50 U/mL penicillin, 50 μg/mL streptomycin, and 0.125 μg/mL amphotericin B. Suspention cultures of up to 75 mL in 250 mL shake flasks or 150 mL in 500 mL shake flasks were grown in orbital shakers at 27°C and 150 rpm. Cultures were routinely passaged every two or three days to keep the cell density between 2×10^6 cells/mL and 6×10^6 cells/mL. Cells were grown in log phase and at more than 90% viability for up to 3 months, after which new cultures were initiated from the frozen stock. Every 4 weeks or before starting expression, the cultures were refreshed by centrifuging at 500 rpm for 5 min and replacing about 75% of the old medium with fresh medium.

To prepare evenly distributed cell monolayers, the required amount of cells was harvested from suspension cultures, diluted with fresh medium, seeded at the proper density (2.5×10^6 cells in 60 mm dishes, or 5×10^6 cells in 100 mm dishes) and allowed to attach for 30 min at room temperature. Once attached, cells can sustain multiple washes without damaging the monolayer. Cells were washed twice with medium without antibiotics or serum before transfection. The cultures were grown at 27°C in a humidified incubator.

Subcloning of human asparagine synthetase cDNA

The human AS encoding cDNA, a gift from Dr. Kilberg, was subcloned in the transfer vector pCR2.1. Human AS cDNA was PCR'ed with high fidelity *Pfu* DNA polymerase over 25 cycles, using a very low amount of template. After 3 min of preheating at 94°C, each of the 25 PCR cycles was composed of denaturation, 45 sec at 94°C, annealing, 45 sec at 52°C, and synthesis, 4 min at 72°C. The 50-μL PCR mixture contained 10 pmol of each primer, various amounts of template, 0.8 mM deoxynucleoside triphosphate, 5 μL 10X reaction buffer (200 mM Tris-HCl, pH 8.8, 100mM KCl, 100 mM $(NH_4)_2SO_4$, 20 mM $MgSO_4$, 1% Triton X-100 and 1mg/mL BSA) and 3.0 U of *Pfu* DNA polymerase.

The forward primer contained a *StuI* restriction site and had the ATG start codon placed in an environment optimal for higher protein-expression levels in baculovirus The reverse primer introduced a c-myc tag followed by an *AvaI* restriction site (Table 3-1) The DNA band corresponding to the amplified fragment was cut out of a 1 2% low melting-point agarose gel and purified with QIAquick Gel Extraction Kit

Single 3' overhanging A's were added to the human AS fragment with *Taq* DNA polymerase in a 20 minute reaction at 70°C The product was purified with QIAquick PCR Purification Kit and ligated in linearized pCR2 1 vector with 3' T overhangs Competent *E coli* Nova Blue cells were transformed and recombinants were selected by blue/white colony screening White colonies were picked and the presence of the cloned human AS fragment was checked by PCR with T7 Promoter and T7 Terminator primers One clone was selected and the whole human AS insert was sequenced

Cloning of human asparagine synthetase in pBAC-1

The pCR2 1/hAS plasmid was simultaneously digested with *AvaI* and *StuI* and the human AS fragment was purified on a 1 2% agarose gel Since *StuI* restriction site in pBAC-1 is sensitive to *dcm* methylation unmethylated pBAC-1 plasmid was prepared from *dcm⁻ dam⁻ E coli* strain GM2929 The unmethylated pBAC-1 was opened by digesting simultaneously with *AvaI* and *StuI* The digestion product was cleaned up on a QIAquick spin column and eluted with 50 µL H_2O The human AS fragment was ligated into the opened pBAC-1 in an overnight reaction with *T4* DNA ligase (Invitrogen) and the product was used to transform *E coli* Nova Blue cells. A dozen colonies were picked and the presence of the cloned human AS fragment was checked by PCR with primers flanking the cloning site Polyhedrin Forward primer and Baculovirus Reverse primer

(Invitrogen) One clone was selected and sequenced to confirm that the human AS was in-frame with the start codon and that no mutations had been introduced

Oligonucleotide-directed *in vitro* mutagenesis

The site directed modifications were performed in the pBAC1/hAS vector using the QuickChange Site-Directed Mutagenesis Kit (Stratagene). Complementing oligonucleotide primers that contain the mutation flanked by correctly annealing sequences were designed and the entire vector was copied over 16 amplification cycles in a polymerase chain reaction catalyzed by 2.5 U of *PfuTurbo* (Stratagene) The methylated unmutated template was digested with *Dpn* I and the product used to transform XL1-Blue *E. coli* competent cells (Stratagene) The transformed cells were plated on LB with 50 μg/mL carbenicillin and incubated overnight at 37°C Next day twenty colonies were picked and amplified in 5 mL cultures Plasmid DNA s were purified and manually sequenced around the mutated fragment One clone with the correct mutation was selected and sent to the DNA Sequencing Facility of the Interdisciplinary Center for Biotechnology Research for complete sequencing of the entire human AS insert

Transfection of insect cells and preparation of human asparagine synthetase recombinant baculovirus

The pBAC1/hAS plasmid DNA used for transfection was prepared from a 200 mL culture of transformed Nova Blue *E. coli* cells grown overnight in Terrific Broth. Plasmid DNA low in endotoxins was purified by CsCl gradient or with Novagen s UltraMobius 1000 Plasmid Kit The transfer plasmid was co-transfected with linearized virus DNA BacVector3000 into insect cells to construct the recombinant virus Working in sterile polystyrene tubes, 100 ng of BacVector3000 DNA was mixed with 900 ng pBAC1/hAS plasmid DNA and antibiotic/serum-free medium to make up a final volume of 25 µL. 5 µL of Eufectin Transfection Reagent (Novagen) liposomes were diluted with 20 µL of nuclease-free water and immediately added over the DNA mixture. After 15 minutes at room temperature, 0.45 mL of medium was added and the mixture was used to transfect Sf9 cells in two experiments. In a direct plaquing procedure, three 5-fold serial dilutions were made and 0.1 mL of each dilution was inoculated onto monolayers of 2.5×10^6 Sf9 cells in 60 mm tissue culture dishes. In a liquid overlay transfection, 0.3 mL of undiluted mixture was added over 2.5×10^6 Sf9 insect cells in a 25 cm^2 flask. The cells were not exposed to antibiotics and serum while reacting with the liposome/DNA mixture. After 1 hour incubation at room temperature, the cells in dishes were overlaid with 6 mL of 1% baculovirus agarose diluted with Sf 900 II medium and 6 mL of medium with antibiotics was added over the cells in the 25 cm^2 flask. Flask and dishes were incubated at 27°C and after 4 to 5 days viral plaques were visible in the agarose overlaid cell monolayer. Plaques were more evident when the monolayer was stained with Neutral Red.

Isolation, amplification and analysis of recombinant virus

Well-isolated plaques were picked by penetrating the agarose with a blunt-end pipette tip and removing the cell monolayer that contains the virus. The agarose plug was transferred into 1 mL of medium and the virus was allowed to diffuse out over 2 hours at room temperature. The virus solution was used to make three 10-fold serial dilutions and was replaqued following a protocol similar to the agarose overlaid transfection. 5×10^6 Sf9 insect cells seeded in 100 mm dishes were infected with 100 µL of undiluted and 1:10, 1:100, 1:1000 dilutions of the eluted virus. Cells and virus were incubated at room temperature for 1 hour and overlaid with 10 mL of 1% baculovirus agarose in Sf-900 II medium. After the agarose has solidified, 5 mL of medium with antibiotics were added to the center of the agarose overlay. The dishes were incubated at 27°C for 4 days or until the plaques became visible. If co-transfection by direct plaquing gave no viral plaques, the medium from liquid transfection was used to isolate the virus in a plaque assay. In this case, at least two rounds of plaque purification were performed.

Small-scale viral stocks were prepared from purified, well isolated plaques by infecting 5 mL cultures of 2.5×10^6 Sf9 cells growing in 25 cm^2 flasks with 0.3 mL of plug-eluted virus. After incubating for 3 to 5 days at 27°C, the medium was harvested and 1 mL was used to purify viral DNA. The presence of the hAS insert was confirmed by PCR analysis of the viral DNA with flanking (Polyhedrin Forward, Baculovirus Reverse) and interior (hASmiddle) primers.

Preparation of high-titer viral stock

One recombinant virus was selected and a high-titer viral stock was made by infecting a 500 mL culture of Sf9 insect cells growing in suspension with 1 mL of small-scale viral stock. The infected culture was incubated at 27°C with constant shaking and the cell viability was monitored by removing small aliquots and counting the cells every 24 hours. After 5 days, more than 90% of cells were dead and the culture was harvested. Cells were separated by centrifugation at 1000×g for 20 minutes, fetal bovine serum was added up to 10%, and the viral stock was stored at 4°C, protected from light. The viral titer was determined in a plaque assay of the stock diluted 10^6, 10^7 and 10^8 fold. Viral DNA was prepared from 100 mL of stock and the whole human AS DNA insert was sequenced.

Time course of human asparagine synthetase expression

A time course experiment was performed to determine the optimal conditions for recombinant human AS expression. Five 100 mL cultures of Sf9 cells growing in suspention at a density of 3×10^5 cells/mL were infected with recombinant virus at different virus to cell ratios (multiplicity of infection or MOI) 10^{-2}, 10^{-1}, 1, 5, and 10. The cultures were monitored by counting the number of cells and collecting 10 mL samples every 12 hours after infection. Harvested cells were separated by centrifugation, medium was discarded, and pellets were stored at -80°C until all samples were collected. All pellets were identically processed by adding 3 mL of lysis buffer (0.1 M EPPS, 10 mM imidazole, 1 mM DTT, 1% Triton X 100, pH 8.0) and incubating on ice for 1 hour. Cellular debris was centrifuged down and the cleared lysates were analyzed by Western blotting and pyrophosphate detection assay. Since the recombinant human AS has two C-terminal tags, two Western blotting experiments were performed, with anti-cmyc and anti HisTag primary antibodies.

Because the pyrophosphate assay was not sensitive enough to detect AS activity in the cell lysate, a purification and concentration step was required. 5 μg of Ni-NTA agarose (QIAGEN) suspended in running buffer (0.1 M EPPS, 10 mM imidazole, 1 mM DTT, pH 8.0) was added over the cell lysate and incubated for 1 hour at room temperature with periodical vortex. The mixture was transferred to a 0.45 μm filtration column (Millipore) and the flow-through was drained by centrifugation at 3000 rpm for 1 min. After washing the column with 2 mL of running buffer, human AS was eluted by resuspending the resin in 50 μL elution buffer (0.1 M EPPS, 0.5 M imidazole, 1 mM

DTT, pH 8.0) and incubating for 10 min. The elute was separated by centrifugation as before.

Western blotting

Sf9 cells harvested during the time course experiment were lysed by sonication in SDS sample buffer, clarified by centrifugation, applied to 12% acrylamide gels (acrylamide/bis weight ratio 29:1) and subjected to electrophoresis at 150 V for 1 hour by the method of Laemmli (252). Following SDS/PAGE, proteins were transferred to 0.45 µm PVDF membranes (Immobilon P, Millipore) by electroblotting at 200 mA for 1 hour. The membranes were incubated for 1 h at room temperature in phosphate-buffered saline (PBS) containing 1% GG-free horse serum (Gibco) to block nonspecific binding and then incubated for 30 min with 1:500 mouse anti His tag 0.2 mg/mL (Santa Cruz Biotechnology) or 1:200 mouse anti c-myc primary antibodies, diluted in blocking buffer. After washing twice with PBS containing 0.5% Tween 20 and once with PBS for 5 min, membranes were incubated for 15 min with 10 mL of alkaline phosphatase-conjugated goat anti mouse IgG (Sigma) diluted 1:5000 in PBS containing 1% horse serum. The blots were finally washed again as above and developed with the BCIP/NBT Substrate Kit (Zymed).

Expression and purification of human asparagine synthetase

A 750-mL culture of Sf9 insect cells growing in suspension at a density of 3×10^6 cells/mL was infected at MOI=5 with 45 mL of recombinant viral stock at 2.5×10^8 pfu/mL (plaque forming units/mL). The infected culture was incubated for 48h at 27°C. Cells were harvested by centrifugation at 1000×g for 10 min and medium was discarded. 50 mL of lysis buffer (100 mM Tris, 10 mM imidazole, 1 mM DTT, 1% Triton X-100, pH 8.0) was added over pellet and allowed to sit on ice for 2h. Cells were resuspended by pipetting up-down and chunks were broken with short sonication bursts. Lysate was centrifuged 30 min at 27 000×g, 4°C and supernatant was filtered through 0.8 µm cellulose acetate membrane. The cleared lysate was loaded on a 2 mL Ni-agarose column preequilibrated with running buffer. The column was washed with 50 mL running buffer (100 mM Tris, 10 mM imidazole, 1 mM DTT, pH 8.0) at a rate of 1 mL/min, and recombinant human AS was eluted with an imidazole gradient made of 25 mL running buffer and 25 mL elution buffer (100 mM Tris, 500 mM imidazole, 1 mM DTT, pH 8.0). 2.5 mL fractions were collected and analyzed on SDS-PAGE. Fractions containing human AS were pooled and proteins were precipitated by slowly adding solid ammonium sulfate to 70% saturation. After sitting on ice overnight, the slurry was centrifuged at 16 000 rpm for 15 min. The supernatant was discarded and the pellet resuspended in 2 mL buffer (100 mM EPPS, 1 mM DTT, pH 8.0). The human AS solution was dialyzed overnight against 3 liters of buffer at 4°C. Glycerol and DTT were added to 20% and 10 mM, respectively. The human AS preparation was aliquoted, snap-frozen and stored at -80°C. Throughout the purification, all steps were performed at 4°C and buffers were ice-cold.

Purification of messenger RNA from A431 human epidermoid carcinoma cells

Messenger RNA encoding the EGFR ED was isolated from A431 human epidermoid carcinoma cells, a cell line that expresses high levels of EGFR. A431 cells at 80% confluency were harvested and about 10^6 cells suspended in isotonic buffer were separated by centrifugation. The cell pellet was resuspended and lysed in 0.4 mL of extraction buffer containing a high concentration of guanidinium thiocyanate, which ensures the rapid inactivation of endogenous RNAses. The extract was diluted three fold with elution buffer (10 mM Tris, 1 mM EDTA, pH 7.5) which reduced the guanidinium thiocyanate concentration to a level low enough to allow efficient binding of the mRNA poly(A) tracts to the oligo(dT) cellulose and high enough to maintain complete inhibition of RNAses. This dilution caused a number of proteins to precipitate and the extract was clarified by a short centrifugation at top speed (14 000 rpm). The supernatant was transferred over 25 mg of oligo(dT)-cellulose, gently mixed, incubated at room temperature for 3 minutes, and centrifuged at top speed for 10 seconds. After being washed five times with high-salt buffer (10 mM Tris, 1 mM EDTA, 0.5 M NaCl, pH 7.5) and low-salt buffer (10 mM Tris, 1 mM EDTA, 0.1 M NaCl, pH 7.5), the oligo(dT)-cellulose pellet was transferred to a microcolumn and bound mRNA was eluted twice with 0.2 mL of elution buffer prewarmed to 65°C. The eluted fractions were mixed and the mRNA was precipitated by adding 10 µL of 10 mg/mL glycogen solution, 40 µL of 2.5 M potassium acetate, and 1 mL of 95% ethanol. The mixture was chilled at -20°C for 30 min and centrifuged at top speed for 5 min. Supernatant was pipetted out, the pellet was dried for 5 min at 37°C and resuspended in 40 µL water. The concentration of total mRNA was determined spectrophotometrically by measuring the absorbance at 260 nm. The mRNA solution was stored on ice and used in the same day for first strand cDNA synthesis.

First-strand cDNA synthesis and amplification

140 ng of mRNA were used as template for the first strand cDNA synthesis catalyzed by Moloney murine leukemia virus reverse transcriptase. After a short denaturation at 65°C for 10 min, the mRNA was added over the first-strand cDNA reaction mix containing a *Not*I d(T)$_{18}$ bifunctional primer or a custom primer

complementary to the EGFR mRNA sequence. The reaction was run for 1 h at 37°C and then the mixture was heated to 95°C for 5 min to denature the RNA-cDNA duplex and inactivate the reverse transcriptase. The first-strand cDNA product was amplified by PCR with *Pfu* or *Tbr* DNA polymerase and EGFR-ED cloning primers (Table 3-2).

Subcloning and restoration of the EGFR-ED wild-type sequence

The DNA band corresponding to the amplified EGFR fragment was cut out of a 1.2% low-melting-point agarose gel and purified with QIAquick Gel Extraction Kit. Single 3' overhanging A's were added to the EGFR-ED fragment with *Taq* DNA polymerase in a 20 minute reaction at 70°C. The product was purified with QIAquick PCR Purification Kit and ligated in linearized pCR2.1 vector with 3' T overhangs. Competent *E. coli* Nova Blue cells were transformed and recombinants were selected by blue/white colony screening. White colonies were picked and the presence of the cloned EGFR-ED fragment was checked by PCR with T7 Promoter and T7 Terminator primers. Five clones were selected and the whole 1863 base-pair insert was sequenced. Sequencing revealed that all clones were identical, having four mutations from the published sequence of human EGFR. Two of these mutations were silent while the other two accounted for A192T and E295G. The non-silent mutations were changed back to the wild-type sequence with Stratagene's QuickChange Site-Directed Mutagenesis Kit, following a protocol described above.

Cloning of EGFR-ED in the pMelBac transfer plasmid

The EGFR-ED cDNA with the correct sequence was cut out of the pCR2.1/EGFR-ED plasmid by simultaneously digesting with *SacI* and *KpnI*, and separated on a 1.2% low-melting-point agarose gel. DNA encoding the EGFR-ED fused to a couple of C-terminal tags was obtained by amplifying the EGFR-ED fragment from pCR® 1 EGFR-ED in a PCR catalyzed by *Pfu* DNA polymerase with a reverse primer designed to introduce a c-myc tag followed by a 6 residue histidine tag (Table 3-2). The PCR product was purified on a QIAquick spin column and digested simultaneously with *SacI* and *KpnI* for 1 h at 37°C. The digested EGFR-ED fragments were cleaned up and ligated into pMelBac B preopened with the same restriction enzymes, in an overnight reaction with *T4* DNA ligase. Competent *E. coli* Nova Blue cells were transformed with 1 µL ligation product and grown overnight on LB with carbenicillin. A dozen colonies were picked and the presence of the cloned EGFR-ED fragment was checked by PCR with primers flanking the cloning site: Polyhedrin Forward primer and Baculovirus Reverse primer. One positive clone from each experiment was selected and sequenced to confirm that the EGFR-ED was in frame with the start codon and that no mutations had been introduced.

Transfection of insect cells and preparation of EGFR-ED recombinant virus

Sf9 insect cells were transfected with pMelBac/EGFR-ED and pMelBac/EGFR-ED cmyc-His tag transfer plasmids together with Bac-N-Blue baculovirus DNA (Invitrogen), following a procedure similar to that for human AS described above. As the virus resulting from recombination of Bac-N-Blue DNA contains the *lacZ* gene, viral plaques where visualized by incorporating X-gal at a final concentration of 150 µg/mL in the agarose-medium mixture used to overlay the transfected cell monolayer. All subsequent steps involving virus purification, analysis, sequencing, and amplification were performed as described above.

Expression and purification of EGFR-ED

Logarithmic phase Sf9 insect cells growing in suspension were harvested and resuspended in fresh Sf 900 II serum free medium to make up a 500 mL culture with a density of 3×10^6 cells/mL. Cells were infected at MOI 5 with 75 mL of recombinant viral stock at 1×10^8 pfu/mL and incubated with shaking for 4 days at 27°C. The culture was harvested, centrifuged for 10 min at 1000×g to pellet the cells and the secreted EGFR-ED was purified from the culture medium. Medium was transferred to fresh tubes and centrifuged at 27 000×g for 30 min to separate the cell debris. Proteins from the cleared medium were precipitated by adding solid ammonium sulfate to 70% saturation at 4°C. A Ni-agarose column was used for the purification of EGFR-ED linked to the 6-histidine C-terminal tag, while an anion exchange column was used to purify the untagged EGFR-ED. For the histidine tagged EGFR, precipitated proteins were separated by centrifugation at 27 000×g for 30 min, resuspended in 25 mL of running buffer (100 mM Tris, 10 mM imidazole, pH 8.0) and filtered through a 0.8 μm cellulose acetate membrane. After loading the protein solution on a 2 mL Ni-agarose column, the resin was washed with 50 mL running buffer at a rate of 1 mL/min, and recombinant EGFR-ED was eluted with an imidazole gradient made of 25 mL running buffer and 25 mL elution buffer (100 mM Tris, 500 mM imidazole, pH 8.0). 2.5-mL fractions were collected and analyzed by SDS/PAGE. The precipitated proteins from expression of the untagged EGFR-ED were resuspended in 100 mL of running buffer (20 mM Tris HCl pH 8.0) and filtered through 0.8 μm membrane followed by 0.2 μm membrane. The cleared solution was loaded on a 10 mL high-performance Q-Sepharose column (Pharmacia), washed with 50 mL buffer, and eluted with NaCl gradient made of 25 mL running buffer and 25 mL elution buffer (20 mM Tris, 300 mM NaCl, pH 8.0). Fractions containing the EGFR-ED were pooled and dialyzed overnight against 3 liters of buffer at 4°C. The EGFR-ED preparation was aliquoted, snap-frozen, and stored at -80°C. Throughout the purification, all steps were performed at 4°C and buffers were ice-cold.

Results and Discussions

Subcloning of Human Asparagine Synthetase cDNA

Subcloning the human AS involved amplification of the cDNA out of a transfer plasmid with high fidelity *Pfu* DNA polymerase, addition of 3' overhanging A's with *Taq* DNA polymerase, and ligation of the purified fragment in preopened pCR2.1 with overhanging T's.

The original plasmid that has the human AS cDNA is also a pCR2.1-type vector and special attention was needed to avoid carrying this plasmid over to the final product. Three parallel PCR's were run with 10-fold serial dilutions of template and the human AS fragment was purified from the reaction with the least amount of template (2 ng) that gave a product visible on agarose gel stained with ethidium bromide.

The PCR primers were designed to introduce two flanking restriction sites that were later used to clone the human AS in the baculovirus transfer vector pBAC1. The forward primer introduced a *StuI* restriction site and provided features for high level protein expression. A review of all recombinant proteins expressed in baculovirus under the control of the *polyhedrin* promoter (253) indicates that expression levels are dependent on the positioning of the start codon. Higher expression is achieved for a shorter distance between the start codon and the *polyhedrin* promoter, and when the start codon context is A_YAUG_Y. The reverse primer introduced a c-myc tag followed by an

XbaI restriction site positioned to keep the histidine tag from pBAC1 in the reading frame

The PCR product of expected size (~2 kb) was purified on agarose gel and single 3' overhanging A's were added with *Taq* DNA polymerase. The human AS cDNA solution obtained after cleaning up the reaction product on QIAquick column had a DNA concentration of 30 ng/µL as determined by optical density at 260 nm.

This human AS fragment was ligated in pCR2.1 in a reaction catalyzed by Quick *T4* DNA ligase (New England Biolabs) at a molar ratio insert/vector of 3/1. Competent Nova Blue cells were transformed by heat shock with 2 µL ligation product and spread on an X-Gal/IPTG LB plate with 50 µg/mL kanamycin. Five white colonies were picked grown in LB with 50 µg/mL kanamycin and the presence of the cloned insert was analyzed by PCR. Plasmid DNA from one positive colony was sent for sequencing of the entire human AS fragment. A standard nucleotide search with BLAST (NCBI) revealed that the cloned sequence was identical to the human AS mRNA.

Cloning of Human Asparagine Synthetase to pBAC-1

The human AS fragment was simultaneously digested with *StuI* and *XbaI* (Promega) out of pCR2.1/hAS and ligated in pBAC1 preopened with the same enzymes. *BamHI* is the first restriction site in pBAC1's multiple cloning region and it allows cloning of the start codon closest to the *polyhedrin* promoter. *BamHI* restriction sites are also present within the human AS cDNA and therefore it could not be used for cloning. The next available restriction site, *StuI*, was instead used and that introduced the ATG start codon 18 bases downstream of the *polyhedrin* promoter (Figure 3-4)

Transfection of Insect Cells and Preparation of Human Asparagine Synthetase Recombinant Virus

Human AS recombinant virus was obtained by co-transfecting insect cells with linearized viral DNA and the *polyhedrin* promoter based transfer vector containing the human AS gene pBAC1/hAS The pBAC1/hAS transfer plasmid has upstream and downstream segments of baculovirus DNA flanking the promoter and the human AS gene Recombination between homologous sequences in the viral DNA and the transfer vector introduces the human AS gene into the baculovirus genome at the *polyhedrin* locus, yielding circular recombinant viral DNA that replicates and forms recombinant virus.

A large number of the over 150 potential genes in AcNPV are unnecessary for growth of the virus in tissue cultures The viral DNA used in transfection BacVector 3000 was generated from a modified virus that lacks the *polyhedrin* gene and seven other non essential genes including a serine protease, v *cath* Digestion of the progenitor BacVector virus to obtain linearized viral DNA resulted in removal of the *polyhedrin* gene and the C terminus of the neighboring ORF1629 Since the ORF1629 is necessary for viral propagation (248) the only way to isolate viable virus is if the ORF1629 sequence is supplied by the transfer vector During transfection, recombination between homologous sequences ORF1629 and ORF603 in the transfer vector and the linearized DNA provides the essential sequence needed for viral replication, resulting in the propagation of only recombinant virus

The co transfection of viral DNA and pBAC1/hAS is mediated by cationic liposomes The positively charged headgroups of liposomes associate with the negatively charged phosphate groups of nucleic acids and form a liposome-DNA complex that is absorbed on the cellular membrane. The liposomes fuse with the membrane and the DNA is taken up by the cells. The purity of the DNA is critical for transfection. The insect cells are sensitive to bacterial endotoxins (lipopolysaccharides from *Escherichia coli*'s outer membrane) that co-purify with the plasmid on anionic resins. The co-transfection was successful only when the plasmid DNA was prepared on CsCl gradient or with the UltraMobius Plasmid Kit (Novagen). Serum proteins can interfere with the formation of liposome-DNA complexes and insect cells were washed twice with serum-free medium before adding the transfection mixture.

Baculovirus plaques were visible on the insect cell monolayer 4 or 5 days after transfection. The number of plaques was consistent with the serial dilutions of the DNA-liposome mixture used for transfection. Plaques were more evident after staining the plates with Neutral Red (Figure 3.2). The pBAC1/hAS transfer vector does not have a reporter gene and recombinant virus was not distinguished from parental virus at this stage.

Virus Analysis, Purification and Amplification

Twelve well-isolated plaques were picked and the virus was purified in a plaque assay. The viral clones were amplified in a 12 well plate seeded with 5×10^5 Sf9 cells per well to make 2 mL low-titer viral stocks. 0.75 mL of each stock was used to purify viral DNA that was analyzed by PCR with primers flanking the human AS cloning site. All PCR's gave a ~2 kb product, identical to the 2070 bp size expected for the human AS insert, suggesting that all viral clones were recombinant.

One clone was selected and a 10 mL viral stock was prepared by infecting 7×10^6 Sf9 insect cells seeded in two 25 cm^2 flasks with 300 μL of the analyzed stock. The infected cultures were harvested after 5 days, the cells were separated by centrifugation for 5 min at 500 rpm and the virus containing medium was transferred to a fresh tube

One mL of this viral solution was used to infect a 500 mL culture of Sf9 insect cells growing in suspention at a density of 2.3×10^5 cells/mL. The infection was monitored by counting the cells every day The culture was harvested 5 days post-infection, when over 90% of cells were dead. The cells were separated by centrifugation and Fetal Bovine Serum was added to 10% making up a viral stock whose titer determined by plaque assay was 2.5×10^8 pfu/mL.

Viral DNA was purified from 100 mL of high titer viral stock and the human AS fragment was completely sequenced to confirm that the insert was intact

Time Course of Human Asparagine Synthetase Expression

The high titer viral stock prepared from plaque purified recombinant virus was used to determine the optimal times and conditions for human AS expression. Insect cell cultures infected with variable amounts of virus were harvested at different times and the level of human AS expression was analyzed by Western blotting and pyrophosphate assay

Cellular lysates were loaded on SDS gels and two Western blots were performed using primary antibodies raised against the c myc and histidine tags fused to the C-terminus of the expressed human AS Both antibodies showed little specificity as they stained other protein bands present in the cell lysate A band that migrates with the recombinant human AS control was becoming visible gradually as the infection times increased Although the Western blot showed evidence that expression of a protein with the expected molecular mass occurred it was not a good experiment to quantify the amount of protein expressed during the time course

An assay that measures the pyrophosphate generated in enzymatic reactions was used to quantify the level of AS expression. No activity was detected in the crude lysates of infected Sf9 cells, probably because the human AS concentration was too low or other cellular proteins interfered with detection of pyrophosphate in the enzyme coupled assay. Cellular lysates from cultures infected with variable amounts of virus and different harvest times were mixed with Ni agarose and bound AS was eluted with 50 µL buffer to obtain relatively pure human AS solutions that showed activity in the pyrophosphate assay. Each assay was done with 10 µL enzyme preparation and the results are shown in Table 3-3. The relative rates of pyrophosphate generation are plotted in Figure 3-3. The time course of human AS expression was performed over a wide range of virus/cell infection ratios (molecularity of infection) 10^{-2}, 10^{-1}, 1, 5 and 10.

The results showed that the human AS expression began 24 h postinfection and gradually increased in the next 24 h. After reaching the maximum around 48 h postinfection, the activity started to decrease, coincidently with cell lysis. The drop in activity after cell death is probably caused by the exposure of the expressed human AS to the oxygen and slightly acidic medium.

Expression and Purification of Human Asparagine Synthetase

Human AS was purified from a 750 mL culture of Sf9 insect cells growing in Sf 900 II serum free medium. Following infection at MOI=5, the culture was monitored by removing small aliquots and counting the cells every 12 h (Table 3-4). As a control, a small aliquot of the cell culture was left uninfected and monitored in parallel with the expression. The culture was harvested 48 h postinfection. The cells were separated by centrifugation and resuspended in 75 mL of buffer containing 1% Triton X-100. The [illegible] centrifugation followed by filtration and loaded on a 2 mL Ni-agarose column. The eluted fractions were analyzed by SDS-PAGE (Figure 3-4). Fractions 7, 8, and 9 were pooled, proteins were precipitated with ammonium sulfate, resuspended in 2 mL of buffer and dialyzed overnight. Total protein concentration, as determined in a Lowry assay, was 9 mg/mL. After adding glycerol and DTT, the human AS solution was divided in 50 μL aliquots, snap-frozen and stored at -80°C. The homogeneity of the protein preparation was checked by running an overloaded SDS-PAGE and a Western blot (Figure 3-5).

N-Terminal Sequence Analysis of the Expressed Human Asparagine Synthetase

Purified protein was electrophoresed on SDS gel and electroblotted on a PVDF membrane, in 10 mM MES buffer, pH 6.0 containing 20% methanol. The membrane was stained with 0.02% Coomassie Brilliant Blue in 40% methanol, 5% acetic acid for 30 sec and destained with 40% methanol, 5% acetic acid for 1 min. After rinsing five times with water, the membrane was dried and a small piece from the protein band at ~60 kDa was excised for N-terminal sequencing. The protein sequencing was performed at the Protein Chemistry Core facility of the Interdisciplinary Center for Biotechnology Research at University of Florida. The results (Figure 3-6) showed that the recombinant human AS had been post-translationally processed in the insect cell expression system, as it lacked the N-terminal methionine. With the exception of cysteines that the sequence analysis method can not identify, all residues were identical to the cognate amino acids of the published human AS sequence.

Cloning, Expression and Purification of Human Asparagine Synthetase Mutants

Five single-residue mutants were expressed in the same baculovirus system as the wild-type AS. Transfer vectors of mutant cDNA's were obtained by site-directed oligonucleotide mutagenesis of the wild type AS with pBAC1/hAS as template for *Pfu* catalyzed PCR s and primers containing the desired mutations. Clones with the correct sequence, selected by DNA sequencing of the entire fragment that encodes the human AS mutants, were further used to transfect insect cells together with BacVector3000 viral DNA and to make recombinant virus. Expression of each mutant was based on a procedure identical to that of wild-type AS and included co-transfection of insect cells, purification, analysis and amplification of recombinant virus. Each mutant was expressed in a 750-mL suspension culture infected at a virus/cell ratio of 5, and was purified based on the C-terminal histidine tag with Ni-agarose columns. The final preparations of the human AS mutants were over 90% pure and the concentrations, as determined in Lowry assays, were: C1A/hAS 3.5 mg/mL, C1S/hAS 2 mg/mL, R339A/hAS 4 mg/mL, R339K/hAS 3 mg/mL and L415F/hAS 4 mg/mL.

Synthesis and Cloning of EGFR-ED cDNA

The DNA sequence encoding EGFR ED was obtained by reverse transcription of the mRNA isolated from A431 human epidermoid carcinoma cells. This cell line was chosen for the high levels of EGFR that it expresses and upregulation of the EGFR gene, which results in accumulation of the corresponding mRNA.

The concentration and purity of mRNA was determined by measuring the UV absorbance at 260 nm of a 100-fold diluted sample and mRNA concentration was calculated with the formula in Equation 3-1.

$$[\text{mRNA}] = A_{260} \times \text{Dilution Factor} \times 40\ \mu\text{g/mL} \qquad (3\text{-}1)$$

The 100-fold diluted sample had $A_{260} = 0.007$, $A_{280} = 0.006$, $A_{260}/A_{280} = 1.17$, and the calculated mRNA concentration was

$$[\mathrm{mRNA}] = 0.007 \times 100 \times 40 = 28\ \mu\mathrm{g/mL} \qquad (3\text{-}2)$$

First strand cDNA synthesis was catalyzed by Moloney murine leukemia virus reverse transcriptase with a universal poly-d(T) primer or a custom primer complementary to the EGFR mRNA sequence. EGFR ED encoding DNA was amplified from the reverse transcription cDNA product in a polymerase chain reaction with specific primers that anneal at the two ends of the desired fragment. The PCR's were catalyzed by high fidelity DNA polymerases *Pfu* or *Tbr* and the products were analyzed by electrophoresis on agarose gel stained with ethidium bromide (Figure 3-7). A DNA fragment with the expected size of about 2 kb was obtained in the reaction with universal poly-d(T) primer and *Tbr*. This product was purified on a 1.2% low melting point agarose gel and single 3' overhanging A's were added with *Taq* DNA polymerase. The DNA fragment was ligated into linearized pCR2.1 vector with 3'-T overhangs and used to transform competent *E. coli* Nova Blue cells. Following blue/white colony screening, twelve white colonies were picked and the size of the cloned fragment was verified by PCR with T7 Promoter and T7 Terminator primers (Figure 3-8).

Five clones harboring the biggest DNA inserts were selected and the cloned fragments were completely sequenced. The sequencing results confirmed that the cloned fragment was indeed the EGFR-ED, but comparison with the receptor's published sequence showed four single point mutations from the wild type EGFR-ED. These mutations were present in all the five selected clones, suggesting that they were not introduced during mRNA reverse transcription and cDNA amplification. Most probably the EGFR-ED that we cloned is the one expressed by the A431 cells and the four mutations are endogenous to this cell line. Two of these mutations are silent and the other two (accounting for A192T and L295G) involve residues largely unconserved throughout the receptor family.

The two non-silent mutations were changed back to the wild type sequence by oligonucleotide directed *in vitro* mutagenesis, a method based on copying the whole DNA plasmid with the exception of an approximately 30 base pair fragment encompassing the mutated nucleotide. Complementary oligonucleotide primers that contain the mutation flanked by correctly annealing sequences were designed and the entire plasmid was copied in a polymerase chain reaction catalyzed by fast, high fidelity *PfuTurbo* DNA polymerase (Stratagene). After selecting a clone with the correct single point mutation, the entire EGFR-ED insert needs to be sequenced, to make sure that unwanted mutations were not introduced elsewhere in the fragment during the PCR.

Cloning the EGFR-ED fragment from pCR2.1/EGFR-ED into pMelBac B was facilitated by the *SacI* and *KpnI* restriction sites that had been introduced with the PCR primers in the cDNA amplification step. The EGFR-ED fragment was simultaneously digested with the two endonucleases and religated in the new host vector, preopened with the same enzymes. Introduction of the C-terminal tags (c-myc and HisTag) was done by amplification of the EGFR-ED fragment from pCR2.1/EGFR-ED with high fidelity *Pfu* DNA polymerase, using a reverse primer that contains the tags' coding sequences inserted between the EGFR-ED C-terminus and a stop codon (Table 3-2). The PCR product was purified on agarose gel, digested with *SacI* and *KpnI* restriction enzymes and ligated in the preopened pMelBac B. Two clones with the tagged and untagged receptor domain were selected and the entire EGFR-ED was sequenced (Figure 3-9).

Human EGFR-ED Recombinant Baculovirus

Since post translational modification of proteins in insect cells closely resembles that in mammalian cells the baculovirus expression system should yield the EGFR-ED in a glycosylated form There is literature precedent for obtaining EGFR ED using baculovirus-based systems in which a leader peptide present in the expressed protein ensures that the processed EGFR ED will be secreted into the medium simplifying isolation and purification protocols (187)

pMelBac is a *polyhedrin* promoter based transfer vector designed to direct expression of recombinant proteins through the insect cell secretory pathway into the extracellular medium The expressed EGFR-ED was cloned at the end of the signal sequence for honeybee melittin (Figure 3-9), a highly expressed and efficiently secreted protein

The homologous sequences flanking the cloning site are the baculovirus ORF 1629 essential for viral propagation and a 1,100 bp *lacZ* fragment that allows recombination of the pMelBac transfer vector only with modified baculovirus DNA containing the *lacZ* gene Insect cells were co-transfected with the pMelBac B/EGFR-ED transfer vector and Bac-N-Blue DNA, a linearized viral DNA that has an incomplete ORF 1629 at one end and the *lacZ* gene at the other end Homologous recombination between these DNA's produced a circular recombinant virus that contains the EGFR ED fragment under the *polyhedrin* promoter and the complete *lacZ* gene under a baculovirus early-to-late promoter Expression of the *lacZ* gene allows identification of the recombinant virus that produces blue plaques in the insect cell monolayer when X gal is added to the agarose-medium overlay (Figure 3 10)

Sf9 insect cells were co-trasnfected with viral DNA and transfer plasmid in a reaction mediated by cationic liposomes. Recombinant blue plaques were selected, purified in two consecutive plaque assays, and amplified to make 5 mL viral stocks. The recombinant virus was analyzed by PCR for the presence on the EGFR-ED insert. One virus clone containing a DNA insert of ~ 2 kb, the expected size for EGFR-ED, was selected and amplified to make 500 mL of high titer viral stock with a titer of 1×10^8 pfu/mL, as determined in a plaque assay. Viral DNA was purified from 100 mL stock and the entire EGFR-ED fragment was sequenced to confirm that the recombinant virus contains the correct, wild type receptor domain.

Expression and Purification of EGFR-ED

EGFR-ED was expressed by infecting serum free medium adapted Sf9 insect cells with recombinant baculovirus at MOI=5. Expression in insect cells that do not require serum supplements facilitates the purification of secreted EGFR-ED out of the medium that does not contain serum proteins.

The lack of an assay to quantify the amount of active EGR-ED did not allow the monitoring of expression levels during the time course experiment. Unlike human AS, the EGFR-ED is an extracellular protein with all cysteine residues involved in disulfide bonds (205), which makes it more stable when exposed to the oxidative factors present in the culture medium. This allowed harvesting the expressed EGFR-ED at very late stages of infection, when over 90% of cells are dead and expression levels are increased.

Both the untagged and the EGFR-ED with consecutive C-terminal tags (c-myc and histidine) were expressed in 500 mL cultures infected at MOI=5. The purification method used was a mild, nonaffinity method, developed with the intention to avoid exposure of the EGFR-ED to the relatively harsh conditions normally used to elute the affinity columns (254). Total proteins were precipitated from the medium harvested 4 days post-infection by adding solid ammonium sulfate to 70% saturation at 4°C. To purify the untagged EGFR-ED, precipitated proteins were dissolved in 100 mL of 20 mM Tris-HCl buffer at pH 8.0, filtered and loaded on a high performance Q-Sepharose column. The expressed receptor domain is retained on the anion exchange column at pH above 7.1, the isoelectric point of the EGFR-ED produced by insect cells. Elution was done with a NaCl gradient from 0 to 300 mM, and most EGFR-ED was recovered in the fractions around 150 mM NaCl. Analysis of eluted fractions by SDS-PAGE showed that the receptor was not purified to homogeneity, as many protein bands with molecular weigh around 60 kDa were visible on the gel stained with Comassie Blue (Figure 3-11). Since none of the eluted proteins was present in higher amounts, it was impossible to identify which band was the EGFR-ED only from the gel picture. One possibility is that the bands separated on the SDS gel are the same protein, EGFR-ED, but with different levels of glycosylation.

Purification of the histidine tagged EGFR-ED by metal chelation chromatography on a Ni-agarose column produced a receptor with over 90% purity, as suggested by SDS-PAGE (Figure 3-12). The total protein concentration of the final EGFR-ED preparation was 0.4 mg/mL, as determined by the method of Lowry.

Table 3.1 Human AS DNA oligonucleotide primers

Oligo name	Sequence
ASpBAC frw	5'-ACGCCTAATATG[illegible]CG[illegible]T[illegible]3'
ASpBACrev	5'[illegible]

Table 3.2 Human EGFR-ED cloning primers

Oligo name	Sequence
Forward	
SacI-EGFR	5'-GCGAGCTCA[illegible]AAA AAAGTTTGC-3'
Reverse	
EGFR-KpnI	5'-GAGGTAC[illegible]AGGACGGGATCTTAGGC[illegible]ATTCG-3'
EGFR-cmyc-6his-KpnI	5'-GAGGTAC[illegible]A[illegible]GTCGTGGTGGTG[illegible]AGATC[illegible]TCTCA ATGAGTTTTTGTTCGG ACCCCATCTTA[illegible]ACCATTCC-3'

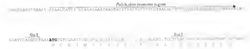

Figure 3.1 The pBAC/hAS cloning sites

Figure 3-2. Viral plaques on the Sf9 cell monolayer

Table 3.3 Time course of human AS expression measured by the rate of pyrophosphate formation.

Harvest time (h)	Molecularity of infection				
	10^{-2}	10^{-1}	1	5	10
12	0.83	0.12	0.61	0.25	0.41
24	0.32	1.84	6.53	9.30	19.45
36	3.01	3.07	15.84	23.12	38.41
48	2.26	6.06	30.31	44.68	60.15
60	1.06	8.14	15.71	20.46	30.43
72	2.60	2.21	7.28	5.81	8.68
84	2.35	3.19	4.85	1.62	6.30

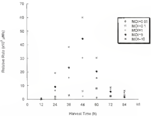

Figure 3.3 Relative rate of pyrophosphate formation of human AS samples collected during the time course

Table 3.4 Cell densities and viabilities during human AS expression

Time postinfection (h)	Alive cells/mL	Dead cells/mL	Viability (% alive)
0	3.0×10^6	1.9×10^5	94%
12	3.9×10^6	2.0×10^5	95%
24	4.4×10^6	4.0×10^5	92%
36	4.5×10^6	8.0×10^6	85%
48	4.2×10^6	1.7×10^6	71%

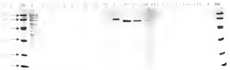

Legend
1–Cell lysate loaded on Ni column (3 µl)
2, 3–Column flow through (3 µl)
E–Elution fractions (10 µl)
4–Column strip (10 µl)

Figure 3-4 Human AS purification on Ni agarose.

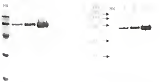

Figure 3.5 Analysis of the human AS preparation by SDS-PAGE and anti-histidine tag Western blot. Increasing amounts of final enzyme preparation were loaded: 1 µL in lane 1, 2 µl in lane 2 and 10 µl in lane 3

Expressed hAS sequence	[illegible] Ala-Leu-Phe-Gly-Ser-Asp-Asp-X-Leu-Ser-Val-Gln
Published hAS sequence	[illegible] Ala-Leu-Phe-Gly-Ser-Asp-Asp-Cys-Leu-Ser-Val-Gln

X – undetermined residue

Figure 3-6 N-terminus sequence analysis of human AS expressed in insect cells

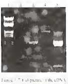

Lane 1 λ marker
2- *Pfu* and poly d(T)$_{18}$
3 *Pfu* and EGFR-KpnI
4- *Thr* and poly d(T)$_{18}$
5 *Thr* and EGFR-KpnI

Figure 3.7 Gel picture of the cDNA amplification product. Each lane was loaded with 10 µl of PCR product catalyzed by *Thr* or *Pfu* DNA polymerase on cDNA templates obtained by mRNA reverse transcription with an universal poly-d(T)$_{18}$ primer or with EGFR-KpnI a specific reverse primer complementary to the EGFR-FD mRNA sequence.

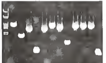

Figure 3.8 Insert [illegible] of potential EGFR-FD cDNA fragments cloned in pCR2.1

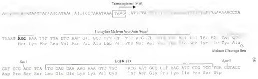
Transcriptional Start
TAAG
Honeybee Melittin Secretion Signal
TAAAT ATG AAA TTC TTA GTC AAC GTT GCC CTT GTT TTT ATG GT
Met Lys Phe Leu Val Asn Val Ala Leu Val Phe Met Val
Melittin Cleavage Site
Sac I
EGFR FD
Kpn I
GAT CCG AGC TCA CTG GAG GAA AAG AAA GTT TGC
Asp Pro Ser Ser Leu Glu Glu Lys Lys Val Cys
ACG AAT GGG CCT AAG ATC CCG TCC TGA GGTACC
Thr Asn Gly Pro Lys Ile Pro Ser Stp

Figure 3 9 Sequence of EGFR FD cloned in pMelBac B

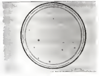

Figure 3-10 Recombinant EGFR-ED viral plaques that stained blue on Sf9 cell monolayer overlaid with medium-agarose containing X-gal

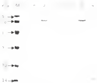

Figure 3-11 Purification of untagged EGFR-ED. SDS/PAGE of fractions eluted from Q-Sepharose column with NaCl gradient.

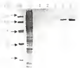

Figure 3-12 Purification of histidine-tagged EGFR-ED SDS/PAGE of fractions eluted from Ni agarose column with imidazole gradient

CHAPTER 4
KINETIC CHARACTERIZATION OF HUMAN ASPARAGINE SYNTHETASE AND ITS MUTANTS

Expression and Characterization of Human Asparagine Synthetase Mutants

Although extensive research data on expression and characterization of *Escherichia coli* AS-B mutants is available (99,157,159,172), very few studies on mutants of the human enzyme have been reported (97). This is most probably because of the difficulties encountered with the expression of human AS. While high quantities of bacterial enzyme can be expressed (up to 40% of the soluble cellular protein) and purified from BL21DE3pLys S *Escherichia coli* transformed with pET expression vectors having the *asnB* gene under the control of the T7 promoter (99), attempts to successfully achieve expression of human AS in bacterial systems have largely failed, as the expression levels were very low and only insignificant amounts of active enzyme were obtained after purification (255). Expression of human AS in yeast has yielded variable amounts of enzyme, depending on the expression system used (95,96).

Sequence alignment together with mutation studies in the glutamine dependent AS family of enzymes provide valuable information on the expected properties of human AS mutants. Mutation of the Arg-325 residue to alanine or lysine in *Escherichia coli* AS-B completely abolishes the synthetase activity (172), suggesting that the corresponding mutations in human AS, at position Arg-339, would have a similar effect. The Cys-1 residue in both human and bacterial AS has been shown to be essential for the glutamine dependent asparagine synthetase activity and glutamine hydrolysis activity (94,97,99), as the nucleophilic thiolate anion of Cys1 makes the first attack on the amide of glutamine. Subsequent hydrolysis of this thioester then regenerates the thiolate and yields glutamate.

A study of a BHK 21 Syrian hamster cell line that was blocked in the G_1 phase of the cell cycle at the non permissive temperature of 39.5°C revealed a single-base mutation that resulted in the substitution of leucine with phenylalanine at a residue located in the C terminal sequence of AS (42). The AS activity in cell extracts sharply decreased during incubation at 39.5°C suggesting that the inability of this cell line to advance to the S phase was due to a mutated thermolabile AS.

The successful use of a baculovirus expression system to produce high levels of human guanosine-5' monophosphate synthetase (138), an enzyme structurally homologous to the AS C terminal domain, suggests that the baculovirus is an effective system for expression of active human AS.

The wild-type human AS and five mutants C1A, C1S, R339A, R339K and L413F were expressed with the pBAC1/BacVector3000 baculovirus system and purified in one step, based on the C terminal histidine tag chelating on a nickel-agarose column. The human AS and its mutants were then characterized for their activity to synthesize asparagine in both the ammonia and glutamine dependent reactions. Expression and purification of all mutants was done using the same procedure, protein concentrations in the final preparations being determined by the method of Lowry.

Pyrophosphate Determination Assay

The initial rate of reaction was determined spectrophotometrically by following the production of pyrophosphate during asparagine synthesis using a coupled assay system based upon literature methods (256). Steady-state kinetic constants (K_M) for human AS substrates were determined by incubating wild type or mutant human AS in a reaction mixture with two substrates present at saturating concentrations and one substrate whose concentration was varied. Reaction mixtures with total volume of 1 mL contained 100 mM EPPS, pH 8.0, 10 mM $MgCl_2$, and 350 µL of reconstituted pyrophosphate reagent (Sigma Chemical Co. Technical Bulletin no. BI-100). The concentrations of the substrates when held constant were 2 mM ATP, 100 mM NH_4Cl, and 10 mM L-aspartate. The glutamine-dependent synthesis of asparagine was assayed using an identical substrate mixture except that ammonium chloride was replaced by 10 mM L-glutamine. The concentrations of the variable substrates were: 0 to 2.0 mM ATP, 0 to 200 mM NH_4Cl, and 0 to 20.0 mM L-aspartate. The mixtures were prewarmed to 37°C, and the reaction was started by the addition of 0.06 nmol of wild-type or mutant human AS. Control experiments contained all of the assay components except the enzyme. All assays were performed in triplicate.

Glutaminase Activity Assay

The rate of glutamine hydrolysis was determined by measuring the amount of L-glutamate produced using glutamate dehydrogenase in the presence of NAD (257). Reaction mixtures with total volumes of 300 µL contained 100 mM EPPS buffer at pH 8.0, 0.2 mM ATP, and 10 mM $MgCl_2$. Freshly made solutions of recrystallized L-glutamine were used to determine the initial rate at various L-glutamine concentrations of up to 50 mM. Reactions were initiated by the addition of 5 µg of wild type human AS or mutants and the mixtures were incubated at 37°C for 15 min. The reactions were stopped by heating 5 min on a boiling water bath. To determine the amount of L-glutamate produced, 200 µL of reaction mixture were transferred over 600 µL coupling reagent containing glycine/hydrazine buffer at pH 9.0 (300 mM glycine, 250 mM hydrazine), 0.5

mM ADP, 1.5 mM NAD, and 2.0 units of glutamate dehydrogenase. The reactions were incubated at room temperature for 1 hour and absorbance at 340 nm was measured, the concentration of glutamate in the samples being determined from a standard curve.

Kinetic Characterization of Human Asparagine Synthetase and its Mutants

Human AS catalyzes the conversion of aspartic acid to asparagine, using either glutamine or ammonia as a source of nitrogen (Figure 1-1).

For each molecule of asparagine formed in the reaction, one molecule of ATP is hydrolyzed to AMP and pyrophosphate (PP_i) [62,82]. The initial rate of reaction can be determined in a continuous spectrophotometric assay, by monitoring the production of PP_i with Sigma's pyrophosphate reagent. The reaction rate is calculated from the decrease in adsorbtion at 340 nm caused by NADH consumption in a series of coupled reactions. Two moles of NADH are oxidized to NAD per mole of PP_i generated during asparagine synthesis.

Rate (μM/s) = Slope (au/s) × 10^3 / (6.22 × 2)

where au = adsorbtion units

6.22 = the millimolar extinction coefficient of NADH at 340 nm

The decrease in adsorbtion at 340 nm was linear with time for at least 30 minutes under the assay conditions. When the concentration of L-aspartate, ATP, ammonium chloride or L-glutamine was separately varied, hyperbolic curves of activity against substrate concentration were obtained. The R339A, R339K, and L413F mutants showed no activity in the pyrophosphate synthesis assay, for both the ammonia- and glutamine-dependent reactions. K_m and k_{cat} values were calculated from V_0 versus [S] plots and double reciprocal plots of $1/V_0$ versus $1/[S]$, where S was the substrate whose concentration was varied and V_0 was the initial reaction rate (Table 4-1) k_{cat} for the ammonia-dependent synthesis activity was estimated at 0 5 s^{-1} assuming the wild-type and mutant human AS preparations were purified to homogeneity ATP was partially inhibiting the reaction at concentrations above 2 mM (Figure 4-11).

The apparent K_m values of human AS for L-glutamine were determined by measuring the initial rate of L glutamate and pyrophosphate formation at varying L-glutamine concentrations (Table 4-2) The glutaminase activity as well as the glutamine-dependent synthetase activity was affected by the presence of anions The rates of these two reactions were dependent on the concentration of chloride and apparent K_m values of human AS for L glutamine hydrolysis were determined at various Cl^- concentrations (Figure 4-12) Assay parameters of length and enzyme concentration were chosen so that L glutamate accumulation did not exceed 5% of the available substrate by the end of the incubation period The initial rate depends on the L-glutamine concentration following a hyperbolic relationship and the apparent K_m values for L glutamine decreased as the concentration of chloride ions increased reaching the lowest K_m of 1 6 mM at chloride concentrations of 50 mM or higher (Table 4-3)

The surprising observation that chloride ions from the ATP/$MgCl_2$ mixture were responsible for the stimulation of glutaminase activity while Mg^{2+} and ATP did not have any effect, encouraged us to explore the influence of other chemical species and anions on this reaction As shown in Table 4-4 only formate nitrate and halide ions had an activating effect, while all the other species tested including the N acylsulfonamide inhibitor 4 did not affect the glutaminase activity The final concentration of the tested chemical species in the assay mixture was 20 mM and all anions were added as Na^+ or K^+

The possibility that the observed stimulation of activity resulted from either sodium or potassium counterions was excluded by running appropriate control experiments.

Glutamine hydrolysis is a partial reaction in the glutamine-dependent asparagine synthesis, suggesting that chloride is also required for the glutamine-dependent synthetase activity. This was demonstrated by determining the amount of pyrophosphate produced by human AS in reactions with recrystallized L-glutamine as the nitrogen source. In the absence of chloride ions, the rate of pyrophosphate formation in the glutamine-dependent synthetase reaction drops to less than 5% of the rate measured in the presence of chloride at concentrations of 50 mM or higher. Unlike the reactions having L-glutamine as a substrate, the ammonia-dependent synthesis of asparagine is not affected by chloride. The effects that various anionic species had on the glutaminase activity and the glutamine dependent synthetase activity were similar (Table 4-4).

The same baculovirus expression system was used to obtain five single point mutants of human AS. The mutations in the hAS coding DNA were made by *in vitro* oligonucleotide directed mutagenesis of the baculovirus transfer vector pBAC1/hAS. After analyzing the hAS mutant clones by completely sequencing the coding DNA fragment, recombinant baculovirus with the correct mutations were produced, purified and amplified following a method identical to the one used for the wild type enzyme. Kinetic characterization of the purified mutants revealed that replacement of Cys-1 by either alanine or serine resulted in loss of glutaminase and glutamine-dependent activity without any significant effect upon ammonia-dependent asparagine synthesis (Table 4-1). The R339A, R339K, and L413F human AS mutants had no detectable synthetase activity but retained their ability to hydrolyze glutamine with catalytic efficiency similar to that of wild-type enzyme.

Discussion

Despite big efforts made in the past to investigate asparagine synthetases from various species, the detailed kinetic and structural studies were greatly limited by the availability of sufficient amounts of pure enzyme. This was especially true for asparagine synthetases from mammalian sources whose characterization has been difficult due to the low abundance and instability of these enzymes.

Prior to our work, only small amounts of recombinant, wild-type human AS could be obtained in a variety of expression systems. *Escherichia coli* systems produced low yields of mostly insoluble human enzyme that still had the N-terminal methionine residue which is normally not found in the native form of the protein (255). Human AS expressed in the eukaryotic host *S. cerevisiae* was soluble, but low yields were a major drawback and presented a problem for enzyme purification (95). Cell extracts of *S. cerevisiae* quickly lost asparagine synthetase activity during enzyme purification, which was tedious and lengthy. The purification protocol was based on affinity chromatography, raising the problem of yeast endogenous asparagine synthetases being copurified with the expressed hAS.

We successfully developed the first efficient protocol for preparing relatively large quantities of recombinant, human AS by using a baculovirus system for protein expression in insect cells. Purification of recombinant enzyme made use of a six residue histidine tag, which allowed that at least 24 mg of homogeneous enzyme be obtained from 1 liter of culture after single step metal chelation chromatography.

The baculovirus expression system presents significant advantages for the production of mammalian proteins: it is not pathogenic. It is easily and reproducibly scaled up, yields very high levels of recombinant proteins that are soluble and post-translationally modified in a similar manner to those expressed in mammalian cells. In a previous study, active glutamine-fructose-6 phosphate amidotransferase (GFAT) of human origin has been successfully expressed in baculovirus, to yield amounts of N terminus nucleophile amidotransferase that could be purified routinely by anion-exchange chromatography (258).

The amount of protein produced by insect cells depends on the efficiency of both transcription and translation, which are influenced by a number of factors. Optimization of the untranslated leader region for size and sequence has been demonstrated to result in a more efficient expression (253). Higher expression in baculovirus systems is achieved for a shorter distance between the start codon and the *polyhedrin* promoter, and when the start codon context is A_YAUG Y.

The recombinant human AS expressed in baculovirus has two C-terminal tags used for protein identification and purification. We anticipated that introducing these additional amino-acids at the C-terminus of hAS would have little effect on the enzyme activity, especially given the wide variation that is observed in this region of the protein when the deduced primary structures for a variety of asparagine synthetases are aligned. Based on the mechanism proposed for the enzyme's glutaminase site, in which the N terminal amine group functions as a general acid/base catalyst and is responsible for the protonation of the ammonium leaving group from glutamine, it was anticipated that the presence of amino-acid residues at the N terminus, in front of Cys 1, will knock-out the glutaminase site. N-terminal amino acid analysis of the purified recombinant hAS expressed in insect cells revealed that cysteine was the first residue (Figure 3-6) indicating that the N terminal methionine was properly processed, unlike the human AS expressed in *E. coli*. The N-terminal sequence analysis was continued for 15 more cycles and the sequence was in exact agreement with the published human AS.

The recombinant baculovirus was analyzed by sequencing the viral DNA to confirm the presence of the correct insert encoding the tagged hAS. The amino acid sequence of the purified recombinant human AS was examined by mass spectrometry of peptide fragments obtained by enzyme trypsinization (Susan Abbanello, unpublished results). Detection of the tryptic peptides of hAS has resulted in positive identification of 43% of the primary sequence (Figure 4-13), twenty five peptides being identified based on their predicted mass. The human AS primary sequence has only one potential N-linked glycosylation site (Asn-Ser-Trp) but the peptide containing it was identified as not having a glycoform. Only one methionine (Met 538) out of the eight methionines present in the identified peptide fragments was identified as being oxidized to methionine sulfoxide, at least to a small extent.

To optimize the production of human AS and determine the best expression conditions, a series of time course experiments were performed, which showed that optimal activity could be obtained by harvesting the cells approximately 48 h after infection. Recombinant human AS expression is under the control of the *polyhedrin* promoter and high levels of protein are expressed during the very late phase of infection. Increase in the amount of expressed human AS with time was evident in Western blotting experiments using anti-c-myc and anti-his tag antibodies, but it did not parallel the profile of asparagine synthetase activity which peaked about 48 h post infection. Most probably exposure of the recombinant enzyme to medium following insect cell death and lysis caused by the infection with virus results in oxidation of cysteine thiols and accounts for the drop in activity at longer expression times The apparent strong susceptibility of the human AS to oxidation was not surprising in view of the instability of this family of enzymes (50 62 259 260) When stored at -87°C in the presence of 1 mM dithiothreitol AS purified from mouse pancreas showed nearly total loss of the ability to utilize L glutamine as amide donor whereas utilization of ammonia continued unaltered (261) When another enzyme from the Ntn class of amidotransferases human GFAT was expressed in insect cells enzyme damage during purification manifested in uncoupling between the glutaminase and aminotransferase activities for preparations that have not been fully protected from oxidation (258)

Multiplicity of infection was also an important experimental variable that was optimized in order to obtain active AS A high multiplicity of infection insures simultaneous infection of the insect cell culture and a peak of the expressed activity

The recombinant, C terminally tagged human AS was assayed for synthetase activity using the standard pyrophosphate assay These experiments showed that the recombinant enzyme could use both ammonia and L glutamine as a nitrogen source for asparagine synthesis In a different set of experiments the enzyme showed the ability to hydrolyze L-glutamine to L-glutamate which was quantified with a glutamate dehydrogenase assay To avoid the possibility that the glutamine was contaminated with ammonia formed during prolonged storage, the L glutamine solutions used in the kinetic experiments were freshly made from recrystallized L glutamine

The presence of the C-terminal tags in the protein was clearly a concern, and a detailed study of the steady state kinetics of the enzyme's activities was performed. The apparent K_m values (Table 4-1 and 4-2) are in good agreement with the values reported for wild type asparagine synthetases from other sources, suggesting that the presence of additional C-terminal residues does not have any significant impact on the ability of the recombinant enzyme to catalyze the glutamine- and ammonia-dependent asparagine formation. The apparent K_m values for L-glutamine in both the glutaminase and glutamine-dependent synthetase activities are the same (Table 4-2), indicating that the two reactions follow an identical catalytic mechanism in regard to the L-glutamine substrate.

A very interesting property of human AS is that the hydrolysis of glutamine and the nitrogen transfer from glutamine to aspartate require chloride or, with somewhat less activity, fluoride, bromide or iodide. The dependence of glutaminase and glutamine-dependent synthetase activities on chloride has been reported for asparagine synthetases of various mammalian origins (62, 88, 262). Formate, nitrate and halide anions can substitute for chloride with lower efficiencies (Table 4-4). Since both the glutamine-employing activities require chloride, while the ammonia-dependent synthetase activity does not, it appears that only the amidotransferase function is anion-mediated. For the glutaminase reaction, chloride concentration does not affect V_{max}, but only the apparent K_m, indicating that chloride affects the binding of glutamine but not the subsequent reaction mechanism steps. This conclusion is reinforced by the independence of the ammonia-dependent synthetase activity on chloride. Chloride has been shown to stimulate the activity of many hydrolytic enzymes (263-265). The mechanism by which [illegible] clear although there is evidence that anions can stimulate enzymatic activity by increasing their stability (264) by shifting the activity versus pH profile (266) and by increasing the affinity for substrate (265) The dependence of the apparent K_m for L glutamine in the glutaminase reaction on chloride concentration suggests that the anion is involved in the initial glutamine binding step In the absence chloride or at very low levels, the rate of glutamine hydrolysis increases continuously without reaching a maximum over the range of L glutamine concentrations that were tested, suggesting an increase in the apparent K_m of L glutamine

The development of this protocol for overexpression of fully soluble and active human AS which is non degraded and properly processed opened up the road to characterization of AS inhibitors with potential clinical utility as anticancer agents A series of N acylsulfonamide analogs of the β aspartyl-AMP intermediate 1 were synthesized by Lukasz Koroniak in our laboratory and examined for their ability to inhibit human AS (Koroniak L 2003 #47) Progress curves generated by incubating the purified enzyme with all necessary substrates in the presence of various concentrations of inhibitor showed that compound 4 inhibited the recombinant human enzyme (Figure 4 14) presumably by binding within the C terminal synthetase site of human AS in a similar fashion to the β-aspartyl-AMP intermediate that is formed in the catalytic mechanism of asparagine production. Further experiments demonstrated that elevated levels of ATP decreased the ability of 4 to inhibit the recombinant human AS suggesting that ATP and 4 compete for the enzyme an observation consistent with the assumption that the inhibitor binds to the C-terminal synthetase site of AS Preparation and characterization of two additional N acylsulphonamide analogs, which are missing either the carboxylate or the amino group, have demonstrated the importance of hydrogen bonding interactions in the recognition of the AS inhibitor with the enzyme. The synthesis and characterization of the N-acylsulfonamide derivative **4** is the first report of a potent human AS inhibitor, and its study provides important information for the rational discovery of compounds that can be employed clinically to treat drug-resistant leukemia.

Having established the steady state behavior of the recombinant wild type hAS, a mutagenesis study was carried out for selected site-specific modifications that exhibited particularly interesting kinetic properties in the bacterial AS. Many previous studies have demonstrated that the glutamine binding domain and the ammonia-dependent synthesis domain of AS, and several other *purF* type amidotransferases, are functionally coupled but topologically separated (267-269). In agreement with previous work on bacterial asparagine synthetase B, replacement of Cys-1 by either alanine or serine completely eliminated the glutaminase and glutamine dependent activities without affecting the ability of the enzyme to synthesize asparagine using ammonia as a nitrogen source. Cys-1 does not appear to possess any essential catalytic function for the ammonia dependent asparagine synthesis. All kinetic constants for the ammonia-dependent synthetase activity of the C1A and C1S mutants were very similar to those of the wild type AS (Table 4-1), indicating very little, if any, structural difference between the mutants and the native hAS. This result is in agreement with the crystallographic structure of the bacterial enzyme, which shows that residue number 1 is in close proximity to the bound L-glutamine and is not part of the asparagine synthetase site. Mutation of the Arg-339 residue to alanine or lysine completely knocked out the enzyme's synthetase activity while leaving the glutaminase activity unchanged. Considering that the crystal structure of bacterial AS-B shows Arg-325 the residue homologous to Arg-339 in the human enzyme not making any contacts with the β-aspartyl-AMP intermediate bound in the synthetase site the role of this asparagine might be to place other active site residues in the right position for catalysis The fact that the Arg 339 mutants retain their glutaminase activity suggests that the folding of the N-terminal domain is unchanged but it does not rule out possible major conformational changes in the C terminal synthetase domain The 15% recovery of catalytic activity in the presence of 50 mM guanidinium chloride showed for the R325K bacterial AS mutant (172) was not observed for the R339K human AS mutant It is possible that if guanidinium helped restore some activity to the human AS mutant the extent of recovery was too small to be detected

Study of a hamster cell line that is blocked in the G1 phase of the cell cycle at the non permissive temperature of 39 5°C identified a single base mutation in the hamster AS gene which was translated in modification of the highly conserved residue leucine-413 to phenylalanine Cytoplasmic extracts of this mutated cell line showed a drop in asparagine synthesis activity during incubation at 39.5°C suggesting that the L413F mutation made the hamster AS thermally unstable The purified human AS L413F mutant that was expressed in insect cells had no synthetase activity over a 25°C to 40°C temperature range but retained the ability to hydrolyze glutamine This result might be another proof of this enzyme s high instability Apparently conservative modifications of residues that are not necessarily in the active site are sufficient to disrupt the asparagine synthetase activity Single point mutagenesis studies of bacterial AS-B identified residues whose mutations resulted in complete loss of synthetase activity (172) but were not part of the β-aspartyl-AMP intermediate binding pocket, as later showed in the crystal structure (98).

Our mutagenesis experiments are the first to identify residues in human AS that have functional roles in the enzyme's activities. The study showed that mutations in both the bacterial and human AS have identical effects, indicating that the mutated residues play the same role in the reaction mechanism. Based on sequence similarity and our mutagenesis study, it is expected that the structure of human AS be analogous to that of the bacterial enzyme.

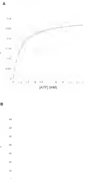

Figure 4-1 Determination of human AS K$_m$ for ATP. Each initial velocity was determined in three parallel experiments. A) Plot of initial velocities against ATP concentrations (0.1, 0.2, 0.3, 0.4, 0.6, 0.8, 1.2, 1.6 and 2.0 mM) at saturating concentrations of other substrates. B) Double reciprocal plot of data from A.

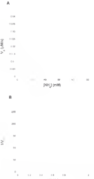

Figure 4 2 Determination of human AS K_m for NH_4 Each initial velocity was determined in three parallel experiments A) Plot of initial velocities against NH4 concentrations (1 2 5 10 20 40 and 80 mM) at saturating concentrations of other substrates B) Double reciprocal plot of data from A

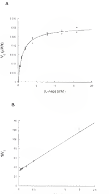

Figure 4-3 Determination of human AS K_m for L-Aspartate. Each initial velocity was determined in three parallel experiments. A) Plot of initial velocities against Asp concentrations (0.5, 1, 2, 4, 8, 12, and 16 mM) in saturating concentrations of other substrates. B) Double reciprocal plot of data from A.

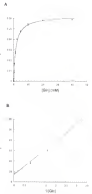

Figure 4-4 Determination of human AS K_m for L-Glutamine. Each initial velocity was determined in three parallel experiments. A) Plot of initial velocities against Gln concentrations (0.31, 0.62, 1.25, 2.5, 5, 10, 20 and 40 mM) at saturating concentrations of chloride and other substrates. B) Double-reciprocal plot of data from A.

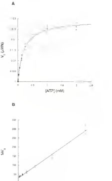

Figure 4-5 Determination of C1A/hAS K_m for ATP. Each initial velocity was determined in three parallel experiments. A) Plot of initial velocities against ATP concentrations (0.03, 0.06, 0.12, 0.25, 0.50, 1.0, and 2.0 mM) at saturating concentrations of other substrates. B) Double-reciprocal plot of data from A.

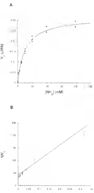

Figure 4-6. Determination of C1A/hAS K_m for NH_4. Each initial velocity was determined in three parallel experiments. A) Plot of initial velocities against NH4 concentrations (3.1, 6.2, 12.5, 25, 50, 100, and 200 mM) at saturating concentrations of other substrates. B) Double reciprocal plot of data from A.

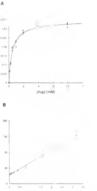

Figure 4-7 Determination of C1A/hAS K_m for L Aspartate Each initial velocity was determined in three parallel experiments. A) Plot of initial velocities against Asp concentrations (0.3, 0.6, 1.2, 2.5, 5.0, 10 and 20 mM) at saturating concentrations of other substrates. B) Double reciprocal plot of data from A

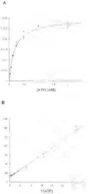

Figure 4-8 Determination of C1S/hAS K_m for ATP. Each initial velocity was determined in three parallel experiments. A) Plot of initial velocities against ATP concentrations (0.03, 0.06, 0.12, 0.25, 0.50, 1.0, and 2.0 mM) at saturating concentrations of other substrates. B) Double reciprocal plot of data from A.

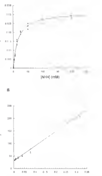

Figure 4 9 Determination of C1S/hAS K_m for NH_4. Each initial velocity was determined in three parallel experiments. A) Plot of initial velocities against NH4 concentrations (3 1, 6 2, 12.5, 25, 50, 100 and 200 mM) at saturating concentrations of other substrates. B) Double reciprocal plot of data from A.

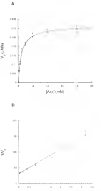

Figure 4-10 Determination of C1S/hAS k_m for L Aspartate. Each initial velocity was determined in three parallel experiments. A) Plot of initial velocities against Asp concentrations (0.3, 0.6, 1.2, 2.5, 5.0, 10 and 20 mM) at saturating concentrations of other substrates. B) Double-reciprocal plot of data from A.

Figure 4-11 Human AS inhibition by ATP at concentrations above 2 mM

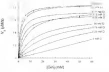

Figure 4-12. Effect of chloride on glutaminase activity. The concentrations of chloride (as NaCl) and L-glutamine in the standard glutaminase reaction mixture were varied as shown. The glutamate formed in 15 minutes was determined.

CGIWALFGSDDCLSVQCLSAMK IAHR GPDAFR FENVNGYTNCCFGFHR
LAVVDPLFGMQPIR VK K YPYLWLCYNGEIYNHK K MQQHFEFEYQTK
VDGEIILHLYDK GGIEQTICMLDGVFAFVLLDTANK K VFLGR
DTYGVRPLFK AMTEDGFLAVCSEAK GLVTLK HSATPFLK
VEPFLPGHYEVLDLK PNGK VASVEMVK YHHCK DVPLHALYDNVEK
LFPGFEIETVK NNLR ILFNNAVK K R LMTDR R
IGCLLSGGLDSSLVAATLLK QLK EAQVQYPLQTFAIGMEDSPDLLAAR
K VADHIGSEHYEVLFNSEEGIQALDEVIFSLETYDITTVR
ASVGMYLISK YIRK NTDSVVIFSGEGSDELTQGYIYFHK APSPEK
AEEESER LLR ELYLFD VLR ADR TTAAHGLELR
VPFLDHRFSSYYLSLPPEMR IPK NGIEK HLLRET FEDSNLIPK
EILWRPK EAFSDGITSVK NSWFK ILQEYVEHQVDDAMMANAAQK
FPFNTPK TK EGYYYR QVFER HYPGR ADWLSHYWMPK
WINATDPSAR TLTHYK SAVK AEQK LISEEDLLEHHHHHH

Figure 4-13 Amino-acid sequence of the expressed human AS and the expected fragments produced by trypsin digestion. The peptides highlighted in blue were identified by mass spectrometry. The only potential glycosylation site is highlighted in red and was found to have no glycosides attached. Methionine-538 is the only residue identified as being oxidized in a very small extent

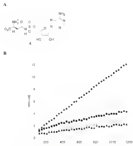

Figure 4.14 A) Structure of the N-acylsulfonamide inhibitor **4**. B) Progress curves showing the effect of N-acylsulfonamide **4** on pyrophosphate production in the ammonia-dependent synthetase reaction catalyzed by recombinant human AS. Key: [4] = 0 µM – filled circles; [4] = 5 µM – open circles; [4] = 10 µM – filled squares; [4] = 25 µM – open squares; [4] = 50 µM – filled triangles. Solid lines represent the theoretical curves computed from a slow-onset inhibition model that best fit the experimental data, and error bars correspond to the standard deviation of the [PP$_i$] concentration measured at a given time point.

Table 4.1 Kinetic constants for the ammonia dependent activity of wild type hAS, C1A and C1S

	Ammonia			Aspartic acid			ATP		
	K_m mM	k_{cat} s^{-1}	k_{cat}/K_m $M^{-1}s^{-1}$	K_m mM	k_{cat} s^{-1}	k_{cat}/K_m $M^{-1}s^{-1}$	K_m mM	k_{cat} s^{-1}	k_{cat}/K_m $M^{-1}s^{-1}$
wt hAS	12	0.65	54	1.2	0.50	417	0.2	0.54	2700
C1A	24	0.53	22	1.2	0.57	475	0.2	0.49	2450
C1S	16	0.51	32	1.1	0.52	473	0.19	0.62	3260

Table 4-2 Kinetic constants of wild type hAS for L glutamine in the glutaminase and glutamine-dependent synthetase activities at saturating amounts of chloride

	K_m (mM)	k_{cat} (s^{-1})	k_{cat}/K_m ($M^{-1}s^{-1}$)
Glutaminase activity	1.65	3.4	2060
Glutamine dependent synthetase activity	1.58	1.04	658

Table 4-3 Kinetic constants of human AS for L glutamine in the glutaminase reaction at various chloride concentrations.

Cl^- mM	L Glu K_m mM	k_{cat} s^{-1}	V_{max} µM/s	V_{max}/K_m ×1000/s
0	-		—	
0.39	68.6	3.5	0.87	0.012
0.78	25.8	2.7	0.68	0.026
1.56	14.8	2.6	0.66	0.045
3.12	8.21	3.1	0.78	0.095
6.25	4.37	2.8	0.70	0.136
12.5	2.76	3.0	0.75	0.272
25	2.26	3.4	0.85	0.376
50	1.65	3.4	0.85	0.515

Table 4-4 Effect of anions and other chemical species on the glutaminase and glutamine-dependent synthetase activities.

Species added	Relative activities %	
	Glutaminase	Glutamine-dependent synthetase
None	–	–
Chloride	100	100
Bromide	93	100
Iodide	77	65
Fluoride	100	Not determined[1]
Carbonate	–	–
Phosphate		Not determined[1]
Pyrophosphate		Not determined[2]
Sulfate		Not determined[2]
Nitrate	90	55
Formate	88	65
Acetate	–	–
Phtalate	–	–
Oxalate	–	–
Tartrate	–	–
$MgSO_4$	–	–
ATP		Not determined[2]
ATP + $MgSO_4$		Not determined[2]
AMP	–	–
AMP + $MgSO_4$	–	–
AMP + PP_i + $MgSO_4$	–	Not determined[2]
L-Asp	–	–
L-Asn	–	–
Inhibitor **4**	–	–
Inhibitor **4** + $MgSO_4$	–	

[1] Cloudiness formed when the quenched reaction mixture was added over the pyrophosphate determination reagent did not allow reading of the change in absorbance at 340 nm.

[2] These species are already present in the synthetase assay mixture.

CHAPTER 5
IDENTIFICATION OF EPIDERMAL GROWTH FACTOR RECEPTOR BINDING PEPTIDES BY PHAGE DISPLAY

Phage Display

The rapid discovery of lead structures with well-defined biological activity in the absence of detailed structural information has been the focus of much research efforts over the past ten years (270,271). As a result, there are now a number of methods for the preparation of large combinatorial libraries of peptides (272) and small molecules (273) and their use in high throughput screening assays has resulted in the identification of compounds with high affinity for cellular receptors, antibodies, or enzymes (274,275). The use of complex mixtures of compounds, as are produced during the synthesis of a combinatorial library (276), in screening experiments has the advantage that many structures can be assayed simultaneously for their ability to interact with the specific biological target. If activity is observed, then the problem becomes one of identifying the compound of interest from the large number of other structures in the combinatorial library. This setback has been solved in a variety of ways (277), one approach being the construction and screening of large peptide libraries displayed on bacteriophage.

Phages are viruses that infect bacteria and have the property that individual bacteria only harbor and replicate one form of the phage. Phage display describes a selection technique in which peptides or proteins are expressed as fusions with coat proteins of bacteriophage, resulting in display of the fused proteins on the exterior surface of the phage virion, while the DNA encoding the fusion resides within the virion (278). Phage display creates a physical linkage between the displayed protein and the viral DNA, allowing rapid identification of the primary structure of selected proteins using DNA amplification and sequencing. Phage-based methods are relatively simple, and are therefore an elegant strategy for identifying both linear and conformationally constrained peptides (279,280), that possess high-affinity for specific biological targets.

Synthetic oligonucleotides, fixed in length but with unspecified codons, are cloned as fusions to gene 3 of M13 bacteriophage where they are expressed as a plurality of peptide-capsid fusion proteins. *Escherichia coli* cells are transformed with the modified phage DNA and a library of phage is created in which the N-terminus of the gene 3 protein (g3p) in the coat of each phage particle is modified so that it has an additional peptide sequence separated by a flexible linker. In this library, a single phage expresses only a single variant peptide sequence.

The random peptide libraries are tested for binding to the target molecules of interest, using a form of affinity selection known as "biopanning" (281). Affinity selection resembles in essence the traditional approach to drug discovery: screening libraries of synthetic compounds or natural products for substances that bind the target receptor and that might therefore be leads to new agonists, antagonists, or modulators. Affinity selection has the key advantage that many structures can be assayed simultaneously and the scale of the search is many orders of magnitude greater than is feasible when chemical libraries must be screened compound by compound.

The library is first incubated with the target molecule followed by the capture and elution of the bound phage. The phage recovered in this manner are then amplified and again selected for binding to the target, thus enriching for those phage that bind. The phage particles are then isolated in individual clones and the phage DNA encoding the modified gIII fusion protein is analyzed to deduce the primary sequence of the peptide that was selected. Pure peptides with the sequences revealed from the phage display procedure can then be synthesized and fully characterized for the desired biological activity

Peptides can be displayed as gene 3 fusions either by cloning directly within the phage genome or by cloning into gene 3 present within a phagemid The "phagemid display" system requires rescue with a helper phage (282) Since the phage particles derived in this way will display g3p from both the wild-type gene 3 of helper phage and the fusion gene 3 from the resident plasmid the method is termed monovalent display This is in contrast to display of g3p fusions encoded within the phage genome itself where all g3p molecules are present as fusions in the technique known as multivalent display (235) It has been shown that display of fusions in a system with only one gene 3, as occurs with phage-display vectors, will give poorer discrimination between binding affinities than phagemid systems using one fused and one wild-type gene 3 (280) Phage-display vectors produce multivalent phage which prevents separation of high affinity peptides from low affinity peptides due to the apparent increased binding capacity of low-affinity clones binding cooperatively In a published study, variants of growth hormone were not readily discriminated according to receptor binding affinities in a polyvalent system However they were discriminated in the monovalent system, allowing for consistent selection of higher affinity variants in randomized libraries of the protein (283)

The quality of the target against which phage are selected is important in several aspects. The target should be relatively pure or consideration must be given to differentiate between clones that bind the target from those that interact with contaminants in the binding reaction. The target must also retain activity during affinity purification of binding phage.

Affinity selection of binding phage from phage displayed random peptide libraries has been performed using two fundamentally different approaches. One approach entails incubating phage libraries with pre-immobilized target such that binding phage are temporarily immobilized onto solid phase while nonbinding phage are washed away. The alternative approach entails incubating library phage with target in solution and subsequently capturing binding phage-target complexes onto solid phase and washing away nonbinding phage. Because phage displayed random peptide libraries express multiple peptides per phage, affinity purification with immobilized target may afford multivalent attachment. Alternatively, solution binding with monovalent target avoids multivalent attachment, thereby enhancing discrimination of high affinity binding clones during affinity purification. In the solution phase binding approach, the effective concentration of the target may be more closely controlled and outcome may be more predictable by the laws of mass action (284).

Elution of phage from the target-phage complex is an important aspect of screening phage displayed random peptide libraries. Generally, bound phage are eluted with drastic pH changes (i.e. glycine-HCl, pH 2; ethanolamine, pH 12), which result in target or peptide denaturation without loss of phage infectivity. Phage may also be recovered by competitive elution from receptors with natural or synthetic ligands (285).

One round of affinity purification with an immobilized target typically results in a ~10^3 fold enrichment of binding over non binding phage (286). Thus, three rounds of affinity purification are generally sufficient for the isolation of binding phage from libraries with complexities smaller than 10^8. However, rates of enrichment will vary from target to target and this must be taken into account when deciding on the number of rounds of affinity purification to perform. Usually, three to four rounds of selection are performed leading to the isolation of one to thousands of binding phage.

After each panning round, the selected phage are propagated by infecting *Escherichia coli* cells. The number of phage particles representing any given binding clone that are recovered from the first round of panning is reduced to the point that binding clones may be lost if subjected to a second round of selection without intervening amplification. Amplification normally results in a 10^4 to 10^7 fold increase in the titer of any given clone from the previous round of affinity purification. This amplified titer is generally sufficient to allow two subsequent rounds of affinity purification without intervening amplification. Phage amplification may be performed in culture dishes or in liquid culture. Liquid culture can accommodate a higher amount of input phage (10^6 pfu/mL culture) than amplification on plates (10^4 pfu/100 mm plate). Amplification on plates, however, has the advantage of minimizing effects of growth or infectivity biases on the representation of different phage clones (287).

Once recombinants have been characterized from phage display libraries, it is often useful to construct and screen a second generation library that displays variants of the selected or consensus sequences. Selective enrichment of stronger binding phage can be accomplished by screening with lower target concentrations. It is possible to include a low concentration of binding competitor in the wash buffer to select for phage that have the slowest off-rate.

Panning of the Phage Display Library against EGFR-ED

Materials and Methods

Iodination of human TGFα

Radioactive labeling of hTGFα was accomplished using the chloramine-T method with the iodination reagent immobilized on a polystyrene support known as Iodo Bead (Pierce Biotechnology, Rockford, IL) (288). 200 µL reaction buffer (10 mM NaH_2PO_4, 0.5 M NaCl, pH 7.4), 10 µL ^{125}I-NaI solution containing 1 milliCurie of ^{125}I (Amersham Biosciences) and one Iodo Bead were placed in a siliconized vial and incubated at room temperature for 5 min with stirring. 5 µg of human TGFα dissolved in 20 µL buffer were added and allowed to stir for 10 min at room temperature. The reaction mixture was applied to a G-50 Sephadex (Pharmacia) column preequilibrated with 10 mL reaction buffer containing 0.1% bovine serum albumine (BSA), 0.05% Tween-20 and washed with 25 mL reaction buffer. Elution was done with the same reaction buffer and 40 drop fractions were collected. 2 µL from each fraction were counted in a γ-counter and the fractions containing the peak activity were pooled.

Binding of ^{125}I-TGFα to EGFR-ED

5 µL of ^{125}I labeled TGFα were mixed with increasing concentrations of unlabeled TGFα and 20 ng of biotinylated EGFR-ED in 0.1 M Tris HCl, pH 7.6 buffer to make a total volume of 500 µL. The solutions were incubated at room temperature for 30 min and ligand-receptor complexes were precipitated by adding 300 µL of 2 mg/mL γ-globulin and 200 µL of 50% polyethylene glycol (PEG). After incubating on ice for 30

min, the solutions were centrifuged at top speed and 4°C for 15 min. The supernatant was removed by aspiration and pellets were counted with a γ scintillation counter.

Solution panning of phage library against EGFR-ED

The phage display library Ph.D.-12 (New England Biolabs) was panned against the biotinylated, histidine tagged EGFR-ED in three rounds of selection and amplification. 10 μL of phage library containing 4×10^{10} plaque forming units (pfu) were mixed with 4 μg of EGFR-ED diluted in Tris-buffered saline (50 mM Tris-HCl, 150 mM NaCl, pH 7.5) with 0.1% (v/v) Tween 20 (TBST) to a total volume of 200 μL and incubated at room temperature for 1 h.

25 μg Ni-NTA agarose (QIAGEN) or 10 μL immobilized avidin gel preequilibrated with 5 mg/mL BSA, 0.1 M $NaHCO_3$, pH 8.6 buffer to block non-specific binding, were washed 4 times with TBST buffer and added over the phage-receptor solution. After incubating at room temperature for 30 min, the gel was washed 10 times with 500 μL TBST buffer. The captured phage-receptor complexes were eluted with 500 μL elution buffer (0.2 M glycine-HCl, 1 mg/mL BSA, pH 2.2) by incubating 10 min at room temperature. The eluted phage solution was neutralized with 75 μL of 1M Tris-HCl buffer, pH 9.1, and 10 μL were used to determine the phage titer in a plaque assay.

The eluted phage was amplified by adding it over 20 mL of mid-log phase *Escherichia coli* Nova Blue cells and incubating at 37°C with vigorous shaking for 4.5 h. The cells were separated by centrifugation for 10 min at 10,000 rpm and 4° in a Sorvall SS-34 rotor. The supernatant was transferred to a fresh tube and re-spun. The upper 80% of the supernatant was transferred to a fresh tube and the phage was precipitated by incubation at 4°C for 2 h after adding 1/6 volume of 20% PEG, 2.5 M NaCl. The PEG precipitation was centrifuged 15 min at 10 000 rpm and 4°C, the supernatant was decanted, and the phage pellet was resuspended in 1 mL Tris-buffered saline (TBS). The titer of the amplified phage was determined in a plaque assay.

The following panning rounds were performed with alternating capturing agent, in identical conditions, except for the buffer used in the binding and washing steps, which was substituted with TBS containing 0.5% (v/v) Tween-20.

Phage titering was done by infecting 200 µL of mid-log phase *Escherichia coli* Nova Blue cultures with 10 µL of serially diluted phage solutions. The dilution range of the amplified phage was 10^8 to 10^{11}, while the eluted, unamplified phage was diluted 10 to 10^4 fold. After incubating the cell and phage mixtures for 5 min at room temperature the infected cells were transferred over 3 mL of melted agarose top (10 g/l bacto-tryptone, 5 g/l yeast extract, 5 g/l NaCl, 1 g/l $MgCl_2 \cdot 6H_2O$, 7 g/l agarose) prewarmed to 45°C and immediately poured onto LB plates. Plates were allowed to cool 5 min at room temperature, inverted and incubated overnight at 37°C. Next day, the plates were inspected and plaques on plates having less than 100 plaques were counted.

After the last panning round, individual phage plaques were amplified and the phage DNA was purified. Well-isolated plaques were picked from titration plates and transferred to tubes containing 1 mL of an *Escherichia coli* overnight culture diluted 1:100 with fresh LB medium. Tubes were incubated at 37°C with shaking for 5 h and cells were separated by centrifugation for 2 min at top speed. 0.5 mL of phage-containing supernatant were transferred to fresh tubes, 200 µL of 20% PEG/2.5 M NaCl was added, mixed and allowed to stand at room temperature for 10 min. The precipitated phage was centrifuged 10 min at top speed, supernatant was removed and pellet was resuspended in

100 µL iodide buffer (10 mM Tris-HCl, 1 mM EDTA, 4 M NaI, pH 8.0). 250 µL ethanol was added and the mixture was incubated for 10 min at room temperature. The precipitated single-stranded phage DNA was separated by centrifugation, washed with 70% ethanol, briefly dried under vacuum and suspended in 30 µl TE buffer (10 mM Tris-HCl, 1 mM EDTA, pH 8.0).

Competition binding assay

Peptide binding to receptors on MDA-231 cells and displacement of ^{125}I-EGF was performed in 24 well plates containing approximately 10 000 cells/well grown in Dulbecco's modified Eagle's medium (DMEM) supplemented with calf serum to 10% (v/v). Cells were washed twice with phosphate-buffered saline (PBS) containing 1 mg/mL bovine serum albumine (BSA) and 200 µL of buffer containing ^{125}I-labeled EGF was added to each well along with 200 µL of buffer containing increasing concentrations of either unlabeled EGF or synthetic peptides. The final concentration of ^{125}I EGF in the assay mixture was approximately 50 pM. After incubation for 1 h at 37°C, the wells were washed twice with PBS-BSA and the cells solubilized with 1 mL of 1 M NaOH solution. The radioactivity was measured with a γ scintillation counter.

Cell proliferation assay

The effects of EGF and synthetic peptides on the growth rate of human skin fibroblasts were determined colorimetrically with Promega's CellTiter 96 Aqueous Non Radioactive Cell Proliferation Assay. Human skin fibroblasts were seeded in 96-well plates and grown in DMEM containing 10% calf serum (v/v). When cells reached ~50% confluency, medium was discarded and replaced with serum-free DMEM to stop cellular growth. Quiescent cells which have been held in serum-free DMEM for two days were grown for 72 hours in 100 µL of serum-free medium containing various amounts of EGF, synthetic peptides, or a mixture of both. 20 µL of aqueous solution containing (3-(4,5-dimethylthiazol-2-yl)-5-(3-carboxymethoxyphenyl)-2-(4-sulfophenyl)-2H-tetrazolium inner salt and phenazine methosulfate were added in each well and the plates were incubated at 37°C for 3 hours. Light absorbance at 490 nm was determined with an ELISA plate reader.

Results

The extracellular domain of EGFR was expressed in a baculovirus system and purified by metal chelation chromatography based on a C-terminal histidine tag. The pure, homogenous receptor was biotinylated and its affinity for the human EGF was determined in a competition binding assay. The soluble receptor was incubated with ^{125}I-labeled EGF and increasing concentrations of unlabeled ligand. The competition binding curve fits the theoretical expectations for a dissociation equilibrium constant $K_d=10^{-8}$ M (Figure 5.1).

A 1.9 x 10^9 peptide sequence library, multivalently expressed on the surface of bacteriophage, was screened against the biotinylated EGFR-ED. The histidine tag at the C-terminus of the EGFR-ED and the biotin label were used to separate the target protein out of the panning solution together with the selected bound phage. Three panning rounds were performed by capturing the target-phage complexes alternatively with immobilized avidin, Ni-agarose, and again avidin. Stringency of selection in the three consecutive panning rounds was risen gradually, by increasing the Tween-20 concentration in binding and washing buffers from 0.1% in the first round to 0.5% in the next rounds. The number of phage added and eluted in each round was [illegible] and the results are shown in Table 5-1.

Phage clones selected in the last round were amplified and the displayed peptides were identified by sequencing the coding DNA (Figure 5-2). Two of these peptides, one with no histidine residues and one with high histidine content (Figure 5-3), were synthesized and tested for their ability to bind the EGFR and stimulate cellular growth. Competition binding assays, where increasing amounts of peptides were incubated with ^{125}I-EGF and EGFR, showed that the amount of bound radioactive ligand decreased as the peptide concentration increased, indicating that peptides compete with the natural ligand for binding to receptor (Figures 5-4 and 5-5). A parallel negative control with a random peptide showed no displacement of the ^{125}I-EGF bound to the receptor. The apparent dissociation constants determined by curve fitting the experimental data to a one-site competition binding model were 50 μM for both selected peptides.

The effects that peptides have on the growth and stimulation of human cells were determined in a cell proliferation assay with cultured human skin fibroblasts. This cell line responds to the presence of growth factors in culture medium by increasing their growth and multiplication rate. Quiescent cells, obtained by subculturing normally dividing cells under medium without serum or growth factors, were incubated with serum-free medium supplemented with various amounts of TGFα or peptides. After incubation for 72 hours at 37°C, the amounts of metabolically active cells were assessed with a non-radioactive assay that measures the change in light absorbance at 490 nm due to enzyme-catalyzed reduction of a tetrazolium salt. The results were plotted in the form of light absorbance at 490 nm versus ligand concentration (Figure 5-6). The EC 50 value for TGFα, which is the amount of TGFα required to reach half the maximal growth rate was estimated at 10^{-11} M

In order to determine the effects of peptides on TGFα-induced cell proliferation, a similar experiment was performed, in which quiescent human skin fibroblasts were grown in serum free medium containing a fixed amount of TGFα (10^{-11} M) and increasing concentrations of peptides (Figure 5.7). Addition of peptide 1 to the cell culture medium reduced the cellular growth rate induced by TGFα, revealing that this peptide has a TGFα-antagonistic activity. The rich-histidine peptide **2** and the random peptide **3** did not show any noticeable competition effect on the cell growth rate.

Discussions

Short synthetic peptides that interact with biologically active molecules can be the basis for development of specific chemical structures that interfere with the function of target molecules. The use of libraries of random peptides expressed on filamentous phage has proved to be an efficient method to identify ligands for antibodies (289), cellular receptors (290), or enzymes (291,292). In the present study, a 12-mer random peptide library displayed on bacteriophage M13 was employed to identify peptides that interact specifically with the extracellular domain of EGFR. The Ph.D.-12 peptide library consists of 1.9 x 10^9 electroporated sequences, amplified once to yield on average 20 copies of each sequence in 10 μL of library. The displayed peptide 12-mers are expressed directly at the N-terminus of gIII protein, *i.e.* the first residue of the mature protein is the first randomized position. The peptide is followed by a short spacer (Gly-Gly-Gly-Ser) and the wild type pIII sequence.

This library was screened against biotinylated EGFR-ED expressed in baculovirus and purified by metal chelation chromatography. The baculovirus expression system is known to produce correctly folded and post-translationally modified proteins. The EGFR-ED was expressed in a secreted, soluble form, flanked by six histidines at the carboxyl terminus. The expression system and the purification method based on metal chelation chromatography on Ni agarose yielded a pure and homogeneous protein, as shown by SDS-PAGE analysis (Figure 3.12).

The biotinylated EGFR-ED bound the EGF ligand, as determined in competition binding assays, with an apparent dissociation constant of 10^{-8} M (Figure 3.1). The affinity of the EGFR-ED expressed in insect cells for EGF is approximately 100-fold lower than that of the cell surface receptor (293), but it is in good agreement with the values reported for the EGFR-ED expressed in insect cells (187) or COS cells (294,295). Previous studies of the EGFR expressed in insect cells showed that decrease in ligand affinity occurred during protein solubilization and purification. The receptor expressed on the surface of intact infected insect cells bound ^{125}I-EGF with a K_d of 2×10^{-7} M, while the apparent binding constant fell to 2×10^{-8} M upon receptor purification (296). The physical basis for this affinity change is not known. It is possible that the local environment of the receptor in the cellular membrane affects the conformation of the receptor-binding site such that it has a higher affinity. Unfortunately, the recently determined crystal structures of the EGFR-ED/ligand complexes do not provide any information about the possible effects of membrane anchorage on ligand binding, as domain IV, the last extracellular domain before the transmembrane region is not visible

The histidine tag at the C-terminus of the EGFR-ED and the biotin label were used to separate the target protein out of the panning solution together with the selected bound phage. Three panning rounds were performed by capturing the target phage complexes alternatively with immobilized avidin, Ni-agarose, and again avidin. Stringency of selection in the three consecutive panning rounds was risen gradually by increasing the Tween-20 concentration in binding and washing buffers from 0.1% in the first round to 0.5% in the next rounds. The number of phage added and eluted in each round was titered and the results are shown in Table 5-1. The increase in phage retention yield observed in the last selection round suggests enrichment of the library for target-binding phage. The phage that eluted in the last panning round was purified, individual clones were amplified, and their DNA was analyzed to determine the sequences of displayed peptides (Figure 5-2).

The phage selection strategy does not require any information concerning the structure of the target molecule, the EGFR-ED. Theoretically, by using this selection method and a random peptide library, we could have selected peptides that bind to any site of the EGFR-ED and not necessarily to the site that interacts with the natural ligand. In previous studies, peptides identified by screening phage-displayed libraries with purified ligand-binding molecules were shown to compete with the natural ligands for binding (297,298), suggesting that during selection, the peptide bearing phage are more likely to bind to a ligand binding site than to a structural portion of the target molecule.

Visual analysis of the amino-acid sequences of identified peptides reveals a higher-than-expected occurrence of histidine residues. Assuming that the original random library was unbiased, the high histidine content raises the possibility that phage was selected for binding to Ni^{2+} ions that could possibly contaminate the EGFR-ED by chelating to the C-terminal 6-histidine tag in the Ni-agarose purification step

Tentative alignment of the phage-selected peptides did not identify any consensus sequence. It was difficult to align all the bacteriophage-derived sequences with each other and especially with the EGF or TGFα This result was not surpris[illegible] since the bacteriophage peptides are linear and the ligand s binding region is discontinuous

Two of the peptides identified by phage display one containing no histidine and one with four histidines (Figure 5-3) were synthesized and evaluated The peptide with high histidine content was expected to have been selected by phage binding to Ni contaminants Surprisingly both peptides were able to compete in some extent with radio labeled EGF for binding to the EGFR While the apparent dissociation constants were approximately 50 μM for both peptides only peptide **1** the peptide with no histidine was able to completely displace the ^{125}I-EGF bound to EGFR (Figures 5-4 and 5-5) A negative control showed that a random 18-residue peptide did not compete with ^{125}I-EGF for binding to the EGFR

Affinity of the synthetic peptides for EGFR is more than three orders of magnitude lower than that of the natural ligand s Selection of phage bearing low affinity peptides could be the result of polyvalent interactions between phage and the biotinylated receptor

Phage were isolated by a two step process in which the pool of phage was first incubated with biotinylated receptor in solution, followed by a second incubation of the mixture with the avidin coated resin. Considering that phage binding is a reversible dynamic equilibrium, it is impossible to know whether the phage is selected by binding to the receptor or to the capturing solid support. Alternation of the capturing agents between rounds should select against the phage that bind to the solid support.

It is possible that by using longer synthetic peptides derived from phage libraries with longer inserts or by extending the 12 mer peptide at both ends with conformation constraining cysteine residues, peptides with higher affinities for the receptor could be identified. The moderate affinity obtained with this 12-mer peptide library might be an intrinsic limitation and may represent the best result one can get in this system for a randomly designed peptide completely unrelated to the natural ligand's structure.

The effect of the two selected peptides on proliferation of human skin fibroblasts was investigated. While increase in cell growth rate was evident for concentrations of TGFα as low as 10^{-12} M, concentrations of peptides up to 100 μM did not stimulate the proliferation of human skin fibroblasts. To determine whether the peptides have any effects on the TGFα induced cell stimulation, a similar assay was performed in which quiescent cells were preincubated with peptides for 12 hours before adding the growth factor to 10^{-11} M final concentration (Figure 5-7). Peptide **1** in a concentration of 10^{-4} M slightly decreased the rate of cell proliferation induced by TGFα, while peptide **2** and the random peptide **3** showed no conclusive effects. The results sugest that peptide **1** is a weak TGFα antagonist, but the rich-histidine peptide **2** is neither antagonist nor agonist. Although both selected peptides competed with TGFα for binding to the receptor, they did not show a similarly strong effect on growth factor-induced cell proliferation. The proliferation assay employs living cells which are known to recycle their receptors through internalization followed by hydrolysis of the bound ligand and transfer of the free receptor back to the cellular surface. This process may result in degradation of the binding peptide during the lengthy proliferation assay The effects that the active peptide **I** has on cell proliferation are small A more substantial effect on TGFα mitogenicity will require compounds resistant to degradation and with binding affinities comparable to the natural ligand s Search of peptides with improved affinities can employ second generation libraries of constrained or biased sequences derived from those identified in this study

Table 5.1. Amount of phage (plaque forming units) selected in three consecutive panning rounds against EFDR-ED

Round	Added phage	Eluted phage	Selection yield
1	4.0×10^{10}	2.9×10	7.3×10^{-6}
2	6.0×10^{10}	4.0×10^{5}	6.7×10^{-6}
3	2.0×10^{10}	2.3×10^{6}	1.2×10^{-4}

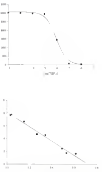

Figure 5-4 Competition binding of ^{125}I- TGFα and unlabeled TGFα to biotinylated EGFR-ED expressed in insect cells A) Competition binding curve B) Scatchard plot derived from the binding curve

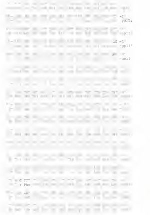

Figure 5-2 Sequences of seventeen peptides selected by panning a random 12 mer phage-displayed library against EGFR-ED

Peptide 1

`Asn Ser [illegible]`

Peptide 2

`His Asn His [illegible]`

Peptide 3 (negative control)

`Gly Val Ile Asp Ile Pro Gly [illegible]`

Figure 5.3 Sequences of the peptides that were synthesized and characterized

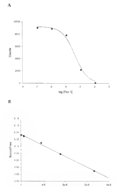

Figure 5-4 Displacement of ^{125}I-EGF from MDA-231 cells by synthetic peptide 1. Plotted values are average results of four separate experimental runs. A) Competition binding curve. B) Scatchard plot derived from the binding curve.

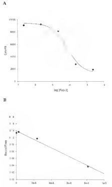

Figure 5-5 Displacement of ^{125}I-EGF from MDA-231 cells by synthetic peptide 2. Plotted values are average results of four separate experimental runs. A) Competition binding curve B) Scatchard plot derived from the binding curve.

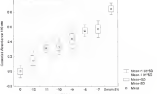

Figure 5 6 Effect of TGFα on proliferation of human skin fibroblats

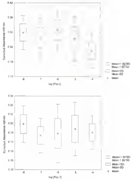

Figure 5-7 Effect of synthetic peptides on TGFα induced cell proliferation at 10^{-11} M TGFα

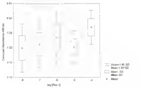

Figure 5-7 Effect of synthetic peptides on TGFα-induced cell proliferation at 10^{-11} M TGFα.

LIST OF REFERENCES

(1) Kidd J G Regression of Transplanted Lymphomas Induced *In vivo* by Means of Normal Guinea Pig Serum 1 Course of Transplanted Cancers of Various Kinds in Mice and Rats Given Guinea Pig Serum, Horse Serum, or Rabbit Serum *Journal of Experimental Medicine* **1953** *98* 565-582

(2) Kidd J G Regression of Transplanted Lymphomas Induced *In vivo* by Means of Normal Guinea Pig Serum .2 Studies on the Nature of the Active Serum Constituent - Histological Mechanism of the Regression Tests for Effects of Guinea Pig Serum on Lymphoma Cells In vitro Discussion *Journal of Experimental Medicine* **1953** *98* 583-606

(3) Broome J D Evidence That L-Asparaginase Activity of Guinea Pig Serum Is Responsible for Its Antilymphoma Effects *Nature* **1961** *191* 1114-1115

(4) Broome J D Evidence That L Asparaginase of Guinea Pig Serum Is Responsible for Its Antilymphoma Effects 1 Properties of L Asparaginase of Guinea Pig Serum in Relation to Those of Antilymphoma Substance *Journal of Experimental Medicine* **1963** *118* 99-120

(5) Broome J D Evidence That L Asparaginase of Guinea Pig Serum Is Responsible for Its Antilymphoma Effects 2 Lymphoma 6c3hed Cells Cultured in a Medium Devoid of L-Asparagine Lose Their Susceptibility to Effects of Guinea Pig Serum in Vivo *Journal of Experimental Medicine* **1963** *118* 121-147

(6) Mashburn L T Wriston J C Tumor Inhibitory Effect of L Asparaginase *Biochemical and Biophysical Research Communications* **1963** *12* 50-55

(7) Mashburn L T Wriston, J C Tumor Inhibitory Effect of L Asparaginase from *Escherichia Coli* *Archives of Biochemistry and Biophysics* **1964** *105* 450-452.

(8) Broome J D Studies on Mechanism of Tumor Inhibition by L Asparaginase - Effects of Enzyme on Asparagine Levels in Blood Normal Tissues and 6c3hed Lymphomas of Mice - Differences in Asparagine Formation and Utilization in Asparaginase Sensitive and Resistant Lymphoma Cells *Journal of Experimental Medicine* **1968** *127* 1055-1072

(9) Schwartz J H Reeves, J Y Broome J D 2 L Asparaginases from *E Coli* and Their Action against Tumors *Proceedings of the National Academy of Sciences of the United States of America* **1966**, *56* 1516 1519

(10) Boyse E A Old L J Campbell H A Mashburn L T Supression of Murine Leukemias by L-Asparaginase - Incidence of Sensitivity among Leukemias of Various Types - Comparative Inhibitory Activities of Guinea Pig Serum L-Asparaginase and *Escherichia Coli* L Asparaginase *Journal of Experimental Medicine* **1967** *125* 17-31

(11) Haghbin, M Tan C Tallal L Wollner N Rosensto J Burchenal J H L-Asparaginase Combination Therapy of Childhood Acute Leukemia *Proceedings of the American Association for Cancer Research* **1970** *11* 33-&

(12) Oettgen, H F, Old L J, Boyse E A, Campbell H A, Philips, F S, Clarkson B D, Tallal L, Leeper R D, Schwartz, M K, Kim J H Inhibition of Leukemias in Man by L-Asparaginase *Cancer Research* **1967** *27*, 2619-2631

(13) Haghbin, M, Tan C, Tallal L, Wollner N, Rosensto J, Burchenal J L-Asparaginase Combination Therapy of Childhood Acute Leukemia. *Proceedings of the American Association for Cancer Research* **1978** *11* 33-&.

(14) Sutow W W, Garcia, F, Starling, K A, Williams T E, Lane D M, Gehan, E A. L Asparaginase Therapy in Children with Advanced Leukemia *Cancer* **1971** *28* 819 824

(15) Terebelo H R, Anderson, K., Wiernik, P H, Cuttner J, Cooper R M, Faso L., Berenberg, J L Therapy of Refractory Adult Acute Lymphoblastic-Leukemia with Vincristine and Prednisone Plus Tandem Methotrexate and L- Asparaginase - Results of a Cancer and Leukemia Group B Study *American Journal of Clinical Oncology-Cancer Clinical Trials* **1986**, *9* 411-415

(16) Hersh, E M Immunosuppression by L Asparaginase and Related Enzymes - Review *Transplantation* **1971** *12* 368-376

(17) Broome J D, Schwartz, J H Differences in Production of L Asparagine in Asparaginase Sensitive and Resistant Lymphoma Cells *Biochimica Et Biophysica Acta* **1967** *138* 637-639

(18) Dollinge Mr Benvenis D Kaufman M, Burchenal Jh Effect of L-Asparaginase (a-Ase) on Asparagine Dependent Mouse Leukemic Cells in Culture *Proceedings of the American Association for Cancer Research* **1969** *10* 20-&

(19) Barr R D Devebe L L Pai K M Andrew M Halton, J Carney A F., Whitton A C Management of Children with Acute Lymphoblastic-Leukemia by the Dana-Farber Cancer Institute Protocols - an Update of the Ontario Experience. *American Journal of Pediatric Hematology Oncology* **1992** *14* 136-139

(20) Lobel J S Obrien, R T, McIntosh S, Aspnes, G T, Capizzi R L Methotrexate and Asparaginase Combination Chemotherapy in Refractory Acute Lymphoblastic Leukemia of Childhood *Cancer* **1979** *43* 1089 1094

(21) Ertel, I J Nesbit, M E, Hammond D, Weiner J, Sather H Effective Dose of L-Asparaginase for Induction of Remission in Previously Treated Children with Acute Lymphocytic Leukemia - Report from Childrens Cancer Study-Group *Cancer Research* **1979** *39* 3893-3896

(22) Capizzi R L Bertino J R Skeel R T Creasey W A Zanes R Olayon C Peterson R G Handschumacher R E L Asparaginase - Clinical Biochemical Pharmacological and Immunological Studies *Annals of Internal Medicine* **1971** *74* 893-901

(23) McCoy T A Maxwell, M Kruse P F Amino Acid Requirements of the Jensen Sarcoma *In vitro* *Cancer Research* **1959** *19* 591-595

(24) Neuman R E, McCoy T A Dual Requirement of Walker Carcinosarcoma 256 *In vitro* for Asparagine and Glutamine *Science* **1956**, *124* 124-125

(25) Haley E E, Fischer G A Welch, A D Requirement for L Asparagine of Mouse Leukemia Cells L5178y in Culture *Cancer Research* **1961** *21* 532-536

(26) Kiriyama Y Kubota M., Takimoto T, Kitoh T Tanizawa, A, Akiyama Y, Mikawa H Biochemical Characterization of U937 Cells Resistant to L-Asparaginase - the Role of Asparagine Synthetase *Leukemia* **1989** *3* 294-297

(27) Chakrabarti R Schuster S M L asparaginase - Perspectives on the mechanisms of action and resistance *International Journal of Pediatric Hematology Oncology* **1997** *4* 597-611

(28) Pieters R Klumper E Kaspers G J L Veerman A J P Everything you always wanted to know about cellular drug resistance in childhood acute lymphoblastic leukemia *Critical Reviews in Oncology/Hematology* **1997** *25* 11-26

(29) Aslanian, A M Fletcher B S Kilberg, M S Asparagine synthetase expression alone is sufficient to induce L asparaginase resistance in MOLT-4 human leukaemia cells *Biochemical Journal* **2001** *357* 321-328

(30) Gong S S Guerrini L Basilico C Regulation of Asparagine Synthetase Gene-Expression by Amino- Acid Starvation *Molecular and Cellular Biology* **1991** *11* 6059-6066

(31) Guerrini, L Gong S S Mangasarian, K Basilico C Cis Acting and Trans Acting Elements Involved in Amino Acid Regulation of Asparagine Synthetase Gene-Expression *Molecular and Cellular Biology* **1993** *13* 3202 3212

(32) Chakrabarti R Chakrabarti D Souba, W W Schuster S M Interaction of the Eukaryotic Peptide Chain Initiation Factor Eif-4a with the Specific Elements at the 5-Untranslated Sequence of Human Asparagine Synthetase Messenger Rna. *Journal of Biological Chemistry* **1993** *268* 1298 1303

(33) Hutson R G Kitoh T Amador D A M Cosic S Schuster S M Kilberg M S Amino acid control of asparagine synthetase Relation to asparaginase resistance in human leukemia cells *American Journal of Physiology Cell Physiology* **1997** *41* C1691 C1699

(34) Barbosa Tessmann I P Pineda, V Nick H S Schuster S M Kilberg M S Transcriptional regulation of the human asparagine synthetase gene by carbohydrate availability *Biochemical Journal* **1999** *339* 151-158

(35) Barbosa Tessmann I P Chen C Zhong, C Schuster S M Nick H S Kilberg M S Activation of the unfolded protein response pathway induces human asparagine synthetase gene expression *Journal of Biological Chemistry* **1999** *274* 31139 31144

(36) Barbosa Tessmann I P, Chen C Zhong, C, Stu, F Schuster S M Nick H S Kilberg, M S Activation of the human asparagine synthetase gene by the amino acid response and the endoplasmic reticulum stress response pathways occurs by common genomic elements *Journal of Biological Chemistry* **2000** *275* 26976-26985

(37) Andrulis I L Barrett M T DNA Methylation Patterns Associated with Asparagine Synthetase Expression in Asparagine-Overproducing and Asparagine Auxotrophic Cells *Molecular and Cellular Biology* **1989** *9* 2922-2927

(38) Worton, K S Kerbel R S Andrulis I L Hypomethylation and Reactivation of the Asparagine Synthetase Gene Induced by L Asparaginase and Ethyl Methanesulfonate *Cancer Research* **1991** *51* 985 989

(39) Andrulis I L Shotwell M Evansblackler S Zalkin H Siminovitch L, Ray P N Fine Structure Analysis of the Chinese Hamster as Gene Encoding Asparagine Synthetase *Gene* **1989** *80* 75-85

(40) Aslanian A. M. Kilberg M. S. Multiple adaptive mechanisms affect asparagine synthetase substrate availability in asparaginase resistant MOLT-4 human leukemia cells *Biochemical Journal* **2001** *358* 59 67

(41) Colletta, G. Cirafici A. M. Tsh Is Able to Induce Cell Cycle Related Gene-Expression in Rat Thyroid Cell *Biochemical and Biophysical Research Communications* **1992** *183* 265-272

(42) Gong, S. S. Basilico C. A Mammalian Temperature-Sensitive Mutation Affecting G1 Progression Results from a Single Amino Acid Substitution in Asparagine Synthetase *Nucleic Acids Research* **1990** *18* 3509 3513

(43) Hongo S. Takeda, M. Sato T. Induction of Asparagine Synthetase During Lymphocyte Activation by Phytohemagglutinin. *Biochemistry International* **1989** *18* 661-666

(44) Huang Y. Z. Knox W. E. Glutamine-Dependent Asparagine Synthetase in Fetal, Adult and Neoplastic Rat Tissues *Enzyme* **1975**, *19* 314 328

(45) Hongo S. Sakagami H. Sato T. Decrease in Asparagine Synthetase Activity During Cell Differentiation of Mouse and Human Leukemia Cell Lines *Leukemia* **1990** *4* 708-711

(46) Cooney D. A. Driscoll J. S. Milman, H. A. Jayaram H. N. Davis, R. D. Inhibitors of L Asparagine Synthetase *In vitro* *Cancer Treatment Reports* **1976** *60* 1493-1557

(47) Cooney D. A., Jones, M. T. Milman H. A. Young D. M. Jayaram H. N. Regulators of the Metabolism of L Asparagine - a Search for Endogenous Inhibitors *International Journal of Biochemistry* **1980** *11* 519 539

(48) Mokotoff M. Bagaglio J. F. Parikh, B. S. Potential Inhibitors of L Asparagine Biosynthesis II Chemistry and Biological-Activity of Beta Hydroxyaspartic Acid and Its Derivatives *Journal of Medicinal Chemistry* **1975** *18* 354 358

(49) Mokotoff M. Brynes S. Bagaglio J. F. Potential Inhibitors of L-Asparagine Biosynthesis III Aromatic Sulfonyl Fluoride Analogs of L Asparagine and L Glutamine *Journal of Medicinal Chemistry* **1975** *18* 888-891

(50) Jayaram H. N. Cooney D. A. Milman H. A. Homan E. R. Rosenbluth R. J. Don Conv and Dons I Inhibition of L Asparagine Synthetase Invitro *Biochemical Pharmacology* **1976** *25* 1571-1582

(51) Jayaram H. N. Cooney D. A. Homan E. R. Milman, H. A. Rosenblu R. Inhibitors of L Asparagine Synthetase of L5178y Asparaginase Resistant Leukemia Ii *Pharmacologist* **1973** *15* 253-253

(52) Jayaram H. N. Cooney D. A. Milman, H. A., Homan E. R. King, V. M. Cragoe E. J. Ethacrynic Acid Inhibitor of L Asparagine Synthetase *Biochemical Pharmacology* **1975** *24* 1787 1792.

(53) Uren, J. R. Chang, P. K. Handschumacher R. E. Effects of Asparagine Synthetase Inhibitors on Asparaginase Resistant Tumors *Biochemical Pharmacology* **1977** *26* 1405-1410

(54) Bohm H. J. Klebe G. What can we learn from molecular recognition in protein-ligand complexes for the design of new drugs? *Angewandte Chemie International Edition in English* **1996** *35* 2589 2614

(55) Richards N G J., Schuster S M Mechanistic issues in asparagine synthetase catalysis *Advances in Enzymology Vol 72* JOHN WILEY & SONS INC New York, 1998 pp 145-198

(56) Buchanan J M Amidotransferases *Advances in Enzymology and Related Areas of Molecular Biology* **1973** *39* 91-183

(57) Hinchman, S K Henikoff S Schuster S M A Relationship between Asparagine Synthetase A and Aspartyl Transfer-Rna Synthetase *Journal of Biological Chemistry* **1992** *267* 144 149

(58) Nakatsu T Kato H Oda, J Crystal structure of asparagine synthetase reveals a close evolutionary relationship to class II aminoacyl-tRNA synthetase *Nature Structural Biology* **1998** *5* 15-19

(59) Hinchman S K Schuster S M Overproduction Preparation of Monoclonal Antibodies and Purification of Escherichia Coli Asparagine Synthetase A *Protein Engineering* **1992** *5* 279 283

(60) Cedar H Schwartz J H Asparagine Synthetase of *Escherichia Coli* I. Biosynthetic Role of Enzyme Purification, and Characterization of Reaction Products *Journal of Biological Chemistry* **1969** *244* 4112 4121

(61) Cedar H., Schwartz, J H. Asparagine Synthetase of *Escherichia Coli* II Studies on Mechanism *Journal of Biological Chemistry* **1969** *244* 4122-4127

(62) Horowitz, B Meister A Glutamine-Dependent Asparagine Synthetase from Leukemia Cells Chloride Dependence Mechanism of Action and Inhibition *Journal of Biological Chemistry* **1972** *247* 6708 6719

(63) Scofield M A Lewis W S Schuster S M Nucleotide-Sequence of Escherichia Coli Asnb and Deduced Amino Acid Sequence of Asparagine Synthetase B *Journal of Biological Chemistry* **1990** *265* 12895-12902

(64) Dang, V D Valens M BolotinFukuhara M DaignanFornier B Cloning of the ASN1 and ASN2 genes encoding asparagine synthetases in Saccharomyces cerevisiae Differential regulation by the CCAAT-box binding factor *Molecular Microbiology* **1996** *22* 681-692

(65) Ramos F Wiame J M Synthesis and Activation of Asparagine in Asparagine Auxotrophs of Saccharomyces-Cerevisiae *European Journal of Biochemistry* **1979** *94* 409-417

(66) Osuna, D Galvez, G Pineda M Aguilar M RT-PCR cloning characterization and mRNA expression analysis of a cDNA encoding a type II asparagine synthetase in common bean *Biochimica Et Biophysica Acta-Gene Structure and Expression* **1999** *1445* 75 85

(67) Yamagata, H Nakajima A Bowler C Iwasaki T Molecular cloning and characterization of a cDNA encoding asparagine synthetase from soybean (Glycine max L) cell cultures *Bioscience Biotechnology and Biochemistry* **1998**, *62* 148 150

(68) Shi L F Twary S N Yoshioka, H Gregerson, R G Miller S S., Samac D A Gantt J S Unkefer P J Vance C P Nitrogen assimilation in alfalfa Isolation and characterization of an asparagine synthetase gene showing enhanced expression in root nodules and dark-adapted leaves *Plant Cell* **1997** *9* 1339-1356

(69) Tsai F Y, Coruzzi G M Dark-Induced and Organ Specific Expression of 2 Asparagine Synthetase Genes in Pisum-Sativum *Embo Journal* **1990** *9* 323-332

(70) Lam, H M Peng S S Y Coruzzi G M Metabolic Regulation of the Gene Encoding Glutamine-Dependent Asparagine Synthetase in Arabidopsis Thaliana *Plant Physiology* **1994** *106* 1347-1357

(71) Lam, H M Coschigano K T Oliveira, I C MeloOliveira, R Coruzzi, G M The molecular genetics of nitrogen assimilation into amino acids in higher plants *Annual Review of Plant Physiology and Plant Molecular Biology* **1996** *47* 569-593

(72) Waterhouse R N Smyth A J, Massonneau A Prosser I M Clarkson D T Molecular cloning and characterisation of asparagine synthetase from Lotus japonicus Dynamics of asparagine synthesis in N-sufficient conditions *Plant Molecular Biology* **1996** *30* 883 897

(73) Ravel, J M Shive W., Norton S J Humphreys J S Asparagine Biosynthesis in *Lactobacillus Arabinosus* and Its Control by Asparagine through Enzyme Inhibition and Repression *Journal of Biological Chemistry* **1962** *237* 2845-2849

(74) Reitzer L J Magasanik B Asparagine Synthetases of Klebsiella Aerogenes - Properties and Regulation of Synthesis *Journal of Bacteriology* **1982** *151* 1299-1313

(75) Deng, W Burland V Plunkett G Boutin, A Mayhew G F Liss P Perna, N T Rose D J Mau B Zhou S G Schwartz, D C Fetherston J D Lindler L E Brubaker R R Plano G V Straley S C McDonough K A Nilles M L Matson J S Blattner F R Perry R D Genome sequence of Yersinia pestis KIM *Journal of Bacteriology* **2002** *184* 4601 4611

(76) McClelland M Sanderson, K E., Spieth J Clifton S W., Latreille P Courtney L Porwollik S Ali J Dante M Du, F Y, Hou, S F, Layman D Leonard S Nguyen C Scott, K Holmes A. Grewal N Mulvaney E Ryan E Sun H Florea, L Miller W Stoneking T Nhan M Waterston R Wilson R K Complete genome sequence of Salmonella enterica serovar typhimurium LT2. *Nature* **2001** *413* 852 856

(77) Bult C J White O Olsen, G J Zhou, L X Fleischmann, R D Sutton, G G Blake, J A FitzGerald, L M Clayton R A Gocayne J D Kerlavage A R., Dougherty B A Tomb J F Adams M D Reich C I Overbeek R Kirkness E F Weinstock K G Merrick J M, Glodek, A Scott, J L Geoghagen N S M Weidman J F Fuhrmann J L Nguyen D Utterback T R Kelley J M Peterson J D Sadow P W Hanna, M C Cotton M D Roberts K M Hurst, M A Kaine B P Borodovsky M Klenk, H P Fraser C M Smith H O Woese C R Venter, J C Complete genome sequence of the methanogenic archaeon Methanococcus jannaschii *Science* **1996** *273* 1058-1073

(78) Bhatia, U Robison, K Gilbert, W Dealing with database explosion. A cautionary note *Science* **1997** *276*, 1724 1725

(79) Smith, D. R.; DoucetteStamm, L. A.; Deloughery, C.; Lee, H. M.; Dubois, J.; Aldredge, T.; Bashirzadeh, R.; Blakely, D.; Cook, R.; Gilbert, K.; Harrison, D.; Hoang, L.; Keagle, P.; Lumm, W.; Pothier, B.; Qiu, D. Y.; Spadafora, R.; Vicaire, R.; Wang, Y.; Wierzbowski, J.; Gibson, R.; Jiwani, N.; Caruso, A.; Bush, D.; Safer, H.; Patwell, D.; Prabhakar, S.; McDougall, S.; Shimer, G.; Goyal, A.; Pietrokovski, S.; Church, G. M.; Daniels, C. J.; Mao, J. I.; Rice, P.; Nolling, J.; Reeve, J. N. Complete genome sequence of Methanobacterium thermoautotrophicum Delta H: Functional analysis and comparative genomics. *Journal of Bacteriology* **1997**, *179*, 7135-7155.

(80) Bowman, S.; Lawson, D.; Basham, D.; Brown, D.; Chillingworth, T.; Churcher, C. M.; Craig, A.; Davies, R. M.; Devlin, K.; Feltwell, T.; Gentles, S.; Gwilliam, R.; Hamlin, N.; Harris, D.; Holroyd, S.; Hornsby, T.; Horrocks, P.; Jagels, K.; Jassal, B.; Kyes, S.; McLean, J.; Moule, S.; Mungall, K.; Murphy, L.; Oliver, K.; Quail, M. A.; Rajandream, M. A.; Rutter, S.; Skelton, J.; Squares, R.; Squares, S.; Sulston, J. E.; Whitehead, S.; Woodward, J. R.; Newbold, C.; Barrell, B. G. The complete nucleotide sequence of chromosome 3 of Plasmodium falciparum. *Nature* **1999**, *400*, 532-538.

(81) Gardner, M. J.; Hall, N.; Fung, E.; White, O.; Berriman, M.; Hyman, R. W.; Carlton, J. M.; Pain, A.; Nelson, K. E.; Bowman, S.; Paulsen, I. T.; James, K.; Eisen, J. A.; Rutherford, K.; Salzberg, S. L.; Craig, A.; Kyes, S.; Chan, M. S.; Nene, V.; Shallom, S. J.; Suh, B.; Peterson, J.; Angiuoli, S.; Pertea, M.; Allen, J.; Selengut, J.; Haft, D.; Mather, M. W.; Vaidya, A. B.; Martin, D. M. A.; Fairlamb, A. H.; Fraunholz, M. J.; Roos, D. S.; Ralph, S. A.; McFadden, G. I.; Cummings, L. M.; Subramanian, G. M.; Mungall, C.; Venter, J. C.; Carucci, D. J.; Hoffman, S. L.; Newbold, C.; Davis, R. W.; Fraser, C. M.; Barrell, B. Genome sequence of the human malaria parasite Plasmodium falciparum. *Nature* **2002**, *419*, 498-511.

(82) Patterson, M. K.; Orr, G. R. Asparagine Biosynthesis by Novikoff Hepatoma Isolation Purification Property and Mechanism Studies of Enzyme System. *Journal of Biological Chemistry* **1968**, *243*, 376-380.

(83) Mehlhaff, P. M.; Luehr, C. A.; Schuster, S. M. Studies of the Ammonia-Dependent Reaction of Beef Pancreatic Asparagine Synthetase. *Biochemistry* **1985**, *24*, 1104-1110.

(84) Arfin, S. M. Asparagine Synthesis in Chick Embryo Liver. *Biochimica Et Biophysica Acta* **1967**, *136*, 233-244.

(85) Heng, H. H. Q.; Shi, X. M.; Scherer, S. W.; Andrulis, I. L.; Tsui, L. C. Refined Localization of the Asparagine Synthetase Gene (Asns) to Chromosome 7, Region Q21.3, and Characterization of the Somatic-Cell Hybrid Line 4af/106/Ko15. *Cytogenetics and Cell Genetics* **1994**, *66*, 135-138.

(86) Hongo, S.; Fujimori, M.; Shioda, S.; Nakai, Y.; Takeda, M.; Sato, T. Immunochemical Characterization of Rat Testicular Asparagine Synthetase. *Archives of Biochemistry and Biophysics* **1992**, *295*, 120-125.

(87) Hongo, S.; Sato, T. Some Molecular Properties of Asparagine Synthetase from Rat- Liver. *Biochimica Et Biophysica Acta* **1983**, *742*, 484-489.

(88) Luehr, C. A.; Schuster, S. M. Purification and Characterization of Beef Pancreatic Asparagine Synthetase. *Archives of Biochemistry and Biophysics* **1985**, *237*, 335-346.

(89) Andrulis, I L Chen J, Ray P N Isolation of Human Cdnas for Asparagine Synthetase and Expression in Jensen Rat Sarcoma-Cells *Molecular and Cellular Biology* **1987** *7*, 2435 2443

(90) Markin R S Luehr C A Schuster S M Kinetic Mechanism of Beef Pancreatic L Asparagine Synthetase *Biochemistry* **1981** *20* 7226-7232

(91) Pfeiffer N E Mehlhaff, P M Wylie D E Schuster S M Monoclonal-Antibodies Specific for Bovine Pancreatic Asparagine Synthetase - Production and Use in Structural Studies *Journal of Biological Chemistry* **1986**, *261* 1914-1919

(92) Mehlhaff P M Schuster S M Bovine Pancreatic Asparagine Synthetase Explored with Substrate Analogs and Specific Monoclonal Antibodies. *Archives of Biochemistry and Biophysics* **1991** *284* 143-150

(93) Beran, R K Schuster S M The Kinetic Properties of Beef Pancreatic L Asparagine Synthetase *International Journal of Biochemistry* **1981** *13* 165 169

(94) Van Heeke G Schuster S M The N Terminal Cysteine of Human Asparagine Synthetase Is Essential for Glutamine Dependent Activity *Journal of Biological Chemistry* **1989** *264* 19475 19477

(95) Van Heeke G Schuster S M Expression of Human Asparagine Synthetase in Saccharomyces- Cerevisiae *Protein Engineering* **1990** *3* 739 744

(96) Sheng S J Moraga, D A Vanheeke G Schuster S M High Level Expression of Human Asparagine Synthetase and Production of Monoclonal-Antibodies for Enzyme Purification *Protein Expression and Purification* **1992**, *3* 337 346

(97) Sheng, S., Moraga-amador D A Vanheeke G Allison R D Richards, N G J Schuster S M Glutamine Inhibits the Ammonia Dependent Activities of 2 Cys-1 Mutants of Human Asparagine Synthetase through the Formation of an Abortive Complex *Journal of Biological Chemistry* **1993** *268* 16771 16780

(98) Larsen T M Boehlein S K Schuster S M Richards, N G J Thoden J B Holden, H M, Rayment I Three-dimensional structure of *Escherichia coli* asparagine synthetase B A short journey from substrate to product *Biochemistry* **1999** *38* 16146-16157

(99) Boehlein S K Richards N G J Schuster S M Glutamine Dependent Nitrogen Transfer in *Escherichia Coli* Asparagine Synthetase B - Searching for the Catalytic Triad *Journal of Biological Chemistry* **1994** *269* 7450-7457

(100) Zalkin, H Smith J L Enzymes utilizing glutamine as an amide donor *Advances in Enzymology* Vol 72 JOHN WILEY & SONS INC New York 1998 pp 87 +

(101) Smith J L Structures of glutamine amidotransferases from the purine biosynthetic pathway *Biochemical Society Transactions* **1995** *23* 894-898

(102) Smith J L Glutamine PRPP amidotransferase snapshots of an enzyme in action *Current Opinion in Structural Biology* **1998** *8* 686-694

(103) Tso, J Y Zalkin, H Vancleumput, M Yanofsky C., Smith, J M Nucleotide-Sequence of Escherichia Coli-Purf and Deduced Amino Acid Sequence of Glutamine Phosphoribosylpyrophosphate Amidotransferase *Journal of Biological Chemistry* **1982** *257* 3525-3531

(104) Badet B Vermoote P Haumont P Y Lederer F Legoffic F Glucosamine Synthetase from Escherichia-Coli - Purification Properties and Glutamine-Utilizing Site Location *Biochemistry* **1987** *26* 1940 1948

(105) Badet-Denisot M A Rene L Badet B Mechanistic Investigations on Glucosamine-6-Phosphate Synthase *Bulletin De La Societe Chimique De France* **1993** *130* 249-255

(106) Vanoni M A Curti B Glutamate synthase a complex iron-sulfur flavoprotein *Cellular and Molecular Life Sciences* **1999** *55* 617-638

(107) Vanoni M A Edmondson D E Rescigno M Zanetti G Curti B Mechanistic Studies on Azospirillum Brasilense Glutamate Synthase *Biochemistry* **1991** *30* 11478 11484

(108) van den Heuvel R H H Ferrari D., Bossi R T Ravasio S Curti B Vanoni, M A. Florencio F J Mattevi A Structural studies on the synchronization of catalytic centers in glutamate synthase *Journal of Biological Chemistry* **2002** *277* 24579-24583

(109) Zalkin H The amidotransferases. *Advances in Enzymology Vol 66* JOHN WILEY & SONS INC New York 1993, pp 203 309

(110) Smith J L Zaluzec E J Wery J P Niu, L W Switzer R L, Zalkin, H Satow Y Structure of the Allosteric Regulatory Enzyme of Purine Biosynthesis *Science* **1994** *264* 1427-1433

(111) Kim J H Krahn J M Tomchick D R Smith J L Zalkin H Structure and function of the glutamine phosphoribosylpyrophosphate amidotransferase glutamine site and communication with the phosphoribosylpyrophosphate site *Journal of Biological Chemistry* **1996** *271* 15549 15557

(112) Chen S H Tomchick, D R. Wolle D Hu, P., Smith J L Switzer R L Zalkin H Mechanism of the synergistic end product regulation of Bacillus subtilis glutamine phosphoribosylpyrophosphate amidotransferase by nucleotides *Biochemistry* **1997** *36* 10718 10726

(113) Krahn, J M Kim J H Burns M R Parry R J Zalkin, H Smith, J L Coupled formation of an amidotransferase interdomain ammonia channel and a phosphoribosyltransferase active site *Biochemistry* **1997** *36* 11061-11068

(114) Muchmore, C R A Krahn J M Kim J H Zalkin H Smith J L Crystal structure of glutamine phosphoribosylpyrophosphate amidotransferase from *Escherichia coli* *Protein Science* **1998** *7* 39 51

(115) Obmolova, G Badetdenisot M A Badet, B Teplyakov A Crystallization and Preliminary-X-Ray Analysis of the 2 Domains of Glucosamine-6-Phosphate Synthase from Escherichia Coli *Journal of Molecular Biology* **1994** *242* 703-705

(116) Isupov M N Obmolova, G Butterworth, S BadetDenisot, M A. Badet, B Polikarpov I Littlechild J A., Teplyakov A Substrate binding is required for assembly of the active conformation of the catalytic site in Ntn amidotransferases: Evidence from the 1 8 angstrom crystal structure of the glutaminase domain of glucosamine 6-phosphate synthase *Structure* **1996** *4* 801 810

(117) Teplyakov A., Obmolova, G Badet Denisot M A Badet B Polikarpov I Involvement of the C terminus in intramolecular nitrogen channeling in glucosamine 6-phosphate synthase evidence from a 1 6 angstrom crystal structure of the isomerase domain *Structure with Folding & Design* **1998** *6* 1047-1055

(118) Teplyakov A Obmolova G Badet-Denisot M A., Badet. B The mechanism of sugar phosphate isomerization by glucosamine 6-phosphate synthase *Protein Science* **1999** *8* 596-602

(119) Teplyakov A Obmolova G Badet B Badet-Denisot M A Channeling of ammonia in glucosamine-6 phosphate synthase *Journal of Molecular Biology* **2001** *313* 1093-1102

(120) Binda, C Bossi R T Wakatsuki S Arzt S Coda A , Curti B., Vanoni M A., Mattevi, A Cross-talk and ammonia channeling between active centers in the unexpected domain arrangement of glutamate synthase *Structure* **2000** *8* 1299-1308

(121) Babbitt P C., Gerlt J A Understanding enzyme superfamilies Chemistry as the fundamental determinant in the evolution of new catalytic activities *Journal of Biological Chemistry* **1997** *272* 30591-30594

(122) Gerlt, J A Babbitt P C Mechanistically diverse enzyme superfamilies the importance of chemistry in the evolution of catalysis *Current Opinion in Chemical Biology* **1998**. *2* 607 612

(123) Gerlt J A Babbitt, P C Divergent evolution of enzymatic function Mechanistically diverse superfamilies and functionally distinct suprafamilies *Annual Review of Biochemistry* **2001** *79* 209-246

(124) Brannigan J A. Dodson, G. Duggleby H J., Moody P C E. Smith, J L Tomchick D R Murzin A G A Protein Catalytic Framework with an N-Terminal Nucleophile Is Capable of Self-Activation *Nature* **1995** *378* 416-419

(125) Oinonen C Rouvinen J Structural comparison of Ntn hydrolases *Protein Science* **2000** *9* 2329 2337

(126) Ponting C P Russell R R The natural history of protein domains *Annual Review of Biophysics and Biomolecular Structure* **2002** *31* 45-71

(127) Duggleby H J Tolley S P Hill C P Dodson E J Dodson G Moody P C E Penicillin Acylase Has a Single-Amino Acid Catalytic Center *Nature* **1995**, *373*, 264 268

(128) Oinonen, C., Tikkanen R. Rouvinen, J., Peltonen, L 3 Dimensional Structure of Human Lysosomal Aspartylglucosaminidase *Nature Structural Biology* **1995** *2* 1102 1108

(129) Lowe, J. Stock D. Jap R. Zwickl P., Baumeister W. Huber R. Crystal Structure of the 20s Proteasome from the Archaeon T. Acidophilum at 3 4-Angstrom Resolution *Science* **1995** *268* 533 539

(130) Groll M. Ditzel L. Lowe, J. Stock D. Bochtler M. Bartunik H. D Huber R Structure of 20S proteasome from yeast at 2 4 angstrom resolution *Nature* **1997** *386* 463-471

(131) Voges D. Zwickl P., Baumeister W The 26S proteasome A molecular machine designed for controlled proteolysis *Annual Review of Biochemistry* **1999** *68* 1015-1068

(132) Bompard-Gilles, C., Villeret, V., Davies, G. J., Fanuel, L., Joris, B., Frere, J. M., Van Beeumen, J. A new variant of the Ntn hydrolase fold revealed by the crystal structure of L-aminopeptidase D-Ala-esterase/amidase from Ochrobactrum anthropi. *Structure with Folding & Design* **2000**, *8*, 153-162.
(133) Kim, Y., Kim, S., Earnest, T. N., Hol, W. G. J. Precursor structure of cephalosporin acylase - Insights into autoproteolytic activation in a new N-terminal hydrolase family. *Journal of Biological Chemistry* **2002**, *277*, 2823-2829.
(134) Tesmer, J. G., Klem, T. J., Deras, M. L., Davisson, V. J., Smith, J. L. The crystal structure of GMP synthetase reveals a novel catalytic triad and is a structural paradigm for two enzyme families. *Nature Structural Biology* **1996**, *3*, 74-86.
(135) Bork, P., Koonin, E. V. A P-Loop-Like Motif in a Widespread Atp Pyrophosphatase Domain - Implications for the Evolution of Sequence Motifs and Enzyme Activity. *Proteins-Structure Function and Genetics* **1994**, *20*, 347-355.
(136) Denessiouk, K. A., Johnson, M. S. When fold is not important: A common structural framework for adenine and AMP binding in 12 unrelated protein families. *Proteins-Structure Function and Genetics* **2000**, *38*, 310-326.
(137) Mantsala, P., Zalkin, H. Cloning and Sequence of Bacillus-Subtilis Pura and Guaa, Involved in the Conversion of Imp to Amp and Gmp. *Journal of Bacteriology* **1992**, *174*, 1883-1890.
(138) Lou, L., Nakamura, J., Tsing, S., Nguyen, B., Chow, J., Straub, K., Chan, H., Barnett, J. High Level Production from a Baculovirus Expression System and Biochemical Characterization of Human Gmp Synthetase. *Protein Expression and Purification* **1995**, *6*, 487-495.
(139) Nakamura, J., Lou, L. Biochemical Characterization of Human Gmp Synthetase. *Journal of Biological Chemistry* **1995**, *270*, 7347-7353.
(140) Kumar, S., Lennane, J., Ratner, S. Argininosuccinate Synthetase - Essential Role of Cysteine and Arginine Residues in Relation to Structure and Mechanism of Atp Activation. *Proceedings of the National Academy of Sciences of the United States of America* **1985**, *82*, 6745-6749.
(141) Surh, L. C., Morris, S. M., Obrien, W. E., Beaudet, A. L. Nucleotide-Sequence of the Cdna Encoding the Rat Argininosuccinate Synthetase. *Nucleic Acids Research* **1988**, *16*, 9352-9352.
(142) Haberle, J., Pauli, S., Linnebank, M., Kleijer, W. J., Bakker, H. D., Wanders, R. J. A., Harms, E., Koch, H. G. Structure of the human argininosuccinate synthetase gene and an improved system for molecular diagnostics in patients with classical and mild citrullinemia. *Human Genetics* **2002**, *110*, 327-333.
(143) Leyh, T. S., Vogt, T. F., Suo, Y. The DNA Sequence of the Sulfate Activation Locus from Escherichia-Coli K-12. *Journal of Biological Chemistry* **1992**, *267*, 10405-10410.
(144) Kurima, K., Singh, B., Schwartz, N. B. Genomic organization of the mouse and human genes encoding the ATP sulfurylase/adenosine 5'-phosphosulfate kinase isoform SK2. *Journal of Biological Chemistry* **1999**, *274*, 33306-33312.
(145) Leyh, T. S. On the advantages of imperfect energetic linkage. *Enzyme Kinetics and Mechanism, Pt E*, ACADEMIC PRESS INC: San Diego, 1999; pp 48-70.

(146) Nicholls A. Sharp K A Honig B Protein Folding and Association - Insights from the Interfacial and Thermodynamic Properties of Hydrocarbons *Proteins Structure Function and Genetics* **1991** *11* 281-296

(147) Bachmann B O Li, R F Townsend C A Beta-Lactam synthetase A new biosynthetic enzyme *Proceedings of the National Academy of Sciences of the United States of America* **1998**, *95*, 9082-9086

(148) Bachmann, B O Townsend, C A Kinetic mechanism of the beta lactam synthetase of *Streptomyces clavuligerus* *Biochemistry* **2000** *39* 11187 11193

(149) McNaughton, H J Thirkettle J E., Zhang, Z H Schofield C J Jensen, S E., Barton, B., Greaves P Beta-lactam synthetase Implications for beta lactamase evolution *Chemical Communications* **1998** 2325 2326

(150) Miller, M T , Bachmann B O Townsend, C A , Rosenzweig A C Structure of beta lactam synthetase reveals how to synthesize antibiotics instead of asparagine. *Nature Structural Biology* **2001** *8* 684-689

(151) Miller M T Bachmann B O Townsend C A Rosenzweig A C The catalytic cycle of beta lactam synthetase observed by x-ray crystallographic snapshots *Proceedings of the National Academy of Sciences of the United States of America* **2002** *99* 14752 14757

(152) Brocklehurst K Willenbrock, F Salih E Cysteine proteases *Hydrolytic Enzymes* Elsevier Biomedical Amsterdam, 1987 pp 39-158

(153) Musil D Zucic D Turk, D Engh R A, Mayr I Huber R Popovic, T., Turk, V Towatari T Katunuma, N Bode W The Refined 2 15 a X-Ray Crystal Structure of Human Liver Cathepsin B - the Structural Basis for Its Specificity *Embo Journal* **1991** *10* 2321-2330

(154) Storer, A. C., Menard R Catalytic Mechanism in Papain Family of Cysteine Peptidases *Proteolytic Enzymes Serine and Cysteine Peptidases* ACADEMIC PRESS INC San Diego. 1994 pp 486-500

(155) Thornberry N A Molineaux, S M Interleukin-1-Beta Converting-Enzyme - a Novel Cysteine Protease Required for Il-1-Beta Production and Implicated in Programmed Cell Death *Protein Science* **1995** *4* 3 12

(156) Earnshaw W C Martins, L M Kaufmann S H Mammalian caspases Structure activation substrates and functions during apoptosis *Annual Review of Biochemistry* **1999** *68* 383-424

(157) Boehlein S K. Richards N G J., Walworth E S Schuster S M. Arginine 30 and Asparagine 74 Have Functional Roles in the Glutamine Dependent Activities of Escherichia-Coli Asparagine Synthetase-B *Journal of Biological Chemistry* **1994** *269* 26789 26795

(158) Boehlein S K Schuster S M Richards N G J Glutamic acid gamma monohydroxamate and hydroxylamine are alternate substrates for Escherichia coli asparagine synthetase B *Biochemistry* **1996** *35* 3031-3037

(159) Boehlein S K RosaRodriguez, J G Schuster S M Richards, N G J Catalytic activity of the N-terminal domain of *Escherichia coli* asparagine synthetase B can be reengineered by single point mutation *Journal of the American Chemical Society* **1997** *119* 5785-5791

(160) Menard, R.; Carriere, J.; Laflamme, P.; Plouffe, C.; Khouri, H. E.; Vernet, T.; Tessier, D. C.; Thomas, D. Y.; Storer, A. C. Contribution of the Glutamine-19 Side-Chain to Transition-State Stabilization in the Oxyanion Hole of Papain. *Biochemistry* **1991**, *30*, 8924-8928.

(161) Dufour, E.; Storer, A. C.; Menard, R. Engineering nitrile hydratase activity into a cysteine protease by a single mutation. *Biochemistry* **1995**, *34*, 16382-16388.

(162) Dufour, E.; Storer, A. C.; Menard, R. Peptide Aldehydes and Nitriles as Transition-State Analog Inhibitors of Cysteine Proteases. *Biochemistry* **1995**, *34*, 9136-9143.

(163) Menard, R.; Plouffe, C.; Laflamme, P.; Vernet, T.; Tessier, D. C.; Thomas, D. Y.; Storer, A. C. Modification of the Electrostatic Environment Is Tolerated in the Oxyanion Hole of the Cysteine Protease Papain. *Biochemistry* **1995**, *34*, 464-471.

(164) Schnizer, H. G.; Boehlein, S. K.; Stewart, J. D.; Richards, N. G. J.; Schuster, S. M. Formation and isolation of a covalent intermediate during the glutaminase reaction of a class II amidotransferase. *Biochemistry* **1999**, *38*, 3677-3682.

(165) Schnizer, H. G.; Boehlein, S. K.; Stewart, J. D.; Richards, N. G. J.; Schuster, S. M. The gamma glutamyl thioester covalent intermediate in the glutaminase reaction catalyzed by *Escherichia coli* asparagine synthetase B. *Enzyme Kinetics and Mechanism, Pt F: Detection and Characterization of Enzyme Reaction Intermediates*. ACADEMIC PRESS INC: San Diego, 2002; pp 260-271.

(166) Kamphuis, I. G.; Kalk, K. H.; Swarte, M. B. A.; Drenth, J. Structure of Papain Refined at 1.65 A Resolution. *Journal of Molecular Biology* **1984**, *179*, 233-256.

(167) Mei, B.; Zalkin, H. A Cysteine-Histidine-Aspartate Catalytic Triad Is Involved in Glutamine Amide Transfer Function in PurF-Type Glutamine Amidotransferases. *Journal of Biological Chemistry* **1989**, *264*, 16613-16619.

(168) Badet-Denisot, M. A.; Badet, B. Chemical Modification of Glucosamine 6-Phosphate Synthase by Diethyl Pyrocarbonate - Evidence of Histidine Requirement for Enzymatic-Activity. *Archives of Biochemistry and Biophysics* **1992**, *292*, 475-478.

(169) Czerwinski, R. M.; Harris, T. K.; Massiah, M. A.; Mildvan, A. S.; Whitman, C. P. The structural basis for the perturbed pK(a) of the catalytic base in 4-oxalocrotonate tautomerase: Kinetic and structural effects of mutations of Phe-50. *Biochemistry* **2001**, *40*, 1984-1995.

(170) Parr, I. B.; Boehlein, S. K.; Dribben, A. B.; Schuster, S. M.; Richards, N. G. J. Mapping the aspartic acid binding site of Escherichia coli asparagine synthetase B using substrate analogs (vol 29, pg 2367, 1996). *Journal of Medicinal Chemistry* **1996**, *39*, 4348-4348.

(171) Parr, I. B.; Boehlein, S. K.; Dribben, A. B.; Schuster, S. M.; Richards, N. G. J. Mapping the aspartic acid binding site of Escherichia coli asparagine synthetase B using substrate analogs. *Journal of Medicinal Chemistry* **1996**, *39*, 2367-2378.

(172) Boehlein, S. K.; Walworth, E. S.; Richards, N. G. J.; Schuster, S. M. Mutagenesis and chemical rescue indicate residues involved in beta-aspartyl AMP formation by *Escherichia coli* asparagine synthetase B. *Journal of Biological Chemistry* **1997**, *272*, 12384-12392.

(173) Blume-Jensen, P.; Hunter, T. Oncogenic kinase signalling. *Nature* **2001**, *411*, 355-365.

(174) Temin, H. M. Studies on Carcinogenesis by Avian Sarcoma Viruses. 3. Differential Effect of Serum and Polycations on Multiplication of Uninfected and Converted Cells. *Journal of the National Cancer Institute* **1966**, *37*, 167-175.

(175) Dulbecco, R. Topoinhibition and Serum Requirement of Transformed and Untransformed Cells. *Nature* **1970**, *227*, 802.

(176) Paul, D., Lipton, A., Klinger, I. Serum Factor Requirements of Normal and Simian Virus 40 Transformed 3t3 Mouse Fibroblasts. *Proceedings of the National Academy of Sciences of the United States of America* **1971**, *68*, 645-648.

(177) Moses, H. L., Proper, J. A., Volkenant, M. E., Wells, D. J., Getz, M. J. Mechanism of Growth Arrest of Chemically Transformed Cells in Culture. *Cancer Research* **1978**, *38*, 2807-2812.

(178) Kaplan, P. L., Anderson, M., Ozanne, B. Transforming Growth Factors(S) Production Enables Cells to Grow in the Absence of Serum - an Autocrine System. *Proceedings of the National Academy of Sciences of the United States of America Biological Sciences* **1982**, *79*, 485-489.

(179) Hunter, T. The Proteins of Oncogenes. *Scientific American* **1984**, *251*, 70-79.

(180) Kelly, K., Cochran, B. H., Stiles, C. D., Leder, P. Cell-Specific Regulation of the C-Myc Gene by Lymphocyte Mitogens and Platelet-Derived Growth-Factor. *Cell* **1983**, *35*, 603-610.

(181) Greenberg, M. E., Ziff, E. B. Stimulation of 3t3 Cells Induces Transcription of the C-Fos Proto-Oncogene. *Nature* **1984**, *311*, 433-438.

(182) Kruijer, W., Cooper, J. A., Hunter, T., Verma, I. M. Platelet-Derived Growth-Factor Induces Rapid but Transient Expression of the C-Fos Gene and Protein. *Nature* **1984**, *312*, 711-716.

(183) Muller, R., Bravo, R., Burckhardt, J., Curran, T. Induction of C-Fos Gene and Protein by Growth Factors Precedes Activation of C-Myc. *Nature* **1984**, *312*, 716-720.

(184) Pierce, J. H., Ruggiero, M., Fleming, T. P., Difiore, P. P., Greenberger, J. S., Varticovski, L., Schlessinger, J., Rovera, G., Aaronson, S. A. Signal Transduction through the Fgf Receptor Transfected in Il-3 Dependent Hematopoietic-Cells. *Science* **1988**, *239*, 628-631.

(185) Schlessinger, J. Signal Transduction by Allosteric Receptor Oligomerization. *Trends in Biochemical Sciences* **1988**, *13*, 443-447.

(186) Jiang, G., Hunter, T. Receptor signaling: when dimerization is not enough. *Current Biology: CB* **1999**, *9*, R568-R571.

(187) Brown, P. M., Debanne, M. T., Grothe, S., Bergsma, D., Caron, M., Kay, C., Oconnormccourt, M. D. The Extracellular Domain of the Epidermal Growth Factor Receptor - Studies On the Affinity and Stoichiometry of Binding, Receptor Dimerization and a Binding-Domain Mutant. *European Journal of Biochemistry* **1994**, *225*, 223-233.

(188) Sherrill, J. M., Kyte, J. Activation of epidermal growth factor receptor by epidermal growth factor. *Biochemistry* **1996**, *35*, 5705-5718.

(189) Lemmon, M. A., Bu, Z. M., Ladbury, J. E., Zhou, M., Pinchasi, D., Lax, I., Engelman, D. M., Schlessinger, J. Two EGF molecules contribute additively to stabilization of the EGFR dimer. *Embo Journal* **1997**, *16*, 281-294.

(190) Ferguson, K. M., Darling, P. J., Mohan, M. J., Macatee, T. L., Lemmon, M. A. Extracellular domains drive homo- but not hetero-dimerization of erbB receptors. *Embo Journal* **2000**, *19*, 4632-4643.

(191) Honegger, A. M., Kris, R. M., Ullrich, A., Schlessinger, J. Evidence That Autophosphorylation of Solubilized Receptors for Epidermal Growth Factor Is Mediated by Intermolecular Cross Phosphorylation. *Proceedings of the National Academy of Sciences of the United States of America* **1989**, *86*, 925-929.

(192) Gotoh, N., Tojo, A., Hino, M., Yazaki, Y., Shibuya, M. A Highly Conserved Tyrosine Residue at Codon 845 within the Kinase Domain Is Not Required for the Transforming Activity of Human Epidermal Growth Factor Receptor. *Biochemical and Biophysical Research Communications* **1992**, *186*, 768-774.

(193) Pawson, T., Schlessinger, J. Sh2 and Sh3 Domains. *Current Biology* **1993**, *3*, 434-442.

(194) Carpenter, G., King, L., Cohen, S. Epidermal Growth Factor Stimulates Phosphorylation in Membrane Preparations In vitro. *Nature* **1978**, *276*, 409-410.

(195) Ullrich, A., Schlessinger, J. Signal Transduction by Receptors with Tyrosine Kinase-Activity. *Cell* **1990**, *61*, 203-212.

(196) Carpenter, G., Wahl, M. I. *Peptide Growth factors and Their Receptors*, Springer, New York, 1991, pp 69-171.

(197) Lemoine, N. R., Lobresco, M., Leung, H., Barton, C., Hughes, C. M., Prigent, S. A., Gullick, W. J., Kloppel, G. The Erbb-3 Gene in Human Pancreatic-Cancer. *Journal of Pathology* **1992**, *168*, 269-273.

(198) Ullrich, A., Coussens, L., Hayflick, J. S., Dull, T. J., Gray, A., Tam, A. W., Lee, J., Yarden, Y., Libermann, T. A., Schlessinger, J., Downward, J., Mayes, E. L. V., Whittle, N., Waterfield, M. D., Seeburg, P. H. Human Epidermal Growth-Factor Receptor Cdna Sequence and Aberrant Expression of the Amplified Gene in A431 Epidermoid Carcinoma-Cells. *Nature* **1984**, *309*, 418-425.

(199) Ushiro, H., Cohen, S. Identification of Phosphotyrosine as a Product of Epidermal Growth Factor-Activated Protein Kinase in a-431 Cell Membranes. *Journal of Biological Chemistry* **1980**, *255*, 8363-8365.

(200) Cummings, R. D., Soderquist, A. M., Carpenter, G. The Oligosaccharide Moieties of the Epidermal Growth Factor Receptor in a-431 Cells - Presence of Complex-Type N-Linked Chains That Contain Terminal N-Acetylgalactosamine Residues. *Journal of Biological Chemistry* **1985**, *260*, 1944-1952.

(201) Mayes, E. L. V., Waterfield, M. D. Biosynthesis of the Epidermal Growth Factor Receptor in A431 Cells. *Embo Journal* **1984**, *3*, 531-537.

(202) Bajaj, M., Waterfield, M. D., Schlessinger, J., Taylor, W. R., Blundell, T. On the Tertiary Structure of the Extracellular Domains of the Epidermal Growth-Factor and Insulin Receptors. *Biochimica Et Biophysica Acta* **1987**, *916*, 220-226.

(203) Ward, C. W., Hoyne, P. A., Flegg, R. H. Insulin and Epidermal Growth-Factor Receptors Contain the Cysteine Repeat Motif Found in the Tumor-Necrosis-Factor Receptor. *Proteins Structure Function and Genetics* **1995**, *22*, 141-153.

(204) Lax, I., Burgess, W. H., Bellot, F., Ullrich, A., Schlessinger, J., Givol, D. Localization of a Major Receptor Binding Domain for Epidermal Growth-Factor by Affinity Labeling. *Molecular and Cellular Biology* **1988**, *8*, 1831-1834.

(205) Abe, Y., Odaka, M., Inagaki, F., Lax, I., Schlessinger, J., Kohda, D. Disulfide bond structure of human epidermal growth factor receptor. *Journal of Biological Chemistry* **1998**, *273*, 11150-11157.

(206) Lax, I., Bellot, F., Howk, R., Ullrich, A., Givol, D., Schlessinger, J. Functional Analysis of the Ligand Binding Site of Egf Receptor Utilizing Chimeric Chicken Human Receptor Molecules. *Embo Journal* **1989**, *8*, 421-427.

(207) Kohda, D., Odaka, M., Lax, I., Kawasaki, H., Suzuki, K., Ullrich, A., Schlessinger, J., Inagaki, F. A 40-Kda Epidermal Growth Factor Transforming Growth Factor- Alpha-Binding Domain Produced by Limited Proteolysis of the Extracellular Domain of the Epidermal Growth Factor Receptor. *Journal of Biological Chemistry* **1993**, *268*, 1976-1981.

(208) Elleman, T. C., Domagala, T., McKern, N. M., Nerrie, M., Lonnqvist, B., Adams, T. E., Lewis, J., Lovrecz, G. O., Hoyne, P. A., Richards, K. M., Howlett, G. J., Rothacker, J., Jorissen, R. N., Lou, M. Z., Garrett, T. P. J., Burgess, A. W., Nice, E. C., Ward, C. W. Identification of a determinant of epidermal growth factor receptor ligand-binding specificity using a truncated, high- affinity form of the ectodomain. *Biochemistry* **2001**, *40*, 8930-8939.

(209) Ogiso, H., Ishitani, R., Nureki, O., Fukai, S., Yamanaka, M., Kim, J. H., Saito, K., Sakamoto, A., Inoue, M., Shirouzu, M., Yokoyama, S. Crystal structure of the complex of human epidermal growth factor and receptor extracellular domains. *Cell* **2002**, *110*, 775-787.

(210) Garrett, T. P. J., McKern, N. M., Lou, M. Z., Elleman, T. C., Adams, T. E., Lovrecz, G. O., Zhu, H. J., Walker, F., Frenkel, M. J., Hoyne, P. A., Jorissen, R. N., Nice, E. C., Burgess, A. W., Ward, C. W. Crystal structure of a truncated epidermal growth factor receptor extracellular domain bound to transforming growth factor alpha. *Cell* **2002**, *110*, 763-773.

(211) Lu, H. S., Chai, J. J., Li, M., Huang, B. R., He, C. H., Bi, R. C. Crystal structure of human epidermal growth factor and its dimerization. *Journal of Biological Chemistry* **2001**, *276*, 34913-34917.

(212) Rigby, A. C., Grant, C. W. M., Shaw, G. S. Solution and solid state conformation of the human EGF receptor transmembrane region. *Biochimica Et Biophysica Acta-Biomembranes* **1998**, *1371*, 241-253.

(213) Downward, J., Parker, P., Waterfield, M. D. Autophosphorylation Sites on the Epidermal Growth-Factor Receptor. *Nature* **1984**, *311*, 483-485.

(214) Margolis, B. L., Lax, I., Kris, R., Dombalagian, M., Honegger, A. M., Howk, R., Givol, D., Ullrich, A., Schlessinger, J. All Autophosphorylation Sites of Epidermal Growth Factor (Egf) Receptor and Her2/Neu Are Located in Their Carboxyl-Terminal Tails - Identification of a Novel Site in Egf Receptor. *Journal of Biological Chemistry* **1989**, *264*, 10667-10671.

(215) Walton, G. M., Chen, W. S., Rosenfeld, M. G., Gill, G. N. Analysis of Deletions of the Carboxyl Terminus of the Epidermal Growth Factor Receptor Reveals Self-Phosphorylation at Tyrosine-992 and Enhanced Invivo Tyrosine Phosphorylation of Cell Substrates. *Journal of Biological Chemistry* **1990**, *265*, 1750-1754.

(216) Bertics P J, Chen W S., Hubler L, Lazar C S., Rosenfeld M G, Gill G N. Alteration of Epidermal Growth Factor Receptor Activity by Mutation of Its Primary Carboxyl-Terminal Site of Tyrosine Self-Phosphorylation. *Journal of Biological Chemistry* **1988** *263* 3610-3617

(217) Stoscheck C M, Carpenter G. Down Regulation of Epidermal Growth-Factor Receptors - Direct Demonstration of Receptor Degradation in Human-Fibroblasts. *Journal of Cell Biology* **1984** *98* 1048-1053

(218) Carpenter G, Cohen S. I125 Labeled Human Epidermal Growth Factor - Binding, Internalization, and Degradation in Human Fibroblasts. *Journal of Cell Biology* **1976** *71* 159-171

(219) Chen W S, Lazar C S, Lund K A., Welsh J B, Chang, C P, Walton G M., Der C J., Wiley H S., Gill G N., Rosenfeld, M G. Functional Independence of the Epidermal Growth Factor Receptor from a Domain Required for Ligand-Induced Internalization and Calcium Regulation. *Cell* **1989** *59* 33-43.

(220) Cohen S. Isolation of a Mouse Submaxillary Gland Protein Accelerating Incisor Eruption and Eyelid Opening in New-Born Animal. *Journal of Biological Chemistry* **1962** *237* 1555-1562

(221) Cohen S., Elliott, G A. The Stimulation of Epidermal Keratinization by a Protein Isolated from the Submaxillary Gland of the Mouse. *Journal of Investigative Dermatology* **1963** *40* 1-5

(222) Savage C R., Cohen S, Inagami T. Primary Structure of Epidermal Growth Factor. *Journal of Biological Chemistry* **1972**, *247* 7612-&

(223) Savage C R., Hash J H., Cohen S. Epidermal Growth Factor - Location of Disulfide Bonds. *Journal of Biological Chemistry* **1973** *248* 7669-7672.

(224) Gregory H. Isolation and Structure of Urogastrone and Its Relationship to Epidermal Growth-Factor. *Nature* **1975** *257* 325-327

(225) Savage C R, Harper R. Human Epidermal Growth Factor-Urogastrone - Rapid Purification Procedure and Partial Characterization. *Analytical Biochemistry* **1981** *111* 195-202

(226) Todaro G J, Delarco J E., Cohen S. Transformation by Murine and Feline Sarcoma Viruses Specifically Blocks Binding of Epidermal Growth Factor to Cells. *Nature* **1976** *264* 26-31

(227) Anzano M A., Roberts A B, Smith J M., Sporn, M B., Delarco J E. Sarcoma Growth-Factor from Conditioned Medium of Virally Transformed Cells Is Composed of Both Type-Alpha and Type-Beta Transforming Growth-Factors. *Proceedings of the National Academy of Sciences of the United States of America-Biological Sciences* **1983** *80* 6264-6268

(228) Marquardt H, Hunkapiller M W., Hood, L E, Twardzik D R., Delarco J E, Stephenson, J R., Todaro G J. Transforming Growth Factors Produced by Retrovirus-Transformed Rodent Fibroblasts and Human-Melanoma Cells Amino-Acid- Sequence Homology with Epidermal Growth-Factor. *Proceedings of the National Academy of Sciences of the United States of America Biological Sciences* **1983** *80* 4684-4688

(229) Mayo K H., Cavalli R C., Peters A R, Boelens, R., Kaptein R. Sequence-Specific H 1-Nmr Assignments and Peptide Backbone Conformation in Rat Epidermal Growth Factor. *Biochemical Journal* 1989 *257* 197-205

(230) Montelione, G. T.; Wuthrich, K.; Nice, E. C.; Burgess, A. W.; Scheraga, H. A. Solution Structure of Murine Epidermal Growth Factor - Determination of the Polypeptide Backbone Chain-Fold by Nuclear Magnetic-Resonance and Distance Geometry. *Proceedings of the National Academy of Sciences of the United States of America* **1987**, *84*, 5226-5230.

(231) Cooke, R. M.; Wilkinson, A. J.; Baron, M.; Pastore, A.; Tappin, M. J.; Campbell, I. D.; Gregory, H.; Sheard, B. The Solution Structure of Human Epidermal Growth-Factor. *Nature* **1987**, *327*, 339-341.

(232) Montelione, G. T.; Winkler, M. E.; Burton, L. E.; Rinderknecht, E.; Sporn, M. B.; Wagner, G. Sequence Specific H-1-Nmr Assignments and Identification of 2 Small Antiparallel Beta Sheets in the Solution Structure of Recombinant Human Transforming Growth Factor-Alpha. *Proceedings of the National Academy of Sciences of the United States of America* **1989**, *86*, 1519-1523.

(233) Tappin, M. J.; Cooke, R. M.; Fitton, J. E.; Campbell, I. D. A High Resolution H-1-Nmr Study of Human Transforming Growth Factor-Alpha - Structure and Ph-Dependent Conformational Interconversion. *European Journal of Biochemistry* **1989**, *179*, 629-637.

(234) Kohda, D.; Shimada, I.; Miyake, T.; Fuwa, T.; Inagaki, F. Polypeptide Chain Fold of Human Transforming Growth Factor Alpha Analogous to Those of Mouse and Human Epidermal Growth-Factors as Studied by Two-Dimensional H-1 Nmr. *Biochemistry* **1989**, *28*, 953-958.

(235) Kline, T. P.; Brown, F. K.; Brown, S. C.; Jeffs, P. W.; Kopple, K. D.; Mueller, L. Solution Structures of Human Transforming Growth Factor Alpha Derived From H-1 Nmr Data. *Biochemistry* **1990**, *29*, 7805-7813.

(236) McInnes, C.; Hoyt, D. W.; Harkins, R. N.; Pagila, R. N.; Debanne, M. T.; OconnorMcCourt, M.; Sykes, B. D. NMR study of the transforming growth factor-alpha (TGF alpha)-epidermal growth factor receptor complex - Visualization of human TGF alpha binding determinants through nuclear overhauser enhancement analysis. *Journal of Biological Chemistry* **1996**, *271*, 32204-32211.

(237) Tam, J. P.; Lin, Y. Z.; Wen, L.; Wang, D. X.; Ke, X. H.; Zhang, J. W. Mapping the Receptor Recognition Site of Human Transforming Growth Factor-Alpha. *International Journal of Peptide and Protein Research* **1991**, *38*, 204-211.

(238) Heath, W. F.; Merrifield, R. B. A Synthetic Approach to Structure - Function Relationships in the Murine Epidermal Growth Factor Molecule. *Proceedings of the National Academy of Sciences of the United States of America* **1986**, *83*, 6367-6371.

(239) Tam, J. P.; Sheikh, M. A.; Solomon, D. S.; Ossowski, L. Efficient Synthesis of Human Type Alpha-Transforming Growth-Factor - Its Physical and Biological Characterization. *Proceedings of the National Academy of Sciences of the United States of America* **1986**, *83*, 8082-8086.

(240) Schultz, G.; Chegini, N.; Grant, M.; Khaw, P.; Mackay, S. Effects of Growth-Factors On Corneal Wound Healing. *Acta Ophthalmologica* **1992**, *70*, 60-66.

(241) Schultz, G. S.; White, M.; Mitchell, R.; Brown, G.; Lynch, J.; Twardzik, D. R.; Todaro, G. J. Epithelial Wound-Healing Enhanced By Transforming Growth Factor Alpha and Vaccinia Growth Factor. *Science* **1987**, *235*, 350-352.

(242) Okamura, K., Morimoto A Hamanaka, R Ono M , Kohno, K , Uchida, Y , Kuwano M A Model System for Tumor Angiogenesis - Involvement of Transforming Growth Factor Alpha in Tube Formation of Human Microvascular Endothelial Cells Induced by Esophageal Cancer Cells *Biochemical and Biophysical Research Communications* **1992** *186* 1471-1479

(243) Luckow, V A Cloning and expression of heterologous genes in insect cells with baculovirus vectors *Recombinant DNA Technology and Applications* McGraw-Hill New York 1991 pp 97-152

(244) Smith G E Fraser M J Summers M D Molecular Engineering of the *Autographa-Californica* Nuclear Polyhedrosis Virus Genome - Deletion Mutations within the Polyhedrin Gene *Journal of Virology* **1983** *46* 584-593

(245) Weyer U Knight S Possee R. D Analysis of Very Late Gene Expression by *Autographa Californica* Nuclear Polyhedrosis Virus and the Further Development of Multiple Expression Vectors *Journal of General Virology* **1990** *71* 1525-1534

(246) Kool M Voncken, J W., Vanlier F L. J Tramper J Vlak J M Detection and Analysis of *Autographa Californica* Nuclear Polyhedrosis Virus Mutants with Defective Interfering Properties *Virology* **1991** *183* 739-746

(247) Kitts, P A Ayres M. D Possee R. D Linearization of Baculovirus DNA Enhances the Recovery of Recombinant Virus Expression Vectors *Nucleic Acids Research* **1990** *18* 5667-5672

(248) Kitts P A Possee R D A Method for Producing Recombinant Baculovirus Expression Vectors at High Frequency *Biotechniques* **1993** *14* 810-&

(249) Gearing K L Possee R D Functional Analysis of a 603 Nucleotide Open Reading Frame Upstream of the *Polyhedrin* Gene of *Autographa Californica* Nuclear Polyhedrosis Virus *Journal of General Virology* **1990** *71* 251-262

(250) Sambrook J Fritsch E F , Maniatis T *Molecular Cloning* Cold Spring Harbor Laboratory Press New York 1989

(251) Sanger F Nicklen S Coulson A R DNA Sequencing with Chain Terminating Inhibitors *Proceedings of the National Academy of Sciences of the United States of America* **1977** *74* 5463-5467

(252) Laemmli U K. Cleavage of Structural Proteins During Assembly of Head of Bacteriophage-T4 *Nature* **1970** *227* 680-685

(253) Matsuura, Y Possee R. D Overton H A Bishop D H L Baculovirus Expression Vectors - the Requirements for High Level Expression of Proteins, Including Glycoproteins. *Journal of General Virology* **1987** *68* 1233-1250

(254) Debanne, M T., Pacheco Oliver M C O Connor-McCourt, M D Purification of the Extracellular Domain of the Epidermal Growth Factor Receptor Produced by Recombinant Baculovirus-Infected Insect cells in a 10-L Reactor *Baculovirus Expression Protocols* Humana Press Totowa, NJ 1995 pp 349-361

(255) Van Heeke G Schuster S M Expression of Human Asparagine Synthetase in Escherichia-Coli *Journal of Biological Chemistry* **1989** *264* 5503-5509

(256) O Brien W E Continuous Spectrophotometric Assay for Argininosuccinate Synthetase Based on Pyrophosphate Formation *Analytical Biochemistry* **1976** *76* 423-430

(257) Bernt, E., Bergmeyer H U *Methods in Enzymatic Analysis*, Academic Press New York 1974 pp 331 358

(258) Broschat, K O Gorka, C , Page J D Martin-Berger C L Davies, M S Huang H C Gulve, E A Salsgiver W J Kasten T P Kinetic characterization of human glutamine fructose-6 phosphate amidotransferase I Potent feedback inhibition by glucosamine 6-phosphate *Journal of Biological Chemistry* **2002** *277* 14764 14770

(259) Patterson M K Jr Orr, G L-Asparagine Biosynthesis by Nutritional Variants of Jensen Sarcoma. *Biochemical and Biophysical Research Communications* **1967** *26* 228-233

(260) Chou, T C Handschumacher R E Kinetic Mechanism of L Asparagine Synthetase of 6c3hed-Rg1 Tumor *Federation Proceedings* **1970** *29* A407

(261) Milman, H A Cooney D A Partial-Purification and Properties of L Asparagine Synthetase from Mouse Pancreas *Biochemical Journal* **1979** *181* 51 59

(262) Hongo S Matsumoto T Sato T Purification and Properties of Asparagine Synthetase from Rat Liver *Biochimica Et Biophysica Acta* **1978** *522* 258-266

(263) Kakiuchi S Tomizawa, H H Properties of Glucagon Degrading Enzyme of Beef Liver *Journal of Biological Chemistry* **1964** *239* 2160 2164

(264) McDonald J K Ellis S Reilly T J Properties of Dipeptidyl Arylamidase I of Pituitary - Chloride and Sulfhydryl Activation of Seryltyrosyl-Beta Naphthylamide Hydrolysis. *Journal of Biological Chemistry* **1966** *241* 1494-1501

(265) Unemoto T Hayashi M Chloride Ion as a Modifier of 2 3 -Cyclic Phosphodiesterase Purified from Halophilic Vibrio Alginolyticus *Biochimica Et Biophysica Acta* **1969** *171* 89-102

(266) Schubert J Choline Acetyltransferase Purification and Effect of Salts on Mechanism of Enzyme-Catalyzed Reaction *Biochimica Et Biophysica Acta* **1966** *122* 470

(267) Mantsala, P Zalkin, H Glutamine Amidotransferase Function Replacement of the Active-Site Cysteine in Glutamine Phosphoribosylpyrophosphate Amidotransferase by Site-Directed Mutagenesis *Journal of Biological Chemistry* **1984** *259* 4230-4236

(268) Pfeiffer N E Mehlhaff P M Wylie D E Schuster S M Topographical Separation of the Catalytic Sites of Asparagine Synthetase Explored with Monoclonal-Antibodies *Journal of Biological Chemistry* **1987** *262* 11565 11570

(269) Lusty C J Liao M Substitution of Glu841 by Lysine in the Carbamate Domain of Carbamyl-Phosphate Synthetase Alters the Catalytic Properties of the Glutaminase Subunit *Biochemistry* **1993** *32* 1278-1284

(270) Gallop M A Barrett R W Dower W J Fodor S P A Gordon E M Applications of Combinatorial Technologies to Drug Discovery 1 Background and Peptide Combinatorial Libraries *Journal of Medicinal Chemistry* **1994** *37* 1233-1251

(271) Gordon, E. M., Barrett, R. W., Dower, W. J., Fodor, S. P. A., Gallop, M. A. Applications of Combinatorial Technologies to Drug Discovery. 2. Combinatorial Organic-Synthesis, Library Screening Strategies, and Future Directions. *Journal of Medicinal Chemistry* **1994**, *37*, 1385-1401.

(272) Houghten, R. A., Pinilla, C., Blondelle, S. E., Appel, J. R., Dooley, C. T., Cuervo, J. H. Generation and Use of Synthetic Peptide Combinatorial Libraries For Basic Research and Drug Discovery. *Nature* **1991**, *354*, 84-86.

(273) Balkenhohl, F., vondemBusscheHunnefeld, C., Lansky, A., Zechel, C. Combinatorial synthesis of small organic molecules. *Angewandte Chemie-International Edition in English* **1996**, *35*, 2289-2337.

(274) Li, B., Tom, J. Y. K., Oare, D., Yen, R., Fairbrother, W. J., Wells, J. A., Cunningham, B. C. Minimization of a Polypeptide Hormone. *Science* **1995**, *270*, 1657-1660.

(275) Wrighton, N. C., Farrell, F. X., Chang, R., Kashyap, A. K., Barbone, F. P., Mulcahy, L. S., Johnson, D. L., Barrett, R. W., Jolliffe, L. K., Dower, W. J. Small peptides as potent mimetics of the protein hormone erythropoietin. *Science* **1996**, *273*, 458-463.

(276) Huc, I., Lehn, J. M. Virtual combinatorial libraries: Dynamic generation of molecular and supramolecular diversity by self-assembly. *Proceedings of the National Academy of Sciences of the United States of America* **1997**, *94*, 2106-2110.

(277) Czarnik, A. W. Encoding methods for combinatorial chemistry. *Current Opinion in Chemical Biology* **1997**, *1*, 60-66.

(278) Smith, G. P. Filamentous Fusion Phage: Novel Expression Vectors That Display Cloned Antigens On the Virion Surface. *Science* **1985**, *228*, 1315-1317.

(279) Koivunen, E., Wang, B. C., Ruoslahti, E. Phage Libraries Displaying Cyclic Peptides With Different Ring Sizes: Ligand Specificities of the Rgd-Directed Integrins. *Bio-Technology* **1995**, *13*, 265-270.

(280) McConnell, S. J., Kendall, M. L., Reilly, T. M., Hoess, R. H. Constrained Peptide Libraries As a Tool For Finding Mimotopes. *Gene* **1994**, *151*, 115-118.

(281) Parmley, S. F., Smith, G. P. Antibody-Selectable Filamentous Fd Phage Vectors: Affinity Purification of Target Genes. *Gene* **1988**, *73*, 305-318.

(282) Bass, S., Greene, R., Wells, J. A. Hormone Phage: an Enrichment Method For Variant Proteins With Altered Binding-Properties. *Proteins-Structure Function and Genetics* **1990**, *8*, 309-314.

(283) Lowman, H. B., Wells, J. A. Affinity Maturation of Human Growth-Hormone By Monovalent Phage Display. *Journal of Molecular Biology* **1993**, *234*, 564-578.

(284) McCafferty, J. *Phage Display of Peptides and Proteins*, Academic Press, 1996, pp 261-276.

(285) Doorbar, J., Winter, G. Isolation of a Peptide Antagonist to the Thrombin Receptor Using Phage Display. *Journal of Molecular Biology* **1994**, *244*, 361-369.

(286) Ladner, R. C. *Phage Display of Peptides and Proteins*, Academic Press, 1996, pp 151-193.

(287) McConnell, S. J.; Uveges, A. J.; Spinella, D. G. Comparison of Plate Versus Liquid Amplification of M13 Phage Display Libraries. *Biotechniques* **1995**, *18*, 803 &

(288) Markwell, M. A. K. A New Solid State Reagent to Iodinate Proteins. I. Conditions for the Efficient Labeling of Antiserum. *Analytical Biochemistry* **1982**, *125*, 427-432

(289) Meulemans, E. V.; Slobbe, R.; Wasterval, P.; Ramaekers, F. C. S.; Vaneys, G. Selection of Phage-Displayed Antibodies Specific For a Cytoskeletal Antigen By Competitive Elution With a Monoclonal- Antibody. *Journal of Molecular Biology* **1994**, *244*, 353-360

(290) Goodson, R. J.; Doyle, M. V.; Kaufman, S. E.; Rosenberg, S. High-Affinity Urokinase Receptor Antagonists Identified With Bacteriophage Peptide Display. *Proceedings of the National Academy of Sciences of the United States of America* **1994**, *91*, 7129-7133

(291) O'Neil, K. T.; DeGrado, W. F.; Mousa, S. A.; Ramachandran, N.; Hoess, R. H. Identification of Recognition Sequences of Adhesion Molecules Using Phage Display Technology. **1994**, 370-386

(292) Rottgen, P.; Collins, J. A Human Pancreatic Secretory Trypsin Inhibitor Presenting a Hypervariable Highly Constrained Epitope Via Monovalent Phagemid Display. *Gene* **1995**, *164*, 243-250

(293) Fitzpatrick, S. L.; Lachance, M. P.; Schultz, G. S. Characterization of Epidermal Growth Factor Receptor and Action on Human Breast Cancer-Cells in Culture. *Cancer Research* **1984**, *44*, 3442-3447

(294) Lax, I.; Mitra, A. K.; Ravera, C.; Hurwitz, D. R.; Rubinstein, M.; Ullrich, A.; Stroud, R. M.; Schlessinger, J. Epidermal Growth Factor (Egf) Induces Oligomerization of Soluble, Extracellular, Ligand-Binding Domain of Egf Receptor - a Low Resolution Projection Structure of the Ligand-Binding Domain. *Journal of Biological Chemistry* **1991**, *266*, 13828-13833

(295) Hurwitz, D. R.; Emanuel, S. L.; Nathan, M. H.; Sarver, N.; Ullrich, A.; Felder, S.; Lax, I.; Schlessinger, J. Egf Induces Increased Ligand-Binding Affinity and Dimerization of Soluble Epidermal Growth Factor (Egf) Receptor Extracellular Domain. *Journal of Biological Chemistry* **1991**, *266*, 22035-22043

(296) Greenfield, C.; Patel, G.; Clark, S.; Jones, N.; Waterfield, M. D. Expression of the human EGF receptor with ligand-stimulatable kinase activity in insect cells using a baculovirus vector. *The EMBO Journal* **1988**, *7*, 139-146

(297) Devlin, J. J.; Panganiban, L. C.; Devlin, P. E. Random Peptide Libraries - a Source of Specific Protein-Binding Molecules. *Science* **1990**, *249*, 404-406

(298) Cwirla, S. E.; Peters, E. A.; Barrett, R. W.; Dower, W. J. Peptides on Phage - a Vast Library of Peptides for Identifying Ligands. *Proceedings of the National Academy of Sciences of the United States of America* **1990**, *87*, 6378-6382

BIOGRAPHICAL SKETCH

Mihai Ciustea was born in Bucharest, Romania, on November 22, 1968. In June of 1987, he graduated in the honor class of Mathematics and Physics High School #3, one of the best ranked high schools in Bucharest. After 9 months of mandatory army service, he started undergraduate studies in the Department of Chemistry at the Polytechnical University of Bucharest. Five years later, he graduated with a Master of Engineering degree in organic chemistry. In the fall of 1996, Mihai entered the University of Florida, to obtain a doctor of philosophy degree in biochemistry and molecular biology.

I certify that I have read this study and that in my opinion it conforms to acceptable standards of scholarly presentation and is fully adequate, in scope and quality, as a dissertation for the degree of Doctor of Philosophy

Nigel Richards

Nigel G.J. Richards, Chair
Associate Professor of Chemistry

I certify that I have read this study and that in my opinion it conforms to acceptable standards of scholarly presentation and is fully adequate, in scope and quality, as a dissertation for the degree of Doctor of Philosophy.

Steven A. Benner
Distinguished Professor of Chemistry

I certify that I have read this study and that in my opinion it conforms to acceptable standards of scholarly presentation and is fully adequate, in scope and quality, as a dissertation for the degree of Doctor of Philosophy

James A. Deyrup
Professor of Chemistry

I certify that I have read this study and that in my opinion it conforms to acceptable standards of scholarly presentation and is fully adequate, in scope and quality, as a dissertation for the degree of Doctor of Philosophy

Gregory Schulz

Gregory S. Schultz
Professor of Biochemistry and
Molecular Biology

I certify that I have read this study and that in my opinion it conforms to acceptable standards of scholarly presentation and is fully adequate in scope and quality as a dissertation for the degree of Doctor of Philosophy.

Jon D. Stewart
Associate Professor of Chemistry

This dissertation was submitted to the Graduate Faculty of the Department of Chemistry in the College of Liberal Arts and Sciences and to the Graduate School and was accepted as partial fulfillment of the requirements for the degree of Doctor of Philosophy.

August 2003

Dean, Graduate School